AN ABSTRACT OF THE THESIS OF

Emily Pierce Verplanck for the degree of Master of Science

in Oceanography presented on January 16, 1985

Title: TEMPORAL VARIATIONS IN VOLUME AND GEOCHEMISTRY OF VOLCANISM IN THE WESTERN CASCADES, OREGON

ABSTRACT APPROVED: Redacted for privacy

ROBERT A. DUNCAN

Fifty-one K-Ar age determinations of basalts, basaltic andesites and ashflow tuffs from the central Western Cascades in Oregon range in age from 32 to 3.0 m.y. The oldest material is exposed on the western margin and ages decrease progressively with increasing elevation and distance eastward. The age data indicate decreasing eruption rates with time in the Western Cascades volcanic arc. There was approximately twice as much volcanic material deposited between 30 and 20 m.y. as between 20 and 10 m.y.

Major and trace element geochemical analyses on the dated samples reveal temporal variations during the Western Cascades eruptive history. There is an increase in calcalkaline relative to tholeiitic volcanism and an increase in K2O/SiO2 and Zr/Nb ratios with time.

It is proposed that the volume and geochemical character of volcanism in the Western Cascades volcanic arc are influenced by changes in the direction and rate of convergence between the Farallon and North American plates. A model of the convergence rate and direction, based on the mantle-fixed hotspot reference frame,

during the Tertiary indicates a factor of five decrease in rate (16.0 to 3.2 cm/yr). When the clockwise rotation of the Coast Range and Western Cascades is compared with the convergence vectors, the convergence angle is found to decrease with time from about 35 m.y. to the present. Apparently, slower, more oblique subduction results in a decrease in eruption rate, an increase in calcalkaline relative to tholeiitic compositions, and an increase in K_2O/SiO_2 and Zr/Nb ratios.

TEMPORAL VARIATIONS IN VOLUME AND GEOCHEMISTRY OF VOLCANISM IN THE WESTERN CASCADES, OREGON

by

Emily Pierce Verplanck

A THESIS

submitted to

Oregon State University

in partial fulfillment of
the requirements for the
degree of

Master of Science

Completed January 16, 1985
Commencement June 1985

APPROVED

Redacted for privacy

Associate Professor of Oceanography in charge of major

Redacted for privacy

Dean of College of Oceanography

Redacted for privacy

Dean of Graduate School

Date Thesis is presented January 16, 1985

Typed by E.P. Verplanck.

ACKNOWLEDGEMENTS

I would like to thank Bob Duncan, my advisor, for his guidance and inspiration. His door was always open when I had questions or when I just needed to talk, and I learned a tremendous amount from him. The quality of the manuscript was greatly improved by his suggestions and by those of Martin Fisk and Ed Taylor. The discussions I had with Dallas Abbott were enlightening and useful for my thesis work.

I also owe a big thank you to George Walker and Norm MacLeod. The thesis research would not have been possible without their guidance in sampling and their financial support for the geochronology. I am also grateful to George for sharing his preliminary geologic map with me.

There are so many people who made the lab work much more enjoyable, and Kris McElwee is number one on the list. I would like to thank her for the help she offered on innumerable occasions and for all the humorous times we had working (and playing) together. My thanks go to Mark Hower for his assistance with the AA and for his wonderful sense of humor. Andy, Jim, Greg and Dick also kindly offered much useful advice. Thank you Lew Hogan for keeping the mass spec in running condition.

Thanks to all the wonderful people in the marine geology department. I have such fond memories of Jamison house folks,

especially the happy corner with Ian, Bruce, Dave and Marta. Thanks also to Kris, Tina, Rolin, John, Todd, Chris & Lenny (his better-2/3), Carolyn & Curt, Mitch, Marty & June, Pat & Bob, Susan, Kim, all the Monday Night Volleyballers and the Friday Squirrel's happy hour regulars. Thank you Mary Jo for helping me to transform my thesis into the acceptable format and for laughing alot. Thank you Dave R. for the excellent photographic work.

There are many other friendly people in Oceanography whom I would like to acknowledge for their kindness, especially, Gary & Heather, Kathryn & Peter, Lynne, Alton, Margaret, Consuelo, Mark B., Harry, Jim, Laurel S., Bob K., Jack, Roger, Jeff, Bruce D., Fa, Marijke & Tom, Katey, Laurel M., Sara C., Sarah H., Pat H., Bobbi & Andy, Enoc & Lily, and Becky.

I owe an enormous thank you to my wonderful parents, Norton and Alice, for their love and support. Chaco and Buckwheat deserve a big thankyou (and a giant milkbone) for their assistance with the field work and for their unfailing good humor and loyalty. Lastly, I thank my dear husband, Philip, for his enthusiasm for my thesis work and, more importantly, for life in general. His friendship and companionship helped me to complete this thesis more than anything else.

TABLE OF CONTENTS

LIST OF FIGURES

LIST OF TABLES

TEMPORAL VARIATIONS IN VOLUME AND GEOCHEMISTRY OF VOLCANISM IN THE WESTERN CASCADES, OREGON

CHAPTER I: INTRODUCTION

OVERVIEW

The Cascade Range is a volcanic arc which extends from northern California to southern British Columbia, a distance of over 1000 km (Figure I-1). Volcanic activity in the Cascades began approximately 42 m.y. ago (Lux, 1981) with the eruption of basalt and basaltic andesite lavas and more siliceous dacitic ash flow tuffs along a linear belt. Continental margin volcanic arcs such as this are widely recognized to be associated with the subduction of oceanic lithosphere beneath a continent. The release of volatiles from the downgoing plate at depth may produce partial melting in the mantle above the slab and thereby stimulate the formation of basaltic magmas (Green, 1980; Ringwood, 1975).

Volcanic eruptions in the Cascade Range have continued to occur since the middle Tertiary, the most recent of which are the Mt. St. Helens eruptions in the spring of 1980. Mt. St. Helens is one of many spectacular Quaternary-age stratovolcanoes that comprise the impressive, snow-capped High Cascade Range. Previous workers (Callahan, 1933; Thayer, 1936; Peck et al., 1964) have chosen to divide the Cascades into two physiographic provinces:the older Western Cascades exposed along the western slope of the range of

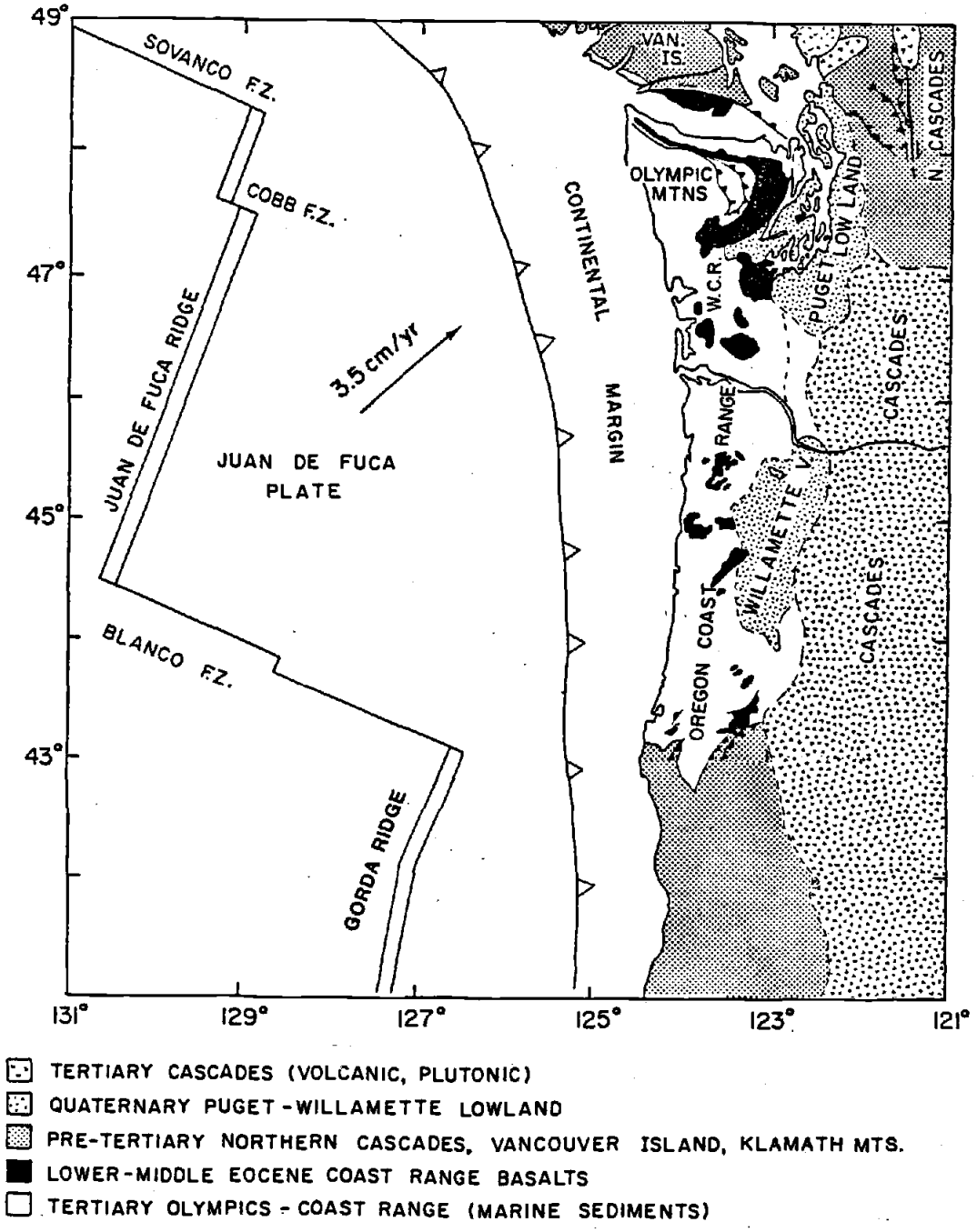

Figure I-1 - Plate boundaries off the coasts of Oregon and Washington.

42-10 m.y. age, and the younger High Cascades on the eastern margin of 10-0 m.y. age. Figure I-2 outlines the boundaries between the early and late Western Cascades and the High Cascades. Temporal variations in the volcanic evolution of the former is the focus of this study.

There are several questions regarding the mid-to-late Tertiary history of the Western Casades which this thesis seeks to evaluate and answer:

1) Eruptive history

a)Has the volume of erupted material been constant or have eruption rates progressively increased/decreased?

b)Have eruptions occurred in distinct pulses separated by intervals of relative quiesence, or have they occurred more or less continuously?

2) Geochemistry

a)Have there been systematic spatial or temporal geochemical variations in the volcanism?

b)Have the degree and depth of melting or the composition of the source region produced distinct primary magmas, as revealed by highly incompatible trace element concentrations?

3) Tectonic setting

a)What is the history of convergence between the Farallon and and North American plates?

b)Do time variations in eruptive history and geochemical character correspond to changes in the pattern of convergence during the formation of the Western Cascades?

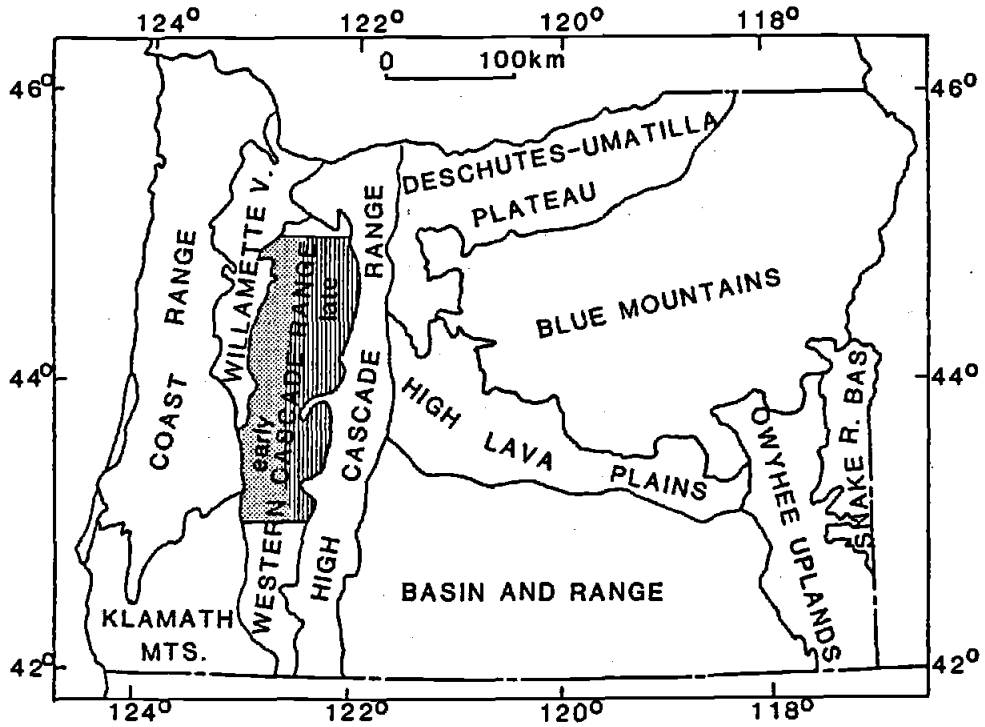

Figure I-2 - Physiographic boundaries of Oregon. Study area is indicated by shaded pattern: dots - early Western Cascades, lines - late Western Cascades.

The Western Cascade Range in central Oregon was chosen as the study area (shaded area, Figure I-2). Samples were collected from a broad region extending from 42° to 44° north latitude and 122° to 123° west longitude on the Salem and Roseburg 2-degree quadrangles. Fifty-one K-Ar age determinations were performed on samples from several volcanic stratigraphic horizons. Major and trace element geochemical analyses were employed on 49 samples.

The major objectives of this study are to describe temporal variations in the eruptive history and geochemical character of the volcanism which produced the Western Cascades and to then correlate these variations with changes in the convergence motion between the Farallon and North American plates. The remainder of Chapter One describes background and previous work on the Western Cascades in Oregon. The second chapter presents the history of convergence between the Farallon and North American plates during Tertiary time. This highly quantitative model was calculated using an absolute reference frame, assuming hotspots are fixed with respect to the mantle, in a similar manner to that described by Engebretson(1983). The third chapter describes the K-Ar geochronology results and uses the ages of volcanic units to estimate eruption rates. Major and trace element geochemical analyses are presented in Chapter IV, and, when combined with the age determinations, temporal geochemical variations are revealed. The convergence model is compared with the geochronological and geochemical results to determine whether the subduction rate influences the volume or geochemical character of volcanism in the associated volcanic arc. Lastly, Chapter V is a summary of the study including broad scale implications and

suggestions for areas of future study. The K-Ar age equation and a list of constants used in the calculations appear in Appendix A. Petrographic descriptions of all samples studied appear in Appendix B.

BACKGROUND AND PREVIOUS WORK

The Western Cascades Range is the older exposed part of the Cascade volcanic arc in which eruptive activity began approximately 42 m.y. ago. This earlier sequence of lavas and ash flows has been uplifted, tilted slightly eastward and subsequently eroded, resulting in a deeply dissected and rugged topography. The steep terrain and extensive vegetative cover have restricted geologists in the past from conducting detailed investigations in the Western Cascades. Recently, however, both the U.S. Geological Survey and the Oregon Department of Geology and Mineral Industries have conducted more extensive mapping programs in some areas of the Western Cascades in Oregon. The following review will begin with a general description of the volcanic stratigraphy and regional structure followed by a summary of relevant geochronological, geochemical and geophysical studies, concluding with a description of volcanic arc petrogenetic processes.

Volcanic Stratigraphy and Regional Structure

The Cascade Range, south of Mt. Hood, was divided into two physiographic provinces designated as the Western Cascades and High

Cascades by Callahan(1933). The boundary between the two divisions is not everywhere agreed upon because it can be a geochemical, chronological, structural or physiographic division. Thayer(1936) recognized the two provinces as "structural units", separated by an east-facing fault scarp which obliquely cuts the folded structure in the North Santiam River section. Peck et al.(1964) described the High Cascades as younger cones and lava flows forming the crest of the range, and the Western Cascades as older, deformed and partially altered flows and pyroclastic rocks. Taylor(1978, 1980, 1981) recognized a 4 to 5 m.y. old north-south trending fault system which separates the Western Cascades from the downward displaced High Cascades graben. The graben possibly extends from Mt. Adams to Crater Lake, but is not entirely continuous. The amount of displacement of the High Cascades axis ranges from several hundred meters to one kilometer.

The Western Cascades volcanic and sedimentary rocks are exposed along the western slope of the Cascade Range and dip gently eastward. The older units may be inclined from 3^{o} to 10^{o} E, but the younger units are often more or less flat-lying. Peck has mapped gentle NE-trending folds, especially in the northern and central parts of the Western Cascades in Oregon. Priest and Vogt(1983) suggest, however, that these folds could be explained by local tilting between fault blocks and also by depositional dips. Farther south, on the Roseburg quadrangle, NW-trending faults are observed (Peck et al., 1964).

The Western Cascades Range consists mainly of volcanic material, both flows and pyroclastic rocks, that range in age from

late Eocene to late Miocene. Priest and Vogt(1983) proposed to divide the volcanic stratigraphy into an early Western Cascades episode of 42 to 18 m.y. and a late Western Cascades episode of 18 to 9 m.y. on the basis of an erosional unconformity which spans 19 to 17 m.y. The volcanic layers overlie and interfinger westward with sedimentary rocks. The following general description of the volcanic stratigraphy is a synthesis of studies by Peck et al.(1964), Priest and Vogt(1983), and Walker (personal communication, 1984).

The oldest rocks in the study area are the Eocene age marine sedimentary rocks of the Spencer, Tyee and Umpqua Formations which lie in the foothills of the Cascades Range south of Eugene. They consist of predominantly sandstone, mudstone and conglomerate marine and submarine strata. The early Western Cascades rocks of 42-18 m.y. age overlie and interfinger with these sedimentary layers, and consist of massive beds of ash flow tuff of andesite to dacite composition, with interbedded olivine basalt and basaltic andesite lava flows. These rocks were referred to as the Little Butte Volcanic Series by Peck et al.(1964), and were originally named by Wells(1956).

The Columbia River Basalt (CRB) is exposed in the study area only in the northern lowlands between the Coast Range and the Cascade Range. The CRB is characterised by columnar jointed flows of dark, fine-grained basalt and its age ranges from 14.5-16.5 m.y. in the study area (Lux, 1981). Geochronological studies by Lux(1981) have determined the southernmost extent of the CRB at Hungry Hill, approximately 16 km north of Lebanon. Therefore, CRB is useful as a stratigraphic marker horizon only north of 44° 40' north

latitude. It unconformably overlies the early Western Cascades lavas and ash flow tuffs in northern Oregon.

The late Western Cascades series, of 18-9 m.y. age, consists of flows and flow breccias of andesite, basaltic andesite and basalt. The lavas are interbedded with continentally derived sediments: volcaniclastic and epiclastic rocks. These approximately horizontally lying strata unconformably overlie the early Western Cascades lavas which generally dip slightly eastward. Much of the late Western Cascades series was referred to as the Sardine Formation by Peck et al.(1964), and was originally named by Thayer (1936). The flows often exhibit curved, platey jointing. The late Western Cascades are most abundant in the north. Proceeding southwards, the exposures decrease and move eastward. The lavas were erupted from NW-trending dikes and related plugs and lava cones, which generally lie to the east of the older, early Western Cascades vents in accordance with the apparent eastward shift of volcanism. Basalt and basaltic andesite volcanic centers of the early Western Cascades are located up to 50 km west of the late Western Cascades volcanic centers (Peck et al., 1964).

The volcanic rocks of the Western Cascades are cut by numerous small intrusive bodies which occur as pipes, dikes, sills and small stocks. Hammond(1979) also describes comagmatic intrusions emplaced during the formation of the Western Cascades. They lie in a belt along the western slope of the Cascades Range in the eastern half of the study area, which is coincident with a zone of hydrothermal alteration. The most common alteration is low-grade zeolite metamorphic facies. Mineral deposits are associated with many of the

intrusive bodies and have yielded minable concentrations of gold and sulfide ore (Callahan and Buddington, 1938).

Younger volcanic rocks of Pliocene and Pleistocene age, from early High Cascades volcanism, are found in the eastern margin of the Western Cascades and also occur as intracanyon flows.

Geochronology

The first age estimates for volcanic rocks from the Western Cascades come from Peck et al.(1964), who made paleontological age determinations on fossil plants from interlayered sedimentary rocks in both the Little Butte Volcanic Series and Sardine Formation. Whole-rock K-Ar age determinations on samples from the central Oregon Cascades were reported by McBirney et al.(1974), Sutter (1978), Hammond(1979) and Priest and Vogt(1983). Fiebelkorn et al.(1983) have compiled K-Ar ages for rocks from the entire state of Oregon. K-Ar and 40Ar/39Ar dating methods were employed by Lux (1981, 1982) on central Western Cascades volcanic rocks.

McBirney et al.(1974) first proposed that a periodicity of volcanic activity occurs in approximately 5 m.y. intervals, since the mid-Miocene, which they correlated with volcanic pulses in the circum-Pacific area. Kennett et al.(1977) examined the record of explosive volcanism from ash layers in deep-sea cores and discovered evidence for synchronous volcanic activity over large regions of the Pacific Basin. The causes of this episodic volcanism in the island-arc and continental-margin areas is possibly due to variations in the rate of plate convergence (Scheidegger and Kulm,

1975; Kennett and Thunell, 1975; Kennett, 1982). Rea and Scheidegger (1979) examined the changes in spreading rates along the East Pacific Rise during the last 4 m.y. and found similar temporal variations between the spreading rates, hotspot volcanism, ash-accumulation and circum-Pacific volcanism.

The geochronological data presented by Sutter(1978) and Lux (1981, 1982) supported the theory of volcanic periodicity in 5 m.y. intervals, which extends back to 40 m.y.. However, the age work of Priest and Vogt(1983) does not support the theory of volcanic episodicity in the Cascade Range. They contended that the periodicity observations could merely be the result of a sampling bias: that a relatively continuous regional volcanic history can be interpreted as episodic due to incomplete sampling, particularly in regions between volcanic centers which may exhibit age gaps in the volcanic stratigraphy. As more areas are mapped and sampled and more age determinations are made, the question of whether the eruptive history of the Cascades has been episodic or continuous can be better decided.

Volume estimates of erupted material in the Cascade Range from the Miocene to the Quaternary show a large pulse of activity in the middle Miocene (16-14 m.y.), followed by smaller episodes in 5 m.y. intervals during the late Miocene (11-9 m.y.), Pliocene (6-4 m.y.) and Holocene (1.5-0 m.y.), (Figure I-3, from McBirney et al., 1974). For younger rocks, such as the Quaternary-age High Cascade volcanoes, reasonably accurate volume estimates can be made. For older rocks, such as those in the Western Cascades, it is impossible to know the original extent of volcanic material. There is an

Figure I-3 - Volumes in km^3 of basalt(B), andesite(A), and rhyolite-dacite(R) for the four latest volcanic episodes of the central Oregon Cascades. Solid areas, volume estimates based on exposed outcrop; stippled areas, probable minimum original volume. From McBirney et al.,(1974).

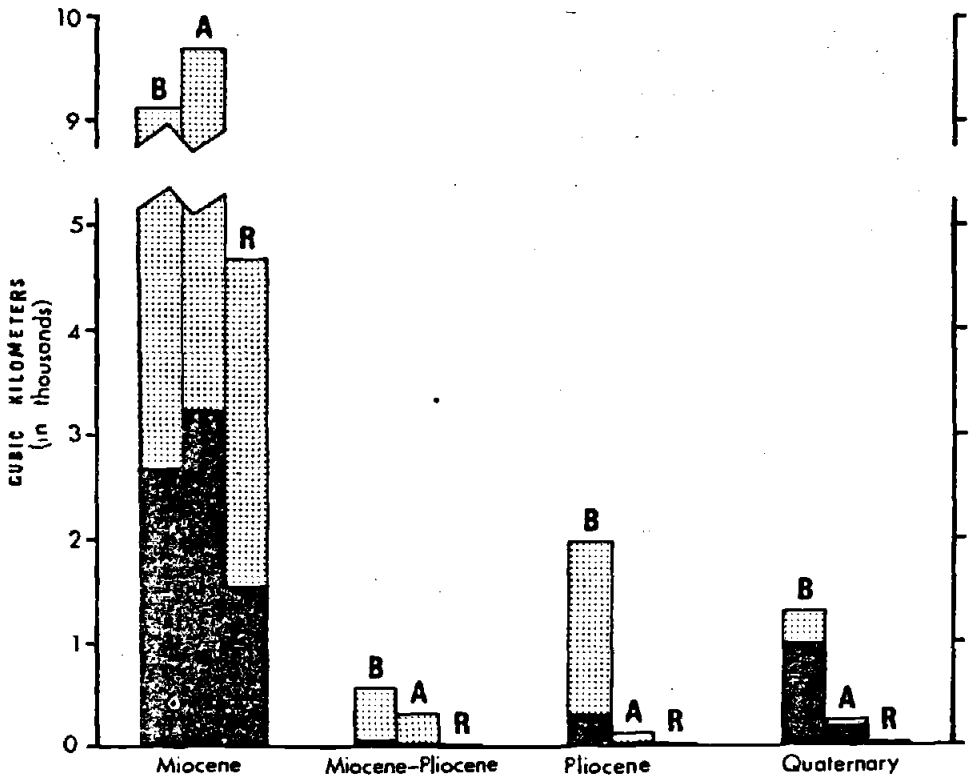

unknown quantity of pyroclastic rock and erosional material removed via wind and water transport. In addition, the extent of older units covered by younger units is unknown. If erosion rates are assumed to be constant, then the relative volumes of older erupted material can be calculated by measuring thicknesses of volcanic layers of known age range in areas where the stratigraphy is well mapped. This study will estimate temporal variations in eruption rates in the Western Cascades by this method.

Geochemistry

Major and trace element geochemical analyses from the Western Cascades in Oregon have been reported by Lux(1981), White(1980) and by Priest and Vogt(1983). Prior to these studies, most of the geochemical research on this volcanic arc had concentrated on the younger High Cascades and the neighboring Columbia River Basalts.

Lux(1981) focused his work on the western margin of the central Western Cascades. The samples were divided into tholeiitic and calcalkaline series, on the basis of degree of Fe-enrichment. Both series are enriched in the light rare earth elements (LREE) relative to the heavy rare earth elements (HREE). The calcalkaline series samples consist of basalts, basaltic andesites, and andesites. The incompatible trace element concentrations appear to increase as the SiO2 content increases, reflecting crystal fractionation of olivine, pyroxene, plagioclase and magnetite (Lux, 1981). On the basis of REE data, Lux(1981) concluded that garnet was not a residual phase after melting and therefore partial melting of peridotite, not eclogite or

other garnet bearing rock, is suggested as a source material for the Western Cascades calcalkaline magmas.

Lux(1981) also measured the 87Sr/86Sr ratios of several samples from the Little Butte Volcanic Series of the Western Cascades. The initial 87Sr/86Sr ratios for all the samples were quite similar and had a range of between 0.70311 to 0.70490. Their average value was 0.7037. This is similar to oceanic island basalts (tholeiitic, 0.7037; alkalic basalts, 0.7038) and volcanic rocks from convergent margins (0.7035), but distinctly higher than mid-ocean ridge basalt values (Atlantic, 0.70264; Pacific, 0.70265; Indian, 0.70314). On the basis of Sr-isotopic data, Lux(1981) concluded that the Western Cascade rocks reflect the isotopic compositon of mantle source materials and that there has been no continental crustal contamination.

Priest and Vogt(1983) present compositional variation diagrams to compare and contrast rocks from the Western Cascades, High Cascades, and Basin and Range provinces. The majority of the Cascades Range rocks have calcalkaline affinities, but their compositions show a temporal geochemical variation. Early Western Cascades rocks consist of both iron-rich tholeiitic basalt to dacite and iron-poor calcalkaline andesite to rhyodacite. The late Western Cascades lavas are iron-poor relative to the early Western Cascades tholeiitic lavas, and consist of primarily calcalkaline basalt to andesite. Priest and Vogt(1983) attribute the decrease in tholeiitic relative to calcalkaline volcanism to maturation of the subduction zone. A temporal variation from tholeiitic to calkaline volcanism has been observed in other volcanic arcs such as Japan and the

Andes.

White and McBirney(1978) compiled selective representative data on igneous rocks of the central Cascades province from various sources to examine geochemical variations with time. The samples were divided into four groups, which range in age from Oligocene to Quaternary, but only the older two groups are from the Western Cascades. The two younger groups are from the Mt. Jefferson area of the High Cascades. The temporal geochemical variations are as follows: 1) an increase in the proportion of basalt relative to andesite or dacite, 2) a decrease in FeO/ FeO+MgO ratios, Rb, REE, and K concentrations, 3) an increase in Na relative to Ca and K/Rb with time. These systematic changes in the geochemical compositions suggest the depth of segregation of the basaltic liquid has become deeper with time (White and McBirney., 1978). Temporal geochemical variations such as those mentioned above, will be examined in this study.

Geophysical Studies

Paleomagnetism

Paleomagnetic data from the Coast Range and Western Cascades Range indicate clockwise rotation of up to 75° since the early Eocene in the former and up to 27° since the late Oligocene in the latter (Simpson and Cox, 1977; Magill and Cox, 1980). The Coast Range basement rocks originated as an oceanic island lineament during early Tertiary time (Snavely and MacLeod, 1977; Simpson and

Cox, 1977; Duncan, 1982). Convergence between the North American and Farallon plates resulted in the emplacement of the Coast Range at approximately 42 m.y. (Heller and Ryberg, 1983). This caused the subduction zone to jump seaward because the oceanic island chain clogged the previous zone (Simpson and Cox, 1977). The initiation of a new subduction zone was coincident with the onset of Cascades volcanic activity. The Coast Range and Cascades Range are presumed to have rotated as a coherent block since the accretion of the Coast Range, because the contacts between the two are depositional rather than fault boundaries.

There is controversy regarding the paleogeographic reconstruction that restores the paleomagnetic vectors to their expected Eocene direction. One theory invokes a continuous clockwise rotation of the Coast Range at a rate of 1.5°/m.y. for the past 50 m.y. (Figure I-4a, Beck and Plumley, 1980). This rotation would include the Western Cascades since the time of Coast Range accretion at 42 m.y. The other theory is a two-phase rotation (Figure I-4b, Magill and Cox, 1980). In Phase I, the Coast Range rotated 45° clockwise about a southern pivot between 55 and 42 m.y. No rotation occured between 42 and 20 m.y. In Phase II, beginning about 20 m.y., the Coast Range, Cascades, and Klamath Mountains rotated 30° clockwise about a northern pivot in response to Basin and Range extension to the south. The Cascades offer an excellent opportunity to resolve the controversy between 1) continuous rotation and 2) stage rotations because of the abundance of new geochronologic data from Western Cascades lava flows and ash flow tuffs. Precise paleogeographic reconstructions for well-constrained time intervals

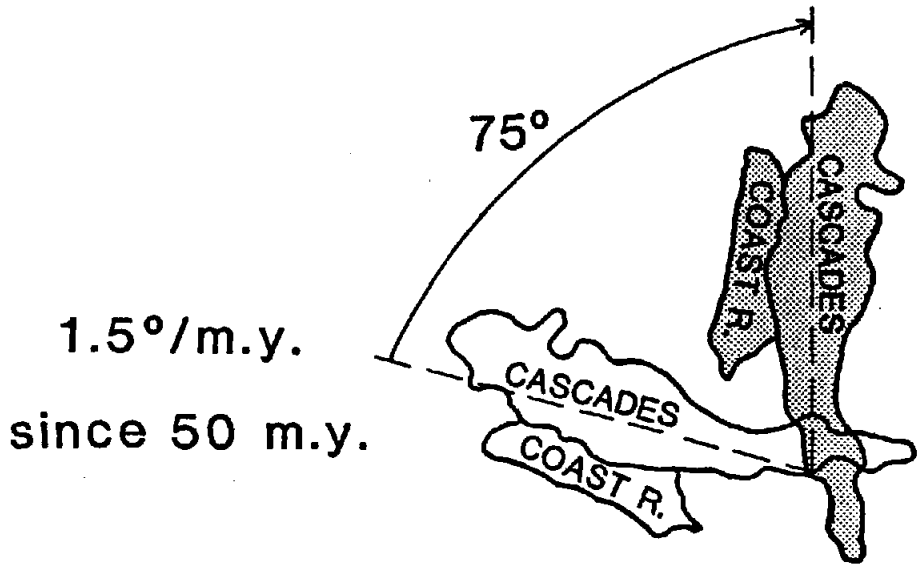

Figure I-4a - Paleogeographic reconstruction for the Coast Range and Western Cascades (after Beck and Plumley, 1980). Paleomagnetic data indicates a continuous clockwise rotation since 50 m.y.

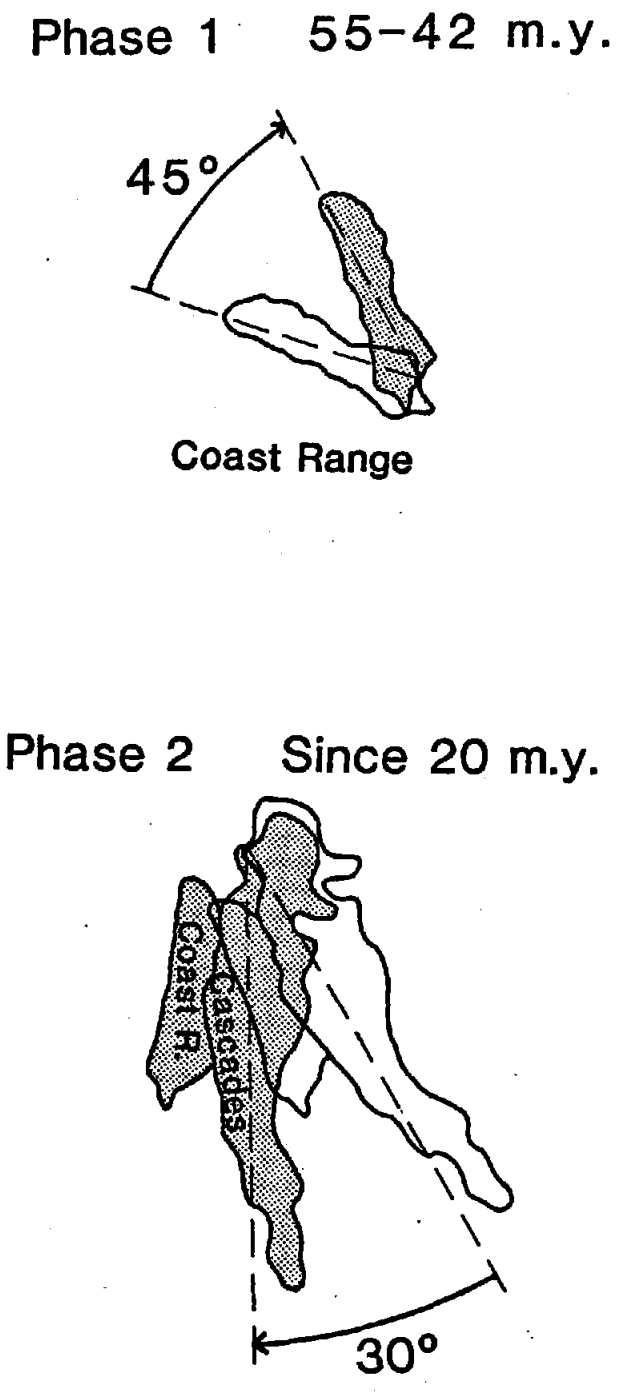

Figure I-4b - Two-phase model for the paleogeographic reconstruction of the Coast Range and Western Cascades (after Magill and Cox, 1980). Phase 1: the Coast Range rotated 45° clockwise about a southern pivot between 55 and 42 m.y. Phase 2: the Coast Range and Western Cascades rotated 30° clockwise about a northern pivot since 20 m.y.

can be made when the paleomagnetic data are measured from dated samples.

Gravity Studies

Gravity measurements in the Cascades Range in Oregon suggest that there are two linear fault systems, oriented approximately N10°E, which delineate a Cascades graben 60 km wide and 350 km long. The western bounding fault is defined by a steep gravity anomaly gradient and extends along the Western Cascades from Crater Lake to the area between Mt. Hood and Mt. Jefferson (Couch and Foote, 1983). Zones of hydrothermal alteration are coincident with the western bounding fault and age determinations of the alteration minerals suggest that the Cascade graben developed between 22 and 9 m.y. ago (Couch, 1984). The eastern side of the graben is less well developed and is oriented parallel to the western side.

Seismic Studies

The subduction zone associated with the Cascades is unusual because there are no deep earthquakes (>100 km) associated with the subduction (Tobin and Sykes, 1968; Crosson, 1976). This is probably a function of the slow subduction rate and youth of the descending Juan de Fuca plate. A younger plate is warmer and therefore reheats and deforms in a ductile manner at a shallow depth, producing few deep earthquakes (Atwater, 1970). Langston(1981) obtained a p-wave low velocity zone between 21 and 45 km depth beneath Corvallis,

Oregon. At 45 km depth, there is a high velocity contrast which he interprets as evidence of a subducting slab (Figure I-5). If the slab is extended beneath the High Cascades axis of volcanism, the seismic model predicts a depth of 70 kilometers for the top of the subducting oceanic plate. This is a minimum estimate because the slab may dip more steeply at greater depths, as is observed at other convergence zones. The crustal thickness beneath the Oregon Cascades Range has been determined by seismic data to increase from 22 km west to 37 km east of the Cascades (Ganoe and Fehler, 1984).

Volcanic Arc Petrogenetic Processes

There are numerous petrogenetic models for the production and evolution of rock series in volcanic arcs. A common feature of all models is that they require a release of water by dehydration in the subducted lithosphere (Green, 1980). The upper few kilometers of the oceanic plate are the most likely source of H_2O and CO_2, because this is the region of hydrothermal alteration (Abbott et al., 1985). Low temperature hydrothermal alteration produces hydrous minerals such as serpentine, talc, epidote, chlorite, smectite and zeolites. The sediments also contain hydrous phases. The subducted slab is reheated by conduction, adiabatic heating and shear melting, consequently, dehydration and decarbonation reactions in the alteration minerals and sediments cause release of volatiles into the overlying asthenosphere (Abbott et al., 1985). Petrogenetic models for the production of tholeiitic and calcalkaline rock series in volcanic arcs are as follows (after Green, 1980):

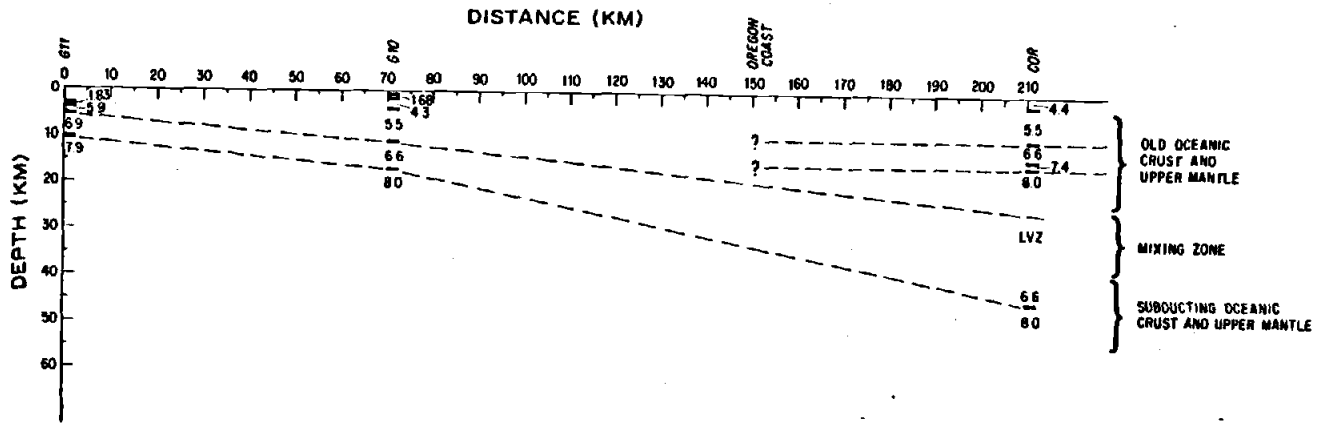

Figure I-5 - Schematic cross section along a profile perpendicular to the Oregon coast and including Corvallis. From Langston(1981).

1) Tholeiitic series magmas are produced by hydrous melting of mantle peridotite at 60-100 km depth (Nicholls and Ringwood, 1973),
2) Calcalkaline series rocks (dominantly andesite) are produced by partial melting of subducted oceanic crust of eclogite composition at depths of 100-200 km, followed by crystallization of olivine, pyroxene, amphibole and magnetite (Green and Ringwood, 1968,1972),
3) Alkaline to tholeiitic series rocks are produced by amphibole-dominated fractionation of a hydrous basic magma (Cawthorne and O'Hara, 1976),
4) Silicic volcanic rocks are produced by hydrous melting of thickened crust (Green, 1972).

There are numerous factors which will affect the composition of volcanic arc magmas. Some of these variables are: crustal thickness, contamination (subducted sediment and/or continental crust), depth of melting, degree of partial melting, extent of crystal fractionation, and age, subduction rate and dip of the subducted oceanic lithosphere. Many of these are dependent upon one another. Previous workers have made attempts to isolate these variables in order that relationships between them can be characterized. The dip and depth of melting on the Benioff zone is apparently dependent upon convergence rate and age of the subducted slab (Abbott and Hoffman, 1984). The subduction rate is proportional to the square root of the age of the plate at the trench (Carlson, 1983).

Both spatial and temporal variations in geochemical compositions have been observed in island and continental volcanic

arcs around the world. Thorpe(1982), in his studies of the Andean volcanic chain, noticed a significant increase in K and Rb, a slight increase in SiO2 and a decrease in Sr with distance from the trench. He suggested that this could reflect a diminishing degree of partial melting, an increase in fractional crystallization, or an increase in contamination in passing eastwards (i.e. away from the plate boundary). Gill(1981) summarized geochemical trends across volcanic arcs from many convergent plate margins. In general, K, Rb, La, Th, U contents and La/Yb, Rb/Sr ratios all increase relative to silica away from the plate boundary.

The most common rocks in immature island arcs are basalts and basaltic andesites of the tholeiitic series, whereas well-developed island arcs are composed of tholeiitic and calcalkaline series rocks (Miyashiro, 1974). This observation suggests that thickening continental crust beneath the arc with time increases the proportion of the calcalkaline relative to tholeiitic series. Miyashiro(1974) noticed a relationship between convergence rate, crustal thickness and composition of volcanic arc rocks (Table I-1). Tholeiitic volcanoes are found to be most abundant in arcs where convergence rates are high (>7 cm/yr) and the crust is thin (<20 km). Where convergence rates are slower (<7 cm/yr) or where the crust is relatively thick (>40 km), less than half the volcanoes are tholeiitic. Intermediate crustal thickness and high convergence rates can correspond to a wide range of volcanic compositions (33-70% tholeiitic). The present crustal thickness beneath the Cascades increases eastward from about 22 km west to 37 km east of the Cascades, but was probably thinner during earlier development of

Table I-1 - RELATIONSHIP BETWEEN CONVERGENCE RATE, CRUSTAL THICKNESS AND COMPOSITION OF VOLCANIC ARC ROCKS.

GROUP I	Convergence rates >7 cm/yr and crust <20 km thick: >80% of volcanoes tholeiitic		
	Kermadec	Mariana	South Sandwich
	Tonga	Izu	
GROUP II	Convergence rates >7 cm/yr and crust 30-40 km thick: 33-70% of volcanoes are tholeiitic		
	New Britain	East Japan	Central America
	Vanuatu	Kuriles	Chile, 33°-47°S
	Java	Kamchatka	
GROUP III	Convergence rates <7 cm/yr or crust >40 km thick: <50% of volcanoes are tholeiitic		
	New Zealand	Cascades	Chile, >47°S
	Sumatra	Mexico	Antilles
	Ryukus	Columbia-Ecuador	Aegean
	Alaska	Peru-Chile, 11°-28°S	Turkey-Iran

From Gill(1981), after Miyashiro(1974).

the volcanic arc (Ganoe and Fehler, 1984). The present subduction rate is very slow (about 2 cm/yr), but was considerably faster during the period of Western Cascades volcanism. This study presents evidence to support the hypothesis that convergence rates influence the geochemical character and volume of volcanic activity in the Western Cascades volcanic arc.

CHAPTER II: THE TERTIARY HISTORY OF CONVERGENCE BETWEEN THE FARALLON AND NORTH AMERICAN PLATES

INTRODUCTION

Changes in the convergence rate and direction at a subduction zone may result in changes in the geochemical character and volume of erupted material in the associated volcanic arc. An excellent site to test this hypothesis is the Cascades volcanic arc. The geologic processes at subduction zones are complex and difficult to isolate. The timing, volume and geochemical character of volcanism may depend on a number of variables: the age of the subducting lithosphere and its volatile content, the percent of sediment which is subducted, the dip angle of subduction, the thickness of overlying continental lithosphere and the convergence rate (Figure II-1). Therefore it is impossible to isolate one variable, i.e. convergence rate. However, the Cascades volcanic arc most nearly approaches the isolation of convergence rate as a controlling factor for the following reasons.

The age of the downgoing slab has remained young (between 10 and 20 m.y. age) during the time of Western Cascades development, and the dip and depth of melting on the Benioff zone is apparently dependent on convergence rate and age of the subducted slab (Abbott and Hoffman, 1984). The amount of sediment which is subducted or accreted is dependent on the convergence rate and the subduction angle (Cloos, 1984). Ganoe and Fehler(1984) have estimated the present crustal thickness beneath the Cascades from seismic data. It

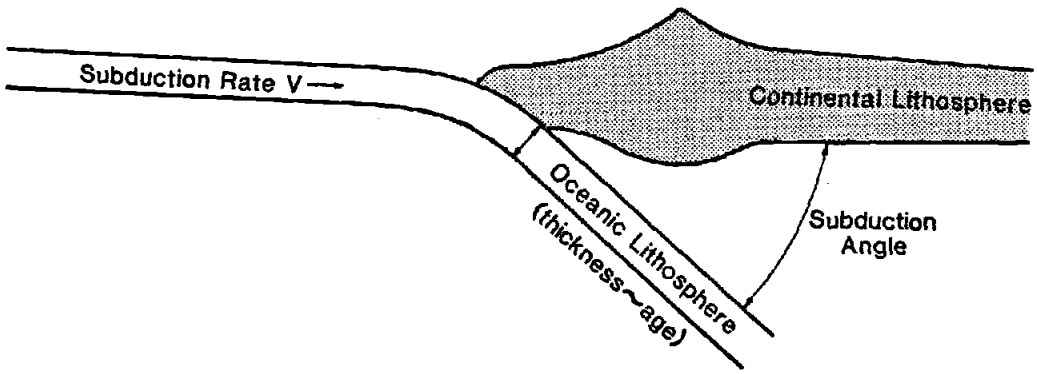

Figure II-1 -Schematic cross section of a convergent margin.

increases eastward from 22 km west to 37 km east of the Cascades, but was presumably slightly thinner during the time of Western Cascades development. There has been a significant decrease in the convergence rate between the Farallon and North American plates during the formation of the older Western Cascades of 42 to 10 m.y. age. Therefore, the effects of slowing subduction on the timing, volume and geochemical character of erupted material can be observed, while other variables remained nearly constant.

The subduction system associated with the Cascades is unique for several reasons. First, there are no deep earthquakes (greater than 100 km) associated with the subduction. This is unusual because most convergent boundaries are characterized by seismic activity to much greater depths (up to 600 km or deeper). Second, the spreading ridge which separates the Pacific plate (west) from the Juan de Fuca plate (east) is exceptionally close to the subduction zone (Figure I-1). This results in unusually young and warm oceanic crust entering the subduction zone. Also younger crust is less dense and will be more likely to subduct at a shallower angle than older, more dense crust (Uyeda and Kanamori, 1979). Between 40 and 80 km depth, basalt transforms to eclogite, yielding a density increase from 2.9 to 3.5 g/cm^3 (Green and Ringwood, 1967). Therefore, a descending oceanic plate will become denser as it subducts.

The convergence rate may also be related to the age of the subducting crust, as denser (older) crust would have a stronger gravitational pull beneath the continental plate than less dense (younger) crust would (McKenzie, 1969; Forsyth and Uyeda, 1975,

Carlson et al., 1983). Plate reconstruction models by Engebretson (1982) and Duncan and McElwee(1984) indicate that the spreading center has been close (within 1000 km) to the subduction zone for the past 40 m.y. Consequently, the age of the subducting plate has been relatively young, 10 to 20 m.y., during this period (Figure II-2). The expected lithospheric thickness of an oceanic plate this age is between 10 and 30 km (Leeds et al., 1974). The subduction of younger plates produces a shallower seismic zone because of a thinner initial thermal thickness. The younger plate will deform in a ductile manner closer to the surface, which explains the absence of deep earthquakes. The subduction angle, rate of convergence and age of oceanic crust are factors which may control the depth of melting, the degree of melting and therefore the geochemical composition and volume of the associated volcanic activity (Abbott and Lyle, 1984).

A third unique characteristic of the Cascades subduction zone is that there is no physiographic expression of a trench at the convergent plate boundary, as found in most convergence zones. This is mainly a result of the high rates of sedimentation off the Oregon and Washington coastal margins, which fills the trench faster than these sediments can be subducted or accreted to the continental margin. Other factors which influence the trench depth are the convergence rate and the plate age (Grellet and Dubois, 1982). When all convergence zones are considered, the maximum trench relief is observed to increase with the log of the lithospheric age. For a given subduction zone, an increase in the subduction rate corresponds to a deepening of the trench. In the Cascades

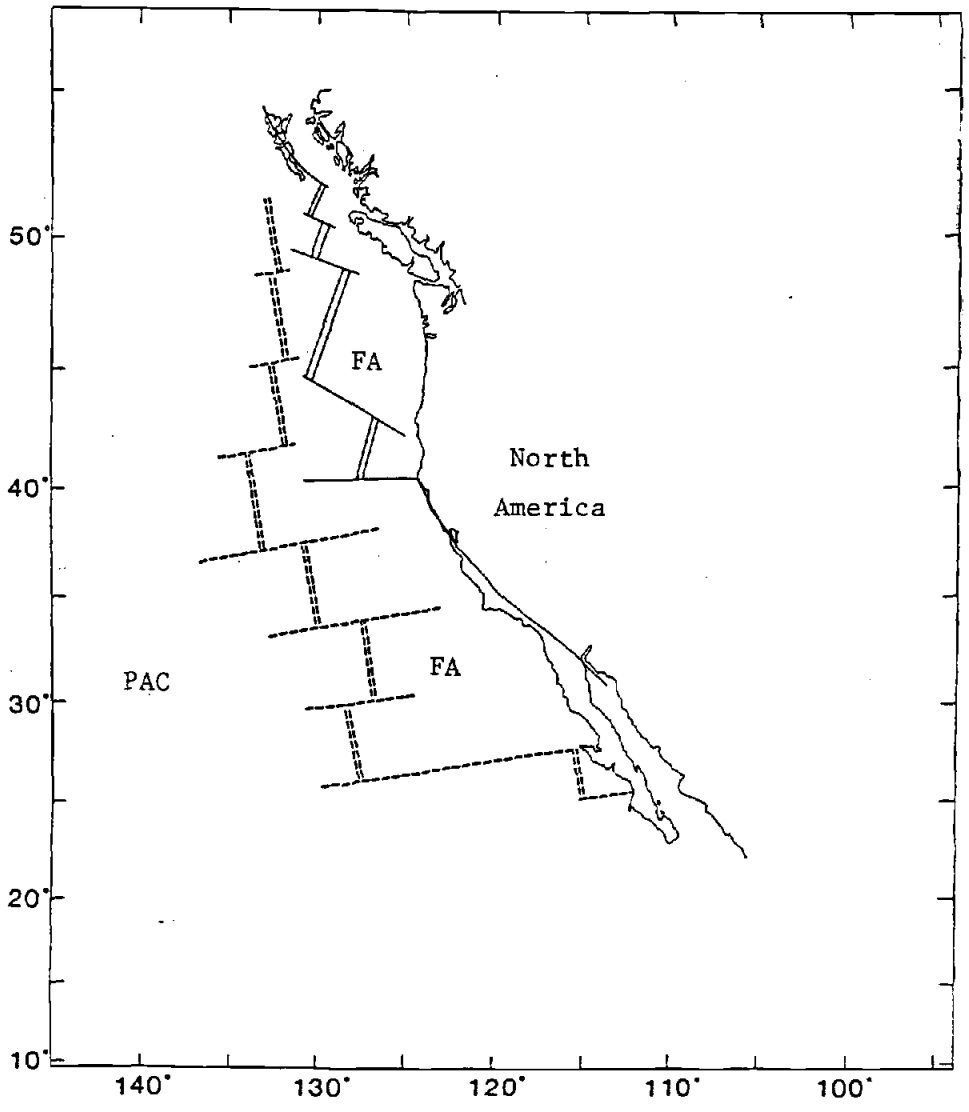

Figure II-2 - Plate boundaries off the coast of North America at 40 m.y. (dashed lines) and at present (solid lines). Double lines are spreading ridges and single lines are fracture zones. From Duncan and McElwee(1984). FA=Farallon plate, PAC=Pacific plate.

convergence zone, the subducting Juan de Fuca plate is both young (11 m.y.) and has a slow subduction rate (normal component 1.4 cm/yr), therefore a minimal trench depth is to be expected.

With changing rates of plate convergence, the amounts of sediment which subducted with the Farallon (ancestral Juan de Fuca) plate may have varied. Sediment contamination is revealed in arc magma geochemical characteristics, e.g. %SiO2, 87Sr/86Sr, 143Nd/144Nd and Pb isotopic ratios (Karig and Kay, 1981; White and Patchett, 1984). Therefore, convergence rates may be a controlling factor in arc magma compositions, as a result of variations in the amount of sediment cover transported to depths of magma genesis.

The first phase of study is to calculate the convergence direction and rate between the Farallon and North American plates during Tertiary time. This model enables correlations to be drawn between changes in the plate convergence pattern and temporal variations in erupted volumes and geochemical character of the volcanism. The convergence model is based on two major assumptions: 1) that hotspots in the Atlantic and Pacific basins have remained fixed with respect to each other and 2) that symmetrical spreading occured along the ocean ridge separating the Farallon and Pacific oceanic plates. The former assumption has been tested by numerous previous workers, (Burke et al., 1973; Molnar and Atwater, 1973; Minster et al., 1974; Molnar and Francheteau, 1975; Minster and Jordan, 1978; Morgan, 1981; Duncan, 1981), the two most recent of which conclude that hotspots move less than 0.5 cm/yr with respect to one another. This is about one order of magnitude less than the absolute plate motions, and therefore is considered an insignificant

amount of interhotspot movement.

The second assumption is necessary because most of the Farallon plate, all that is older than 11 m.y. (polarity chron 5), has been subducted beneath North America. Therefore, the only record of the spreading rate, prior to late Miocene time, is the magnetic anomaly pattern on the Pacific plate. Symmetrical spreading is most likely a valid assumption because it has been observed in the last 11 m.y. at the Juan de Fuca-Pacific ridge south of the Sovanco Fracture Zone (Riddihough, 1977). There is no method possible to prove or disprove this assumption prior to polarity chron 5, however, because the evidence has been subducted. Medium to fast spreading ridges elsewhere have been observed to be symmetric.

The methods of the convergence calculations can be described in three steps (Figure II-3). First, the absolute motion of the Pacific and North American plates is determined from the reference frame of hotspots which are fixed with respect to the mantle. The presence of fixed hotspots (stationary thermal anomalies originating in a convecting mantle) was proposed by Carey(1958), Wilson(1963), and Morgan(1971, 1972). In this model, the linear volcanic features on the ocean floor, such as the Hawaiian Ridge and Emperor Seamounts, are a result of the movement of the Pacific oceanic plate over a hotspot (now under the island of Hawaii and Loihi Seamount). Geochronological data and the geographic distribution of these numerous oceanic ridge lineaments have enabled the calculations of Pacific and North American plate motions relative to fixed hotspots in the mantle (Duncan and Clague, 1984; Duncan, 1984).

Once the Pacific and North American plates absolute motion is

a)

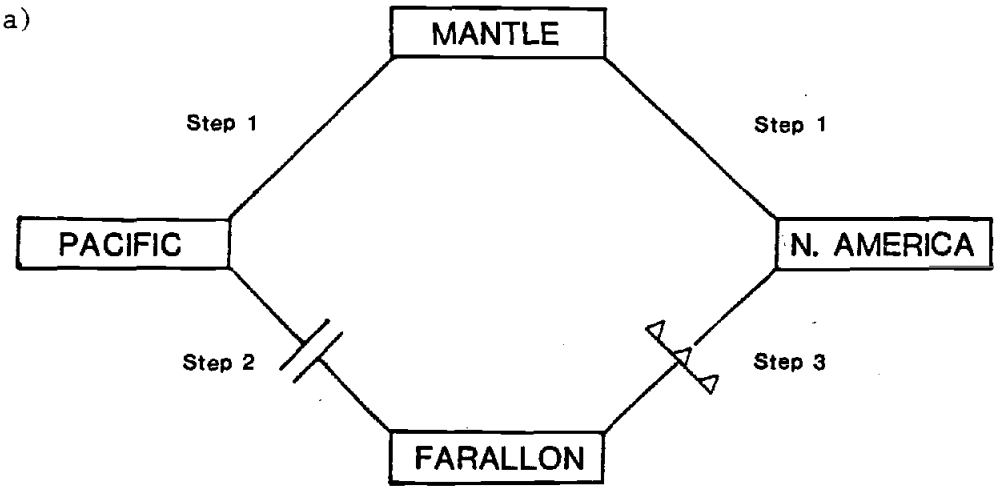

b)

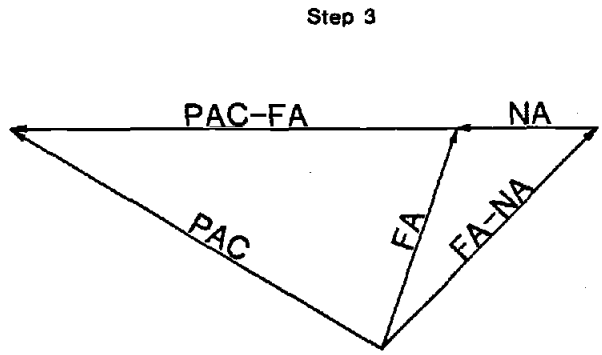

Figure II-3 - a) Diagram illustrating the model of convergence between the Farallon and North American plates.

b) Vector diagram of plate motions. PAC=Pacific, FA=Farallon, NA=North America. PAC-FA=motion of the Pacific plate relative to the Farallon plate, FA-NA=motion of the Farallon plate relative to the North American plate.

determined, the second step is to establish the motion of the Farallon plate relative to the Pacific plate. The magnetic lineations on the Pacific and Juan de Fuca plates (Atwater and Menard, 1970; Riddihough, 1977) are used in conjunction with the magnetic polarity time scale (Harland et al., 1982) to determine the Farallon-Pacific spreading rate and direction. The third step is to add the Farallon-Pacific relative motion to the Pacific absolute motion - their sum is the absolute Farallon motion. The North American absolute motion is added to the absolute Farallon motion; their resultant is the Farallon-North American convergence vector.

DETAILS OF THE MODELING

Farallon-Pacific Relative Motion

The first step, as mentioned above, is to establish the absolute motion of the Pacific and North American plates relative to the mantle-fixed hotspot reference frame. This has been accurately determined by Duncan and Clague(1984) for the Pacific, and by Duncan (1984) for North America, for Tertiary time. The second step is to calculate Farallon-Pacific relative motion. All of the calculations for the relative motion of the Farallon and Pacific plates are based on the northeast Pacific and Juan de Fuca plates magnetic lineations maps by Atwater and Menard(1970) and Riddihough(1977), (Figure II-4). First, the distances between each magnetic lineation were measured for each of the areas confined by fracture zones. For example, the distance between magnetic anomaly 6 and 6A is 0.5

a)

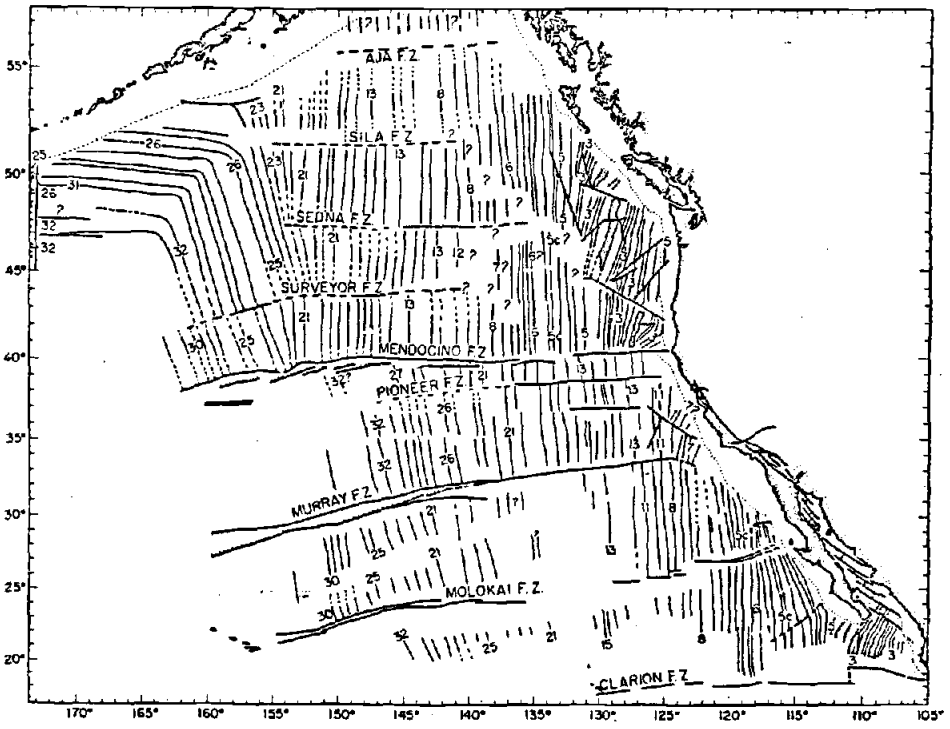

b)

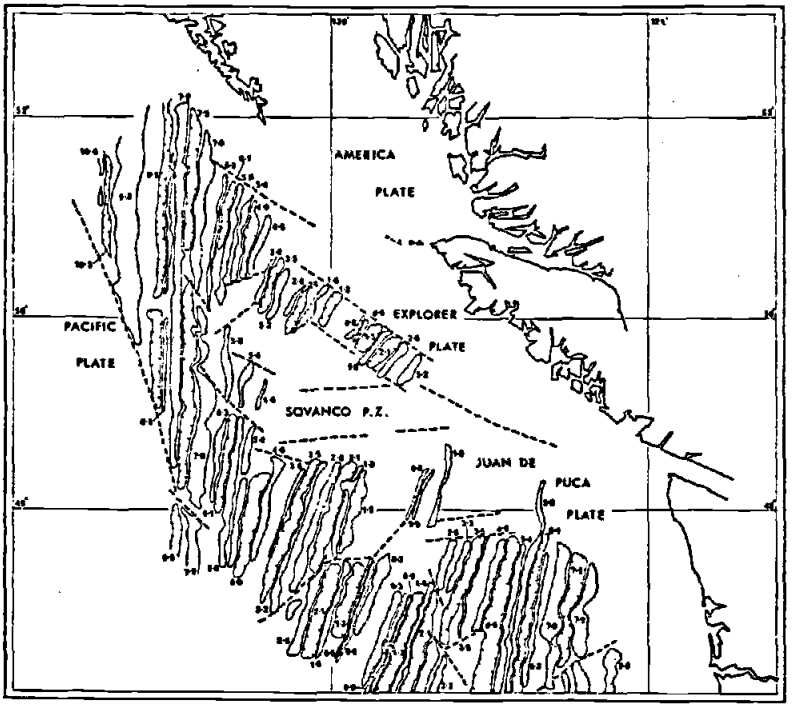

Figure II-4 - a) Magnetic anomalies in the northeast Pacific. From Atwater and Menard(1970).
b) Magnetic anomalies off Washington and Vancouver, B.C. Dates are in m.y., shaded-positive, hachured-negative. From Riddihough(1977).

degrees longitude between Aja and Sila fracture zones, 0.6 degrees longitude between Sila and Sedna fracture zones, 0.3 degrees longitude between Sedna and Surveyor fracture zones, etc. The velocity for each interval is simply the distance divided by the time between magnetic lineations. All the velocities calculated for each magnetic anomaly time interval were plotted versus time for 76 m.y. to present, or magnetic lineations 33 to 1 (Harland et al., 1982).

Time intervals of relatively constant velocity (five are chosen) were isolated and the best fitting stage pole of rotation for each was determined. The expected relation between the linear velocity, v, and the angular distance to the stage pole, Θ, is a sine function, where the maximum velocity is at a distance of $\Theta=90$, (Figure II-5). Several "trial" stage poles are used to plot v versus Θ for a given time interval. Each curve represents a different "trial" stage pole. The one which most closely fitted the velocity data to a sine function was chosen as the correct stage pole. Five stage poles of Tertiary relative motion between the Farallon and Pacific plates were selected and are listed in Table II-1.

An average velocity for more closely spaced time intervals were selected (seventeen were chosen), and the angular velocity, ω, was calculated for each ($\omega=v/\sin\Theta$). The amount of rotation (α) is ω(degrees/m.y.) X t(m.y.). Table II-1 lists the relative stage poles (latitude, longitude) and angle of rotation (α) for the Farallon-Pacific plate relative motion for several time intervals during Tertiary time.

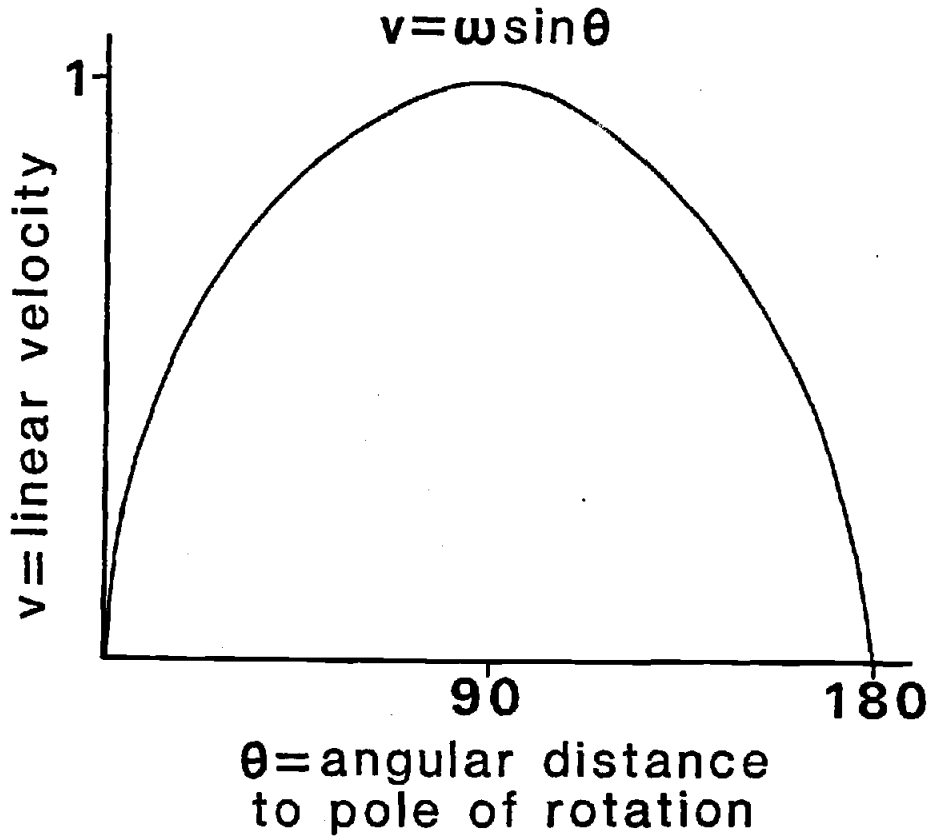

Figure II-5 - Graph of V(linear velocity) vs. θ(angular distance to the pole of rotation). ω = angular velocity.

Table II-1

PACIFIC-FARALLON RELATIVE MOTION

TIME M.Y.		STAGE POLES LATITUDE	LONGITUDE	ROTATION DEGREES
2	0	2.0	-133.0	-3.48
6	2	2.0	-133.0	-4.82
10	6	2.0	-133.0	-8.30
14	10	-10.0	-132.5	-2.16
15	14	-10.0	-132.5	-1.02
19	15	-10.0	-132.5	-3.30
20	19	-10.0	-132.5	-1.02
24	20	-52.5	-137.0	-3.58
26	24	-52.5	-137.0	-1.04
37	26	-52.5	-137.0	-9.78
39	37	85.0	40.0	4.40
42	39	85.0	40.0	5.05
48	42	85.0	40.0	6.46
52	48	76.0	161.0	3.55
56	52	76.0	161.0	3.55
71	56	76.0	161.0	10.56

Table II-2

FARALLON ABSOLUTE MOTION (CUMULATIVE)

TIME M.Y.	STAGE POLES LATITUDE	LONGITUDE	ROTATION DEGREES
5	24.55	-122.7	-8.76
10	21.2	-122.4	-19.72
15	23.3	-119.5	-24.51
20	23.1	-117.6	-30.20
25	20.4	-116.4	-33.18
30	18.5	-114.7	-36.35
35	16.4	-113.3	-39.65
40	10.99	-112.1	-40.96
45	4.17	-110.99	-41.95
50	2.38	70.52	43.45
55	8.66	73.23	44.65
60	12.9	75.98	46.40
65	16.3	78.7	48.40
70	18.6	82.9	50.79

West and south are negative, clockwise rotation is negative.

Absolute Farallon-North America Convergence Motion

This part of the modeling relies on the assumption that hotspots in the Atlantic and Pacific regions have remained fixed with respect to each other. As explained above, this is not entirely accurate but is valid for the purpose of determining plate motions across a convergent margin. All of the calculations were performed by computer programs written by W.J. Morgan, and modified by R.A. Duncan. The plate motions (both relative and absolute) were quantified in terms of stage poles and angular rotations. Spherical trigonometry was employed to add and subtract plate motions. The resultant stage poles and degrees of rotation were converted to velocity vectors in 5 m.y. intervals.

The absolute Farallon plate motion (as previously illustrated in Figure II-3) is determined by adding Farallon-Pacific plate relative motion to Pacific plate absolute motion. Table II-2 lists the stage poles and rotations, in 5 m.y. intervals. The convergence of the Farallon plate relative to North America is the difference between the absolute motions of the North American and Farallon plates. Table II-3 lists the stage poles and rotations for the convergence motions, 70 m.y. to present, in 5 m.y. intervals.

The final step is to now use the convergence stage poles of rotation to calculate velocity vectors. Cape Blanco, Oregon was chosen as the site of convergence. Its ancestral geographical coordinates, in 5 m.y. intervals, are calculated by knowing the absolute motion of North America. The convergence rate is then a straight forward calculation: $v=\omega\sin\Theta$, i.e., the angular velocity,

Table II-3

FARALLON-NORTH AMERICA CONVERGENCE

TIME M.Y.		STAGE POLES LATITUDE	LONGITUDE	ROTATION DEGREES	ANGULAR VELOCITY DEGREES/M.Y.
5	0	27.2	-90.6	-2.9	0.58
10	5	27.2	-90.6	-2.9	0.58
15	10	15.3	-87.6	-3.2	0.64
20	15	9.3	-86.7	-3.0	0.60
25	20	51.4	142.3	3.1	0.62
30	25	51.6	148.7	3.1	0.62
35	30	52.0	148.9	3.1	0.62
40	35	42.7	116.4	4.0	0.80
45	40	45.9	107.4	6.9	1.38
50	45	48.8	120.2	7.2	1.44
55	50	46.1	142.6	6.4	1.28
60	55	48.3	145.9	6.0	1.20
65	60	49.5	147.9	5.8	1.16
70	65	31.1	134.4	7.5	1.50

West and south are negative, clockwise rotation is negative.

ω, times the sine of the great circle distance between the stage pole and Cape Blanco, θ. The convergence direction is simply a vector oriented perpendicular to the great circle azimuth.

CONVERGENCE MODEL RESULTS

Figure II-6 illustrates the results of the convergence model in terms of vectors whose length indicate the rate and whose azimuth is the direction of convergence between the Farallon and North American plates at Cape Blanco. Each vector is an average over a 5 m.y. interval and the number beside each vector indicates the beginning of the time interval. It is apparent that the convergence has always been to the northeast during the Tertiary with a variable component of northward translation. There has been a drastic decrease in convergence rate, however, from 16.5 cm/yr at 70 m.y. to the present rate of 3.4 cm/yr. The decrease occurs relatively continuously with time except for a more sudden decrease at 40 m.y. This significant decrease in rate is partly a result of the change in Pacific plate absolute motion recorded by the Emperor Seamounts and Hawaiian Ridge intersection at 43 m.y. (Clague et al., 1975). Perhaps not coincidently, this is also the time of the Coast Range accretion (Duncan, 1982; Heller and Ryberg, 1983) and the initiation of Western Cascades volcanic activity. Figure II-7 illustrates the percent change in rate versus time, in 5 m.y. intervals. Most of the changes are negative or only slightly positive, except for between 60 and 45 m.y. where a small increase occurs.

Engebretson(1982) and Jurdy(1984) have also modeled the

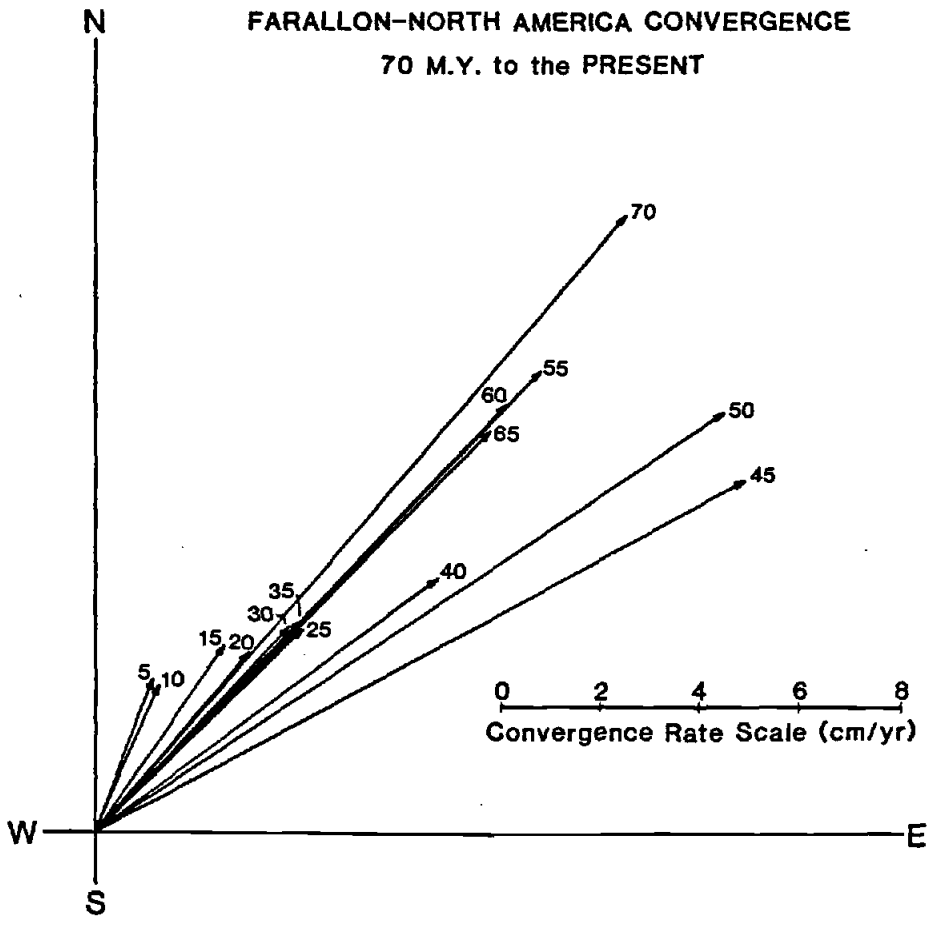

Figure II-6 - Farallon-North America convergence model. The vectors indicate the rate and direction of convergence between the Farallon and North American plates at Cape Blanco, Oregon during the Tertiary. The number beside each vector indicates the beginning of a 5 m.y. time interval.

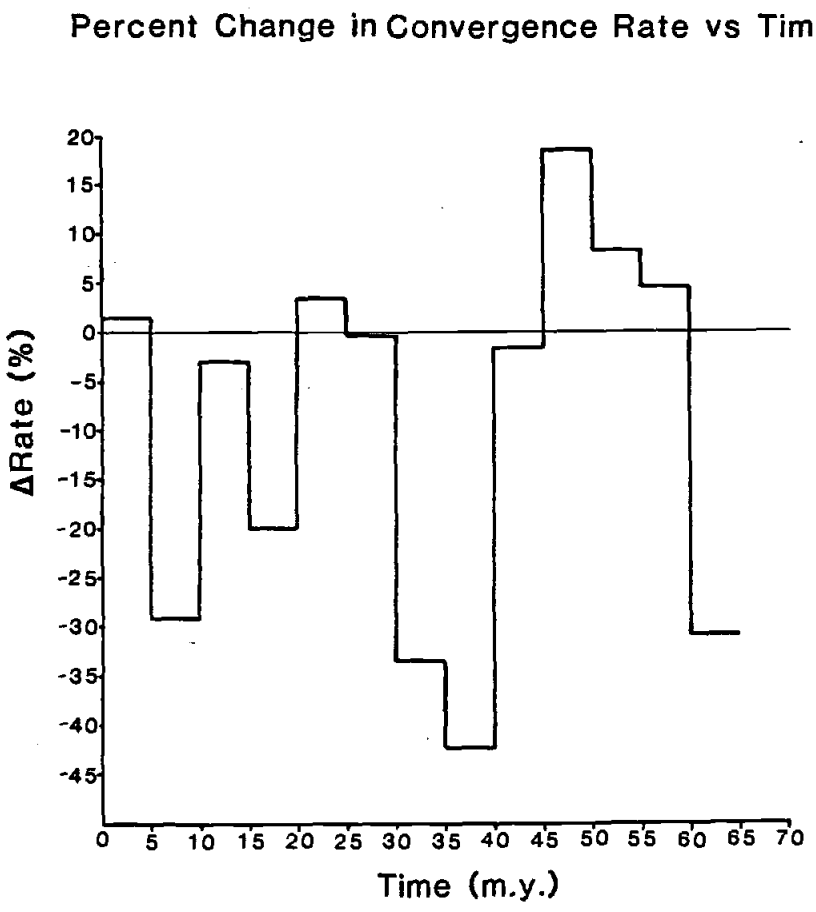

Figure II-7 - The percent change in convergence rate vs. time for the Farallon and North American plates.

convergence of the Farallon plate and North America during Tertiary time. Engebretson's calculations are also based on the absolute reference frame (mantle-fixed hotspots). Jurdy's model was derived by adding the relative plate motions in a circuit through Antarctica (i.e. NOAM-AFRI-ANTA-PCFC-FARA = NOAM-FARA), therefore she does not rely on the hotspot reference frame. Both of their results are similar to those above and are compared in Figure II-8. The normal component of convergence near present-day San Francisco (Engebretson's model) and near present-day Cape Blanco (this study) are quite comparable.

Engebretson(1982) also included an age estimate of the Farallon plate that was descending beneath North America at the latitude of San Francisco through Tertiary time (Figure II-8). The Farallon-Pacific spreading ridge has remained close to the western edge of North America during the time period of Cascades volcanic arc development (as illustrated above, Figure II-2). Therefore, the age of the descending plate has always been relatively young, between about 20 and 10 m.y. age.

The direction of convergence between the Farallon and North American plates during Tertiary time has an average azimuth of N45^{o}E. Since 40 m.y. ago, however, the 5 m.y. interval convergence vectors have rotated progressively in a counterclockwise direction from N53^{o}E to N20^{o}E. At the same time, the Oregon Coast Range and Western Cascade Range have rotated in a clockwise manner, thereby increasing the obliquity of convergence motion with time. Paleomagnetic data from the Oregon Coast Range indicate 51^{o} clockwise rotation since 37 m.y. ago (Simpson and Cox, 1977). The

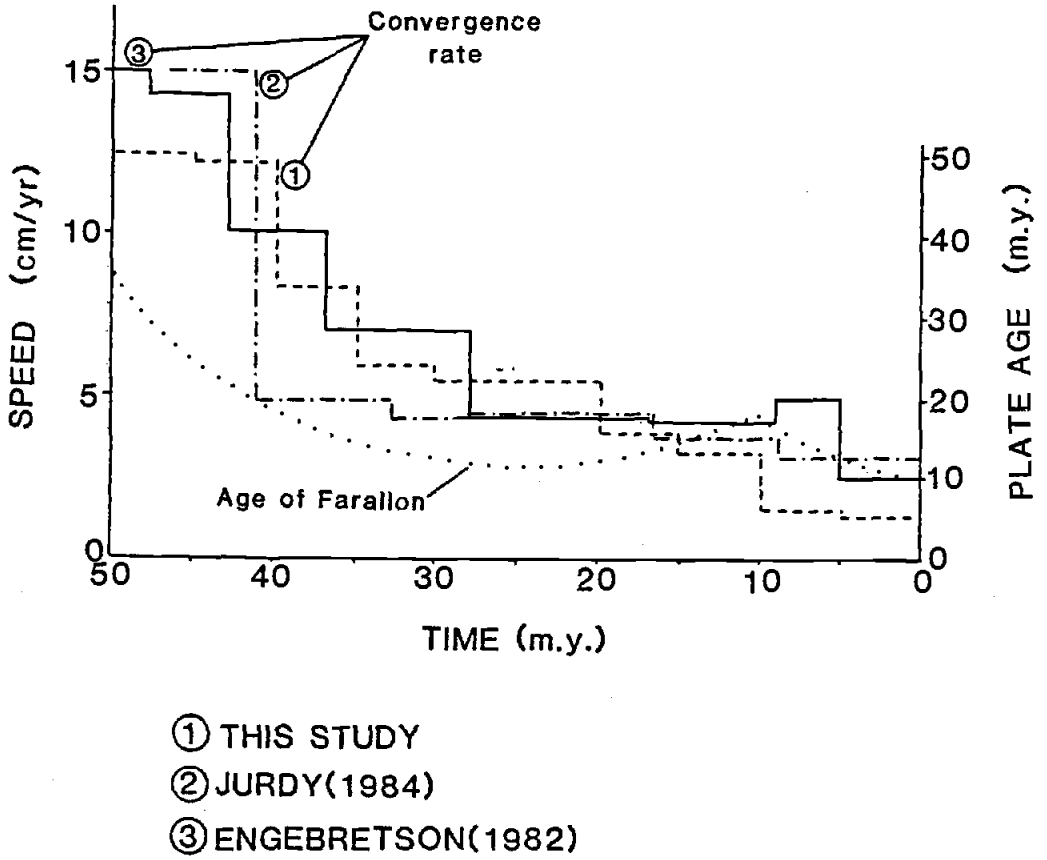

Figure II-8 - The normal component of convergence between the Farallon and North American plates since 50 m.y. 1 - This study. The model is based on the absolute reference frame and the site of convergence is Cape Blanco, Oregon. The normal component of convergence is calculated assuming the Western Cascades have rotated clockwise since 40 m.y., as determined from paleomagnetic data (see text). 2 - Jurdy(1984). The model is derived by adding the relative plate motions in a circuit through Antarctica. 3 - Engebretson(1982). The model is based on the absolute reference frame and the site of convergence is San Francisco, California. The age of the Farallon plate at the subduction zone is also shown (dotted line) from 50 m.y. to the present.
The three methods give similar results and all indicate a decrease in the convergence rate with time.

Western Cascades have also been rotated clockwise, 25° since 25 m.y. ago (Magill and Cox, 1980). If one assumes the Cascades and Coast Range have rotated together since the accretion of the latter at about 42 m.y., then the orientation of the subduction zone associated with Cascades volcanism can be reconstructed. Figure II-9 illustrates the changes in both the convergence motion and the subduction zone orientation with time, in 5 m.y. intervals, since 40 m.y. ago. Prior to 40 m.y. and the Coast Range accretion, the orientation of the northwestern margin of the United States is not well enough constrained to make predictions of the convergence angle.

In conclusion, the rate and orthogonal component of convergence motion between the Farallon and North American plates has decreased during the evolution of the Western Cascades volcanic arc. The orthogonal rate has decreased by a factor of five, from 8.45 to 1.60 cm/yr, and the angle of convergence has decreased by two-thirds, from 90° to 30°, between 40 and 10 m.y. ago. The next step is to compare this quantitative convergence model to temporal variations in volume and geochemistry of volcanism in the Western Cascades.

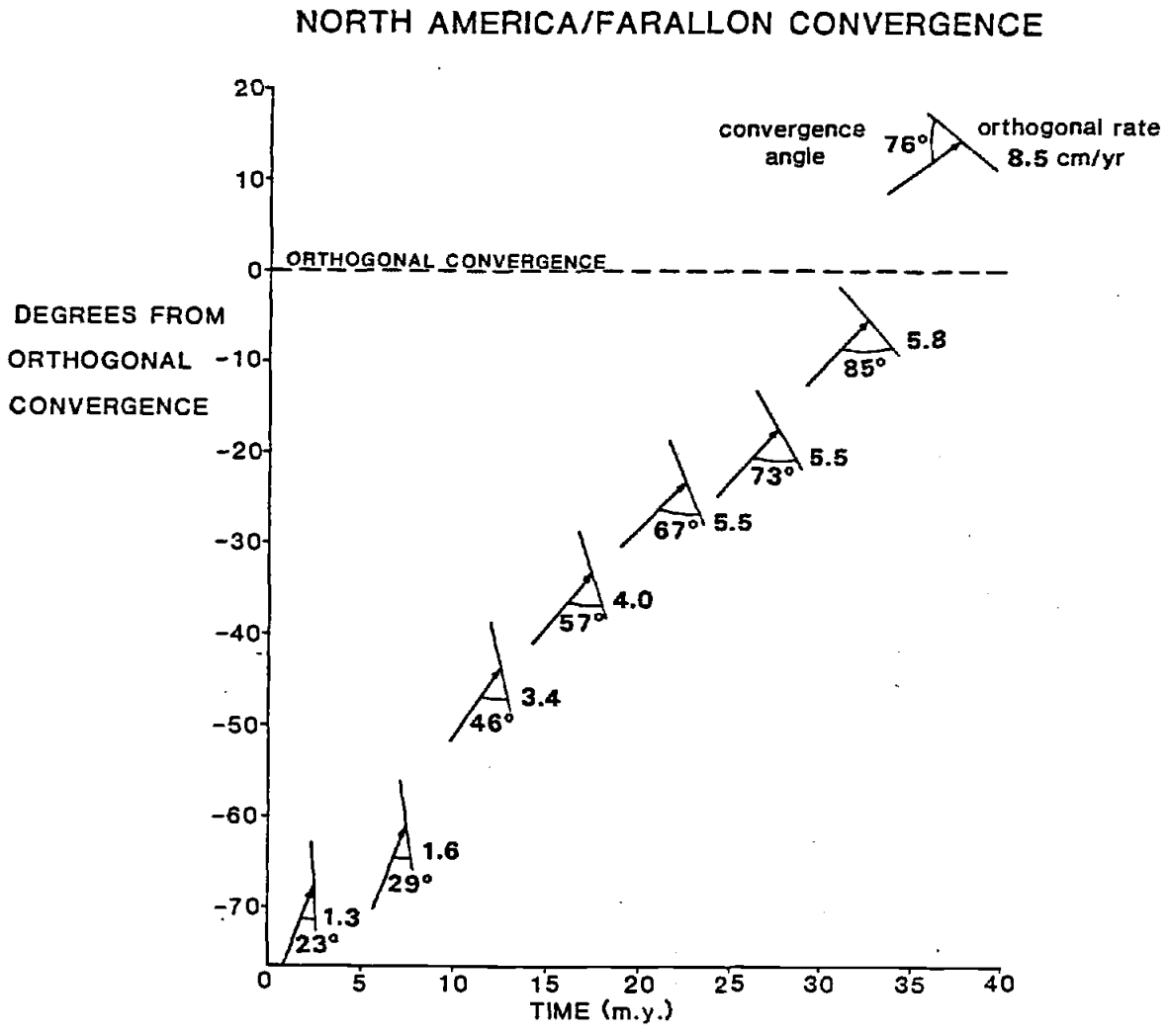

Figure II-9 - The change in the convergence motion between the Farallon and North American plates since 40 m.y. The vectors indicate the direction of convergence and the lines illustrate the orientation of the continental margin as deduced from paleomagnetic data from the Coast Range and Western Cascades. The numbers on the right are the orthogonal rates of convergence (cm/yr) and those on the left are the convergence angle. The convergence has become increasingly oblique with time since about 35 m.y.

CHAPTER III: GEOCHRONOLOGY

INTRODUCTION

The main objective of the geochronological study is to estimate eruption rates in the Western Cascades volcanic arc and to determine if the changes in subduction rate (described in the preceding chapter) influence the amount of volcanic activity. Wells et al.(1984) suggested that changes in the character of volcanism in the Cascades correlates with the decrease in Farallon-North America convergence rate. There are obviously other factors besides subduction rate which affect the volume of volcanic material erupted in the asssociated arc: the age of the subducting lithosphere and its volatile content, the percent of sediment which is subducted, the dip angle of subduction, and the thickness of overlying continental lithosphere. Therefore, while it is impossible to isolate one variable, such as the convergence rate, the Cascades volcanic arc is an excellent site to most nearly approach the isolation of convergence rate as a controlling factor for the following reasons. The age of the downgoing slab has remained young, between 20 and 10 m.y. (Engebretson, 1982), during the time of Western Cascade development, and the dip and depth of melting on the Benioff zone is apparently dependent on convergence rate and age of the subducted slab (Abbott and Hoffman, 1984). The amount of sediment which is subducted or accreted is dependent on the convergence rate and the subduction angle (Cloos, 1984). Ganoe and Fehler(1984) have estimated the present crustal thickness beneath

the Cascades from seismic data. It increases eastward from 22 km west to 37 km east of the Cascades, but was presumably slightly thinner during the time of Western Cascade development because there was less volcanic material in the arc. Convergence rate, therefore, appears to be the controlling factor on eruption rates in the Western Cascades because the other factors have remained more or less constant or are also dependent upon the convergence rate.

Two other objectives of the geochronological work are to 1) determine the spatial variation of ages in the Western Cascades volcanic stratigraphy, and to 2) determine whether the volcanic activity has been episodic or continuous during the past 42 m.y. The field work and K-Ar analytical methods are described first, followed by the results and conclusions from the age distribution study.

FIELD WORK

The field work for this study was done in collaboration with researchers from the U.S. Geological Survey. Samples were collected during the 1983 and 1984 field seasons. George W. Walker and Norman MacLeod, geologists from the U.S.G.S., spent the summers of 1980 to 1984 in the Western Cascades of Oregon working on a reconnaissance mapping program of the Salem and Roseburg 1:250,000 sheets. The present investigation was planned to complement their mapping by providing K-Ar age determinations on critical lava flows and ash flow tuffs. Forty-four K-Ar age determinations were performed on the samples collected during the 1980 to 1984 field seasons with the guidance of the U.S.G.S. and R.A. Duncan, O.S.U. College of

Oceanography. Five additional samples were collected for K-Ar age analysis by R.A. Duncan and the author in the 1984 field season. The sample names that begin with GWW and M were collected with guidance from G.W. Walker and N. MacLeod, respectively. Those samples beginning with P were collected by R.A. Duncan and the author. We thus have a total of 51 new K-Ar age analyses from the central Western Cascades in Oregon. When combined with the age determinations of Lux(1981, 1982), Sutter(1978), Hammond(1979), Priest and Vogt(1983), and summarized by Fiebelkorn et al.(1983), there are now over 150 K-Ar age determinations of volcanic rocks from the Western Cascades of Oregon.

All of our samples are found between 42° and 44° north latitude and 122° and 123° west longitude, on the Salem and Roseburg 2-degree quadrangles. The regional volcanic stratigraphy dips gently eastward, ranging from 3° to 10°E. The attitude of most of the younger lavas (<15 m.y.) is approximately horizontal (Walker, personal comm., 1984). The types of outcrops sampled include roadcuts, active and abandoned quarries, stream cuts, and ridge capping lavas. Fresh outcrops were not always obtainable because the terrain is deeply dissected, eroded and extensively vegetated. Intrusive rocks were avoided because of their uncertain stratigraphic relation with the lavas and ash flow tuffs. With the guidance of Walker and MacLeod, we were able to sample over 60 fresh-appearing rocks from critical stratigraphic horizons.

Most of the rock specimens are basalt or basaltic andesite lava flows, except for a few ash flow tuff samples of dacitic or rhyodacitic composition. Almost all of the basalts and basaltic

andesites are plagioclase phyric, and some also contain clinopyroxene phenocrysts. A few of the samples have olivine phenocrysts, most of which have been replaced by iddingsite or clay alteration products. Opaque minerals, such as magnetite and ilmenite are relatively abundant (up to 10% modal abundance) in many of the samples.

Thin sections were made of all samples considered for age determinations and geochemical studies. The K-Ar dating method requires that all radiogenic 40Ar, produced by the decay of 40K, be retained within the crystal lattices of the minerals. Alteration or devitrification are signs of probable argon loss and will result in lowering the K-Ar age. Therefore, petrographic examination was used to select fresh samples. A small percentage of the samples were rejected after this process. Four ash flow tuffs were selected for mineral separation (plagioclase) and one for glass separation prior to age determination. The remainder were chosen for whole rock K-Ar age analyses. (See Appendix B for petrographic descriptions.)

ANALYTICAL METHODS

Conventional K-Ar techniques (Dalrymple and Lanphere, 1968) were employed to determine ages for the 51 samples from the central Western Cascades in Oregon: 46 were whole rock, 4 were plagioclase separates, and one was a glass separate. The rock samples were sawed to remove the weathered surfaces, and then crushed to 0.84-2.00 mm size fraction. The crushed samples were washed in distilled water, dried, and split into two aliquots: one was used

for Ar-analysis and the other was powdered and used for K-analysis. A heavy liquid mineral separation technique was used for the plagioclase separates. The glass separate was picked by hand from the crushed fraction using a microscope to select the freshest pieces. K concentrations were measured with an atomic absorption spectrophotometer, described in the geochemistry chapter. Argon isotope concentrations were measured by means of 38Ar isotope dilution with an AEI-MS10 mass spectrometer equipped with two in-line high vacuum extraction systems. The samples were weighed, placed in molybdenum crucibles and fused by an external induction heater. The radio frequency field from the induction heater coil induces a current flow in the crucible which is thus heated. The 36Ar, 38Ar, and 40Ar peaks were read by hand off a recording chart and peak heights were regressed to the time of sample introduction to the mass spectrometer to obtain isotope ratios. Absolute abundances of 40Ar were determined by pipetting a known amount of 38Ar into the extraction line during sample fusion. (See appendix A for K-Ar radiometric age determination equation and values of decay and abundance constants used in the calculations.)

RESULTS

Fifty-four K-Ar age determinations are listed in Table III-1, (three of the fifty-one samples were repeated). The sample locations begin with the one farthest north and proceed southwards. The four plagioclase and one glass separates are noted, in parentheses, beside the calculated age. All the other samples are whole rocks.

Table III-1 K-AR AGE DETERMINATIONS

SAMPLE NO.	LOCATION	K(WT%)	Rad. ^{40}Ar $\times 10^{-6}$ (cc/g)	Rad. %^{40}Ar	Age $\pm\sigma$ ($\times 10^{6}$ m.y.)
	SALEM QUADRANGLE				
GWW-113-83	SE/4,NE/4,S25;T 9S,R3E	1.41	.1298	60.89	23.5 ±0.3
GWW-104-83	SW/4,S28;T 9S,R4E	1.40	.6815	42.29	12.5 ±0.2
P84-65	NE/4,SE/4,S 5;T10S,R1E	.540	.4808	77.17	22.8 ±0.3
GWW-102-83	NW/4,S21;T10S,R3E	.74	.9110	65.05	31.4 ±1.8
		.74	.3723	64.52	12.9 ±0.2
GWW-73-83	NW/4,S22;T10S,R2E	.465	.5188	82.96	28.5 ±0.4
GWW-67-83	cE/2,S24;T10S,R1W	1.46	.7973	84.09	14.0 ±0.2
GWW-99-83	NW/4,NW/4,S27;T10S,R4E	.59	.3634	29.27	15.8 ±0.3
GWW-32-83	NE/4,S15;T11S,R2E	.22	.0235	23.23	2.7 ±0.1
		.22		30.3	3.3 ±0.6
GWW-28-83	NW/4,SE/4,S35;T11S,R1E	.795	.7012	81.92	22.6 ±0.3
GWW-42-83	S/2,NE/4,S11;T12S,R4E	.595	.1456	44.97	6.3 ±0.1
GWW-15-83	NW/4,S13;T12S,R2W	1.065	1.3241	83.35	31.7 ±0.4
GWW-24-83	NE/4,S29;T12S,R2E	.26	.3202	45.41	32.1 ±0.9*
GWW-21-83	NE/4,SW/4,S 3;T13S,R1E	.375	.3336	66.22	22.8 ±0.4
GWW-10-83	SW/4,S18;T13S,R2W	.61	.2826	22.89	11.9 ±0.3
P84-1	SE/4,SW/4,S16;T13S,R1E	.965	.1693	8.49	4.51±0.28
P84-2	NW/4,NW/4,S20;T13S,R3E	.607	.4705	84.71	19.8 ±0.2
P84-3	NE/4,SW/4,S29;T13S,R3E	.992	.7441	38.13	19.2 ±0.3
GWW-82-45	E/2,SE/4,S15;T14S,R1W	.376	.4592	87.27	31.2 ±0.3
GWW-82-43	NE/4,SE/4,S35;T14S,R1E	.162	.1378	34.70	21.8 ±0.3
GWW-82-41	NE/4,S 2;T15S,R1E	.469	.4370	28.20	23.8 ±0.3
P84-6	NW/4,SE/4,S12;T15S,R1E	.556	.5080	72.40	23.4 ±0.4
GWW-81-141	NW/4,S23;T16S,R1W	.279	.2856	68.89	26.2 ±0.3
GWW-82-22	NW/4,S19;T16S,R1E	.381	.4195	51.40	28.1 ±0.3
GWW-111-81	NW/4,S17;T17S,R2W	.369	.4473	77.45	31.0 ±0.4*
GWW-191-81	NW/4,S13;T17S,R1W	.172	.1572	59.85	23.4 ±0.3
GWW-56-81	NW/4,S17;T17S,R1E	.251	.2601	50.10	26.5 ±0.3
GWW-175-81	SW/4,S21;T17S,R2E	.984	.5359	54.34	14.0 ±0.2
GWW-76-81	NE/4,NW/4,S30;T17S,R1W	.361	.4091	50.45	28.9 ±0.3
GWW-87-81	NW/4,S31;T17S,R5E	1.344	.5428	41.63	10.4 ±0.1
GWW-114-81	SW/4,S 1;T18S,R4E	1.925	.5821	71.22	7.7 ±0.1
GWW-81-158	W/2,NW/4,S15;T18S,R3E	.39	.3231	67.49	21.2 ±0.3*
		.39	.3573	82.06	23.4 ±0.3*

Table III-1 (continued)

SAMPLE NO.	LOCATION	K(WT%)	Rad. ^{40}Ar $\times 10^{-6}$ (cc/g)	Rad. %^{40}Ar	Age $\pm\sigma$ ($\times 10^{6}$ m.y.)
	ROSEBURG QUADRANGLE				
M3-30	SW/4,S20;T19S,R2E	2.17	1.8241	70.77	21.5 $\pm$0.3
M3-29	NW/4,NW/4,S30;T19S,R3E	.765	.2154	55.61	7.2 $\pm$0.2
M3-25	W/2,S17/18;T21S,R2E	.66	.5108	29.40	19.8 $\pm$0.4
M2-25	SW/4,S29;T21S,R1E	.18	.1740	16.35	24.7 $\pm$1.0
M3-26	NE/4,S29;T23S,R4E	.71	.3410	83.88	12.4 $\pm$0.1
M2-24	NE/4,S36;T23S,R2E	.48	.4418	57.76	23.5 $\pm$0.5
M3-34	NE/4,SW/4,S24;T25S,R3E	.545	.1953	19.08	9.2 $\pm$4.1
		.545	.3227	63.1	15.5 $\pm$0.3
M2-23	SW/4,SE/4,S23;T25S,R2E	1.24	.9764	28.41	20.2 $\pm$0.4
M2-17	cS/2,S 1;T26S,R3W	.43	.4804	16.92	28.5 $\pm$0.8
M3-32	NE/4,NE/4,S10;T26S,R1W	1.50	1.1944	34.89	20.4 $\pm$0.4
		1.50	1.0311	28.73	18.0 $\pm$0.3
M2-22	SE/4,S7;T26S,R1E	.71	.7465	32.05	26.9 $\pm$0.5
M3-31	SW/4,NW/4,S17;T26S,R1W	.955	.4542	14.43	12.2 $\pm$0.4
M3-33	NE/4,SE/4,S17;T26S,R3E	.64	.3446	14.55	13.8 $\pm$1.4
M2-19	SE/4,S30;T26S,R1W	.41	.4058	53.94	25.3 $\pm$0.3
M3-37	SE/4,NW/4,S32;T26S,R1E	.395	.3474	27.83	22.5 $\pm$0.4
M3-38	SE/4,NW/4,S12;T27S,R1W	1.305	.9460	55.57	19.0 $\pm$0.2
M3-36	NE/4,NW/4,S 6;T28S,R2E	.99	.6711	58.99	17.8 $\pm$0.2**
M3-35	SE/4,NE/4,S 9;T28S,R3E	.875	.5523	60.40	16.2 $\pm$0.2

All samples are whole rock unless otherwise noted.
*plagioclase separate
**glass separate

The K content (wt.%), abundance of radiogenic 40Ar (cc/g x 10^{-6}), percent radiogenic 40Ar, and calculated age (m.y.) $\pm 1\sigma$ analytical uncertainty are listed for each sample. The samples range from 3.0 to 32.1 m.y., but most fall between 12 and 32 m.y.. The geochronological results are used to determine: 1)spatial variations of ages in the Western Cascades, 2) the nature of the eruptive history, that is, episodic or continuous and 3) eruption rates.

Spatial Variations

The Western Cascades volcanic stratigraphy consists primarily of ash flow tuffs of dacite and rhyodacite and lava flows of basalt and basaltic andesite composition. As described in the Chapter I, the Western Cascades volcanic units are underlain by and intercalated with marine and continentally derived sediments. The regional dip is 5-10°E, except for some of the younger units (<15 m.y.) which are approximately horizontal. With a relatively continuous regional stratigraphy, it is logical to expect that the gentle eastward dip results in the oldest volcanic rocks being exposed on the western margin, with ages decreasing progressively eastward. Not surprisingly, this is what is observed in the distribution of crystallization ages in the Western Cascades. There are complicating factors, such as minor faults, folds and intracanyon flows, which disrupt the continuous stratigraphic relations, but overall the ages of the Western Cascades volcanic units decrease with increasing elevation and distance eastwards.

The spatial variations of the ages of the volcanic units are

Figure III-1 - Spatial variation of age determinations in the Western Cascades, Oregon.
Closed circles: geochronologic data from this study.
Open circles: geochronologic data from Sutter(1978), Lux(1981, 1982), Fiebelkorn et al.(1983) and Priest and Vogt(1983).
Dashed lines: isochrons of 20, 25, 30, and 35 m.y.

Figure III-1

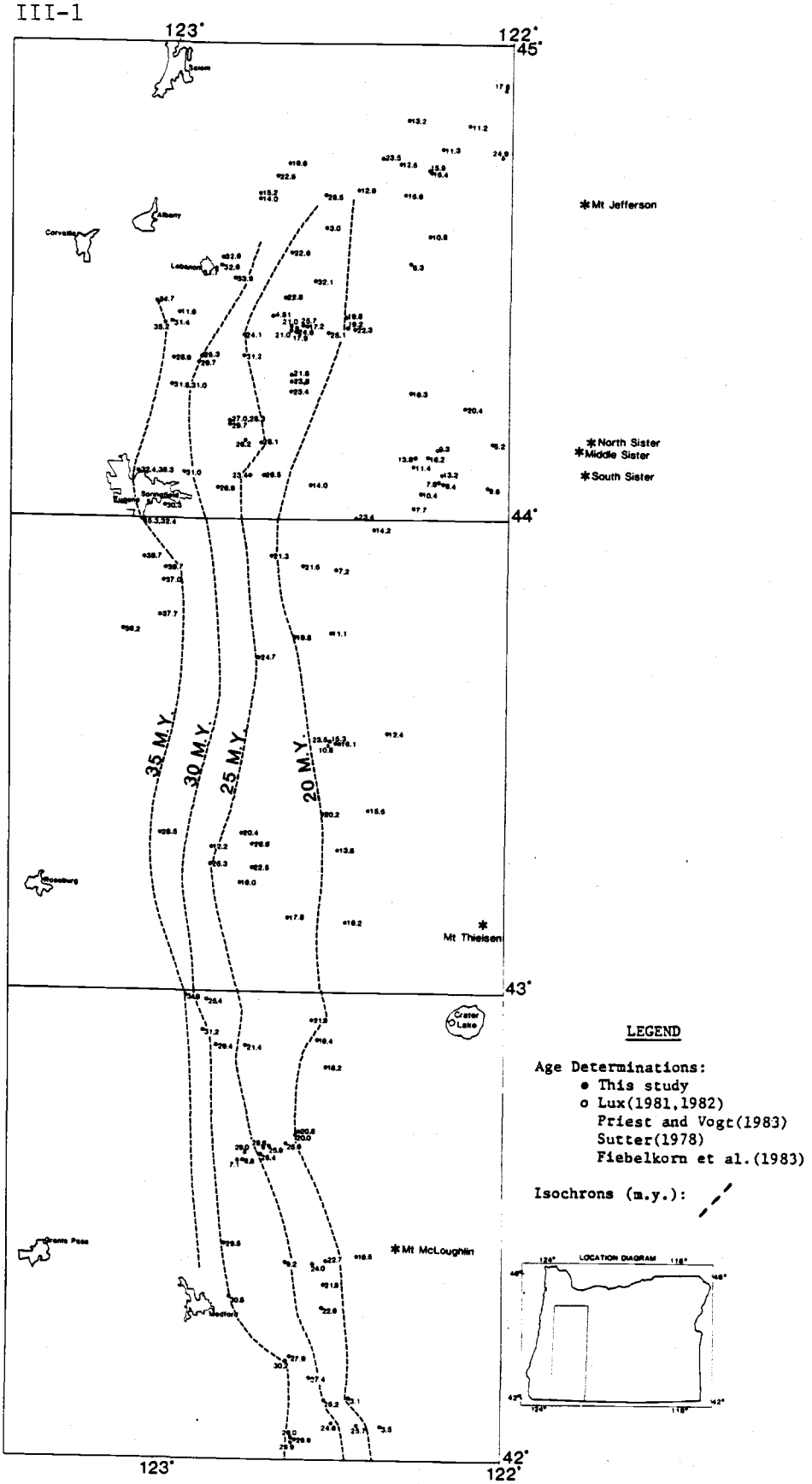
123°
122°
45°
44°
43°
42°
123°
122°
Salem
Albany
Corvallis
Lebanon
Springfield
Eugene
Roseburg
Grants Pass
Medford
Crater Lake
35 M.Y.
30 M.Y.
25 M.Y.
20 M.Y.
Mt Jefferson
North Sister
Middle Sister
South Sister
Mt Thielsen
Mt McLoughlin
LEGEND
Age Determinations:
• This study
o Lux(1981,1982)
Priest and Vogt(1983)
Sutter(1978)
Fiebelkorn et al.(1983)
Isochrons (m.y.):
LOCATION DIAGRAM

illustrated in Figure III-1. The new K-Ar age determinations are combined with reported geochronological data from the Western Cascades (Sutter, 1978; Lux 1981, 1982; Priest and Vogt, 1983; and Fiebelkorn et al., 1983). Isochrons, lines of constant age, are constructed by interpolation between dated locations. The isochrons are in 5 m.y. intervals between 35 and 20 m.y. and are oriented approximately north-south. In general, the isochrons follow the topographic contours. Where drainages are crossed (most flow east to west), the isochrons are continued straight to simplify the diagram. Otherwise, they would make a V-pattern up every drainage.

The isochrons are nearly parallel to one another. The gentle indulations are mainly a result of variations in the distance from eruptive centers. Wider areas between isochrons suggests that thicker amounts of volcanic material were deposited, assuming the volcanic stratigraphy has a constant dip. The isochrons bow out towards the west near Eugene. Further south, the isochrons are approximately straight until the area east of Grants Pass, where they squeeze closer together and move eastward. This indicates either a steepening dip or a decrease in the thickness of erupted material to the south.

Periodic or Continuous Volcanism?

McBirney et al.(1974) first proposed that a periodicity of volcanic activity in the central Oregon Cascades occurred in approximately 5 m.y. intervals and correlates with volcanic pulses in the circum-Pacific area. The volcanism was suggested to be

concentrated in 1-2 m.y. intervals, separated by periods of relative quiescence. Subsequent studies by Kennett et al.(1977), Sutter(1978), and Lux(1981,1982) also supported the theory of volcanic periodicity. Kennett et al.(1977) examined the record of explosive volcanism from ash layers in deep-sea cores and discovered evidence for widespread synchronism of volcanic activity over large regions of the Pacific Basin. Variations in the rate of plate convergence were suggested to be the cause of the observed episodicity in island-arc and continental margin volcanic activity (Scheidegger and Kulm, 1975; Kennett and Thunell, 1975; Kennett, 1982). Temporal relations between the East Pacific Rise spreading rate, hotspot volcanism, ash-accumulation and circum-Pacific volcanism during the last 4 m.y. were observed by Rea and Scheidegger(1979).

The 51 new K-Ar age determinations plus all of the reported K-Ar and 40Ar-39Ar age determinations for the volcanic rocks of the Cascades province are plotted on a histogram in Figure III-2. The results do not appear to support the theory of periodic volcanism. There are no periods of hiatus. The data indicate more or less continuous volcanic activity throughout the mid-to-late Tertiary, with some periods of more active volcanism: 13-16 m.y., 22-26 m.y. and 29-31 m.y.. Priest et al.(1983) contend that the periodicity observations could merely be the result of a sampling bias: that a relatively continuous regional volcanic history can be interpreted as episodic due to incomplete mapping and sampling, particularly in regions between volcanic centers which may exhibit age gaps in the volcanic stratigraphy.

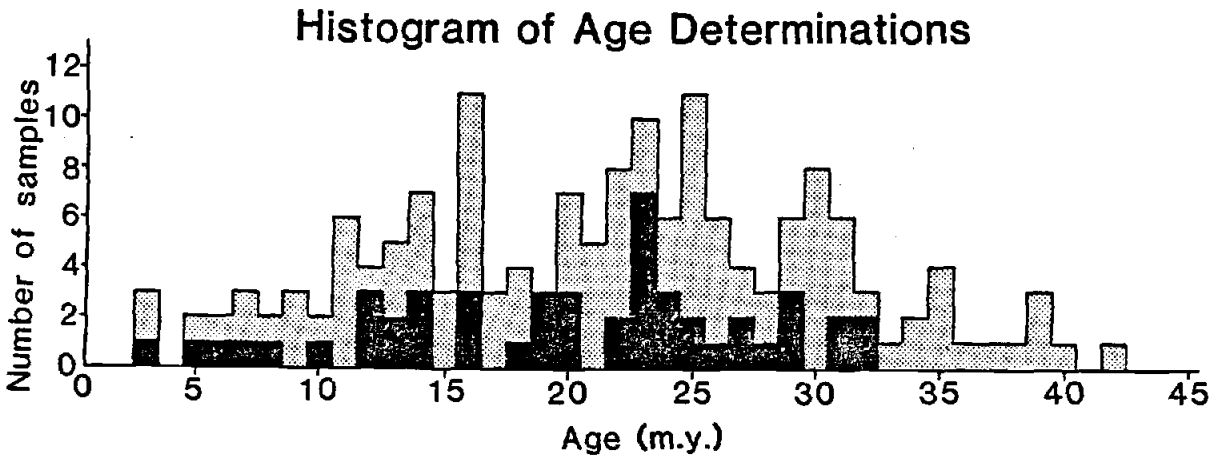

Figure III-2 - Histogram of age determinations (K-Ar and 40Ar/39Ar). Solid color: this study. Stippled pattern: Lux(1981, 1982), Priest and Vogt(1983), Sutter(1978), and Fiebelkorn et al.(1983). All data is from the Western Cascades, Oregon.

Eruption Rates: Temporal Variations

Previous workers have attempted to estimate volumes of erupted material in the younger, Quaternary-age, High Cascades volcanoes where the exposures are good and the volcanic units have been well-mapped (McBirney et al., 1974). Reasonably accurate quantitative volumetric data have been obtained; the only serious unknown factor being the amount of pyroclastic rock and erosional material removed via wind and water transport. The Western Cascades are deeply disected by drainages and extensively covered by vegetation, therefore it is difficult to estimate volumes of erupted material. Also, the volcanic material produced by the Western Cascades volcanoes is more extensive than the High Cascade lavas. Recent work by Robinson et al.(1984) suggests that, beginning about 37 m.y. ago, voluminous dacitic to andesitic air-fall material of the John Day Formation of north-central Oregon was derived from the volcanoes within the Western Cascades Range. Therefore, there is presumably Oligocene and Miocene age volcanic material underlying the High Cascades whose volume cannot be measured.

Instead of volume calculations, relative thickness estimates can be used to compare rates of volcanic activity through time. There are, however, certain assumptions which must be taken into account. First, the erosion rates are assumed to be more or less constant during the time period 40-10 m.y. Second, the variation in distances from volcanic centers is assumed to be averaged by the density and breadth of sampling. In general, proximity to a volcano

will result in thicker lava deposition. This effect can be neglected if sufficient transects are taken, thereby averaging out the variations in distances from eruption sites. Third, the relatively thin sedimentary layers are assumed to be interbedded in approximately equal proportions between the volcanic units throughout the Western Cascade stratigraphic sequence. The sediment input increases the eruption rate estimates, but the erosion of material decreases the estimates by a greater amount. Therefore, the calculated eruption rates are probably minimum estimates of the original thicknesses of volcanic material deposited with time.

In areas where the volcanic stratigraphy and structure are well understood, it is possible to use the geochronological data to construct cross-sections with isochrons (lines of constant age), (Figure III-3). The reported age of Sutter(1978), Lux(1981) and Priest and Vogt(1983), open circles, are combined with the new K-Ar age determinations, closed circles. Elevation is in meters (y-axis) and distance is degrees longitude (x-axis). The vertical exaggeration is 21:1, and the topography is diagramatically illustrated on each cross-section by the curved solid lines. Each east-west swath covers an area between 5' and 15' wide and they proceed from north at the top to south, as shown in the location map. They all lie within the study area, between 43^{o} and 45^{o} north latitude.

Ten, twenty and thirty m.y. isochrons are shown in dashed lines on each of the five swaths across the central Western Cascades. They appear to dip steeply eastward due to the vertical exaggeration but most are dipping $<5^{o}$E in accordance with the volcanic stratigraphy.

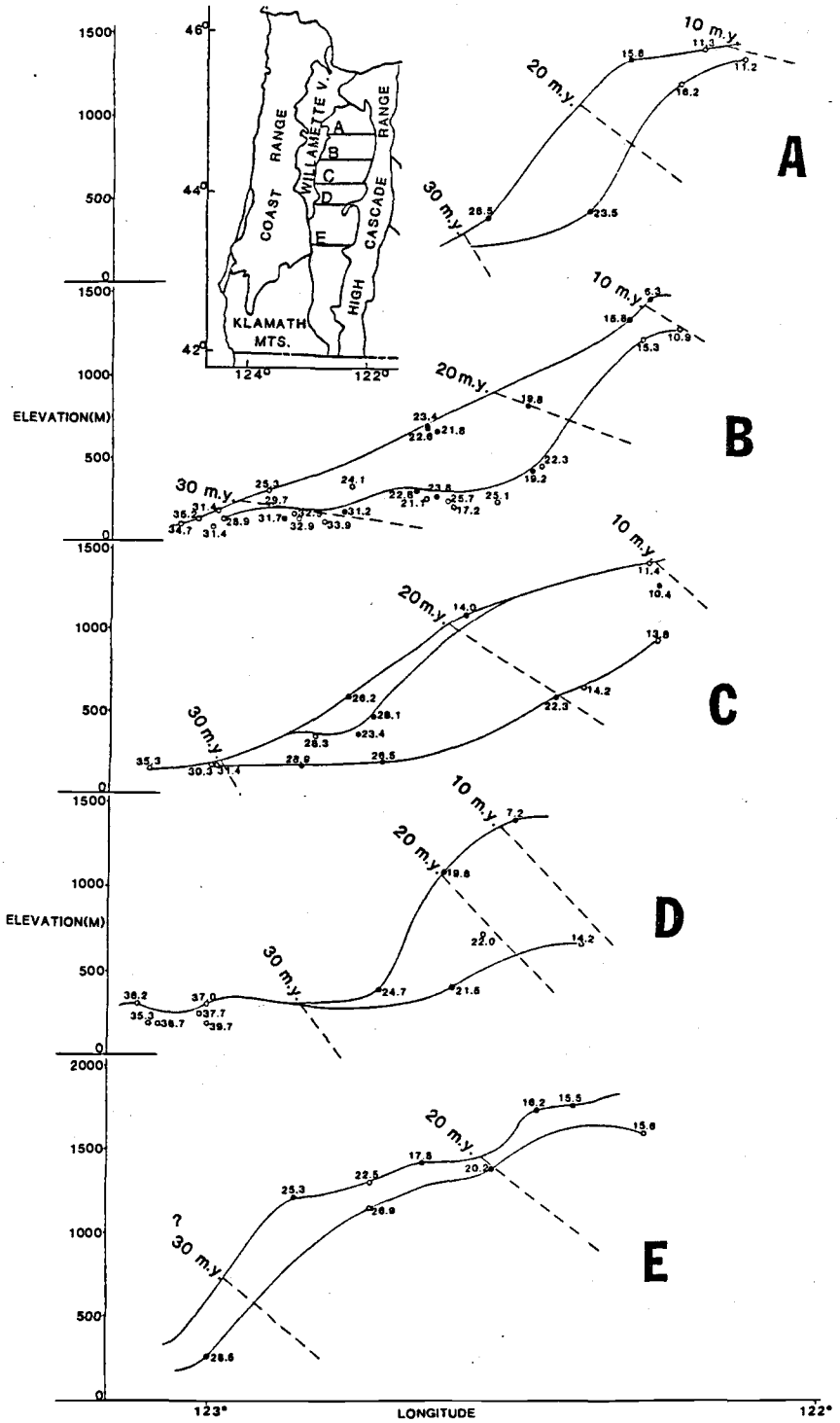

Figure III-3 - Five cross-sections of the Western Cascades, Oregon. The age data are used to construct isochrons of 10, 20 and 30 m.y. Open circles are K-Ar and 40Ar/39Ar age determinations from Lux(1981, 1982), Sutter(1978) and Priest & Vogt(1983). Closed circles are K-Ar age determinations from this study. Vertical exaggeration is 21:1.

The perpendicular distance between isochrons is an estimate of the thickness of volcanic material deposited during the 10 m.y. time intervals. The thickness for a given interval varies from one transect to another due to variations in the distance from volcanic centers. All of the swaths exhibit the same trend of decreasing thicknesses of volcanic material deposited with time. The thicknesses are converted to eruption rates by dividing by the 10 m.y. time interval.

One method which may be proposed to explain the decrease in thickness of volcanic material is the progressive eastward migration of volcanic centers. The basalt and basaltic andesite volcanic centers of the early Western Cascades are located up to 50 kilometers west of the late Western Cascades centers (Peck et al., 1964). However, the early Western Cascades volcanic stratigraphy is exposed west of the late Western Cascades volcanic stratigraphy. The horizontal distance between the 30 m.y. and 10 m.y. isochrons varies from about 25 to 60 kilometers. Therefore, the distance from the ancestral volcanic centers to the site of deposition of volcanic material has not changed by a significant amount with time. The decrease in thickness of volcanic material with time apparently reflects a decrease in eruption rate.

Table III-2 compares eruption rates for the 30 to 20 m.y. interval (early Western Cascades) with the 20 to 10 m.y. interval (late Western Cascades) for each of the swaths. The eruption rates are consistently greater during the earlier time interval. The average eruption rate is 2100 meters/m.y. between 30 and 20 m.y. and decreases to 1000 meters/m.y. between 20 and 10 m.y. There is a 50%

Corrections for page 65. 4/1/87

Table III-2 ERUPTION RATES

LOCATION	TIME (m.y.)	ERUPTION RATE (m/m.y.)	% DECREASE
A. North Santiam/Thomas Creek			
44°, 40-45'N Lat.	30-20	374	-53%
	20-10	176	
B. South Santiam/Calapooya R.			
44°, 20-25'N Lat.	30-20	240	-9%
	20-10	218	
C. McKenzie R.			
44°, 5-10'N Lat.	30-20	490	-57%
	20-10	210	
D. Lower Mid. Fork Willamette			
43°, 45-44'N Lat.	30-20	380	-67%
	20-10	127	
E. North Umpqua			
43°, 10-25'N Lat.	30-20	362	-19%
	20-15	292	

Table III-2 ERUPTION RATES

LOCATION	TIME (m.y.)	ERUPTION RATE (m/m.y.)	% DECREASE
A. North Santiam/Thomas Creek 44°, 40-45'N LAT.	30-20	2080	
	20-10	1172	-44%
B. South Santiam/Calapooya R 44°, 20-25'N LAT.	30-20	705	
	20-10	590	-16%
C. McKenzie R 44°, 5-10'N LAT.	30-20	2990	
	20-10	1108	-63%
D. Lower Mid Fork Willamette 43°,45'-44 , 0'N LAT.	30-20	1951	
	20-10	650	-67%
E. North Umpqua 43°,10-25'N LAT.	30-20	2927	
	20-10	1563	-47%

decrease, approximately, in eruption rates between the early and late Western Cascade volcanism.

Correlation of Eruption Rates with Convergence History

This study provides evidence that the temporal variation in eruptive history is a result of the change in subduction rate of the Farallon plate beneath North America. When an oceanic plate, such as the Farallon, subducts beneath a continent, such as North America, it is postulated that the release of volatiles (H2O and CO2) at depth results in partial melting of both/either the overlying asthenosphere and/or the oceanic plate itself (Green and Ringwood, 1968; Nicholls and Ringwood, 1973; Cawthorne and O'Hara, 1976; Green, 1980). Experimental petrology studies confirmed that andesitic magmas can be produced through partial melting of ocean floor tholeiites at P(H2O) equal to 5 kbar (Heltz, 1976). High pressure hydrous partial melting of peridotite can produce high alumina tholeiites, alkaline basalts and calcalkaline andesite at progressively deeper levels (Green, 1972). The volatiles are released by decarbonation and dehydration reactions involving the breakdown of hydrous minerals such as amphibole, talc and serpentine. The depth of partial melting is dependent on the age and subduction rate of the oceanic lithosphere (Abbott and Hoffman, 1984). In the Cascades volcanic arc, the subducting Farallon plate has remained young (10-20 m.y., Engebretson, 1982) for the past 40 m.y. and therefore the age of the descending plate is not a variable. The convergence rate, however, is a variable and decreases

drastically by a factor of 5 during the evolution of the Western Cascades (Chapter II).

Faster convergence rates increase the depth at which the subducting plate attains thermal equilibrium with the surrounding mantle (Abbott and Hoffman, 1984), and therefore, more volatiles are transported to the depths of melting (60-200 km). This causes more melt and consequently more magma to be produced. Intuitively, one would expect that more subducted material would result in a greater amount of volcanism in the overlying arc. Karig(1982) suggested that intensity of arc volcanism is influenced by the rate of subduction. This study provides evidence to support this hypothesis.

The average subduction rate during the early Western Cascades volcanism was 6.3 cm/yr and decreased to 3.0 cm/yr during the late Western Cascades volcanism. The average eruption rate was 2100 meters/m.y. between 30 and 20 m.y. and decreases to 1000 meters/m.y. between 20 and 10 m.y., approximately one-half the earlier rate. Therefore, it appears that subduction rate and eruption rate are roughly proportional to one another during the evolution of the Western Cascades volcanic arc. This is an important result because it can be used to correlate plate motions and magma production in volcanic arcs around the world.

The convergence rates were significantly greater (11 to 16 cm/yr) prior to 40 m.y. It would be an interesting future study to compare the eruption rates of volcanic material which predates the Western Cascades and test whether the subduction rate and eruption rate are indeed proportional to one another. The subduction zone is

thought to have been located further east in the past and volcanism was located along the Challis axis in Washington and Idaho. The emplacement of the Coast Range at approximately 42 m.y. (Duncan, 1982) clogged the previous subduction zone and thereby caused the subduction to jump seaward (Simpson and Cox, 1977). One would expect the eruption rates of volcanic material in the ancestral volcanic arc to greatly exceed those of the Western Cascades, if all other factors remained the same.

CHAPTER IV: MAJOR AND TRACE ELEMENT GEOCHEMISTRY

INTRODUCTION

The major objectives of the geochemical study are to isolate temporal geochemical variations in the Western Cascade volcanism and then to correlate these variations with changes in convergence rate and direction. The convergence history between the Farallon and North American plates was quantitatively modeled in Chapter II. The results indicate a drastic decrease in the rate of convergence (8.45 to 1.60 cm/yr, orthogonal component) and a change from approximately orthogonal to more strike-slip convergence since 40 m.y.

Changes in the rate and direction of subduction and the age of the subducting plate may result in variations in the dip and depth of melting on the Benioff zone (Abbott and Hoffman, 1984). Young oceanic lithosphere, which is thermally buoyant, subducts at a shallower angle and results in a reduced volume of igneous activity. Younger lithosphere also descends more slowly, (Carlson et al., 1983), and therefore has more time to heat up at a given depth. This results in a shallower loss of volatiles, such as H_2O and CO_2. Old oceanic lithosphere subducts at a steeper angle and a faster rate and therefore releases volatiles at a greater depth. This results in deeper partial melting and a greater volume of igneous activity. The age of the descending oceanic plate is not a variable in the Cascades because it has remained young, between 10 and 20 m.y., during the past 40 m.y. The subduction rate is a significant

variable, however, and has decreased by a factor of five during the evolution of the Cascades.

The depth of melting directly influences the geochemical character of the magmas produced. Calcalkaline lavas are suggested to be the product of partial melting of the subducted oceanic crust at 100-200 km depth (Green and Ringwood, 1972), whereas tholeiitic lavas are thought to be produced by hydrous melting of mantle peridotite at a shallower depth of 60-100 km (Nicholls and Ringwood, 1973). There remains controversy regarding the source region and petrogenesis of various volcanic arc magmas, however. The volatile content also influences the percentage of partial melt produced and therefore the geochemical character of the resultant volcanism.

Forty-nine samples from the Western Cascades were analyzed for ten major element and three trace element (Zr, Nb, and V) concentrations. K-Ar age determinations were performed on all but seven of the forty-nine samples. With the ages and geochemical character of volcanic stratigraphic units known, temporal variations in the volcanism can be investigated.

METHODS

All the rock samples were sawed to expose a fresh surface, then crushed and sieved to 0.84-2.00 mm size fraction. After washing and drying, the crushed samples were split into separate aliquots: one for atomic absorption, colorimetric, and x-ray fluoresence geochemical analyses, and the other for Ar isotopic analysis (see Geochronology Chapter III).

The crushed fractions were powdered in a tungsten carbide mixer mill. The weight percents of K20, Na20, A1203, and MgO were determined using a Jarrell Ash dual channel, double beam atomic absorption spectrophotometer. The powdered samples were dissolved in an HF/Nitric acid solution according to the method outlined in Fukui(1976). U.S.G.S. standards AGV, BCR and BR, were used for calibration.

SiO2 concentrations were measured by U.V.-visible colorimetric analysis. An ammonium paramolybdate reagent was used and the absorbance was measured on a Bausch and Lomb spectrophotometer. The analyses were compared to U.S.G.S. standards BCR and BR for callibration.

Fe, Mg, Mn, Ca, Ti and P major element concentrations and V, Zr, and Nb trace element concentrations were measured by a Phillips PWW 1600 simultaneous x-ray fluoresence spectrometer, which holds 20 samples and has an automatic sample changer. The major and trace element concentrations were converted to weight percent oxides and parts per million, respectively. The XRF pellets were made with polyvinylalcohol as a binding agent.

GEOCHEMICAL RESULTS

The major and trace element geochemical data on the forty-nine Western Cascades samples are listed in Table IV-1. Weight percent H2O and CO2 was not measured in the samples, which may account for some of the low totals.

TABLE IV-1 - MAJOR AND TRACE ELEMENT GEOCHEMICAL RESULTS AND NORMATIVE MINERAL CALCULATIONS

major oxides (wt%)	GWW 10-83	GWW 15-83	GWW 21-83	GWW 28-83	GWW 32-83	GWW 42-83	GWW 56-81
SiO2	53.11	56.34	51.65	56.52	49.27	50.77	50.49
TiO2	1.85	1.33	1.27	1.69	1.38	1.43	1.43
Al2O3	15.03	15.56	18.71	14.39	16.79	17.66	19.40
FeO*	10.78	7.84	9.72	10.07	9.45	9.31	10.26
MnO	0.29	0.27	0.27	0.27	0.25	0.23	0.27
MgO	4.27	3.53	3.07	2.97	8.44	6.19	4.74
CaO	8.69	7.59	9.69	6.69	10.26	9.18	11.07
Na2O	3.26	3.42	3.08	3.86	3.13	3.95	2.45
K2O	1.14	1.28	0.45	0.96	0.27	0.72	0.30
P2O5	0.25	0.23	0.14	0.32	0.27	0.32	0.18
total	98.67	97.39	98.05	97.74	99.51	99.76	100.59
trace elements(ppm)							
V	312.6	203.3	217.2	238.6	200.0	203.3	240.8
Zr	130.3	206.2	96.3	156.6	137.3	148.4	87.5
Nb	19.7	18.0	17.3	18.0	17.3	15.8	16.7
C.I.P.W. NORMS(WT%)							
Q	3.13	8.74	3.46	9.16	---	---	1.24
Or	6.74	7.56	2.66	5.67	1.60	4.26	1.77
Ab	27.59	28.94	26.06	32.66	26.49	33.43	20.73
An	23.01	23.33	35.91	19.10	30.97	28.33	41.05
Di	15.40	10.67	9.45	10.10	14.83	12.40	10.59
Hy	16.92	13.80	16.16	15.42	5.81	1.84	20.39
Ol	---	---	---	---	15.02	14.50	---
Mt	1.93	1.40	1.74	1.80	1.69	1.66	1.83
Il	3.51	2.52	2.42	3.21	2.62	2.72	2.72
Ap	0.59	0.53	0.33	0.75	0.62	0.74	0.41

TABLE IV-1 (cont.)

major oxides (wt%)	GWW 65-83	GWW 67-83	GWW 73-83	GWW 76-81	GWW 81-141	GWW 82-18	GWW 82-22
SiO2	51.18	55.89	52.01	51.40	51.82	51.48	52.24
TiO2	1.68	2.12	1.91	1.68	1.47	1.95	1.59
Al2O3	19.03	13.85	15.35	16.18	19.10	17.02	19.05
FeO*	9.48	11.04	12.15	9.46	9.98	11.45	10.40
MnO	0.27	0.27	0.29	0.27	0.28	0.31	0.27
MgO	3.64	3.46	4.26	7.72	3.60	4.25	3.08
CaO	10.06	7.01	8.27	10.52	10.39	9.50	9.98
Na2O	2.99	3.19	3.12	2.46	2.91	3.01	2.88
K2O	0.52	1.76	0.56	0.43	0.34	0.22	0.46
P2O5	0.30	0.28	0.27	0.24	0.21	0.28	0.22
total	99.19	98.87	98.19	100.35	100.1	99.73	100.13
trace elements(ppm)							
V	256.9	318.0	310.5	251.5	233.3	294.4	240.8
Zr	123.8	168.6	115.9	130.6	102.1	100.7	97.4
Nb	15.3	20.1	18.6	21.0	14.5	14.4	12.9
C.I.P.W. NORMS(WT%)							
Q	2.46	8.04	3.95	0.56	3.08	3.26	4.33
Or	3.07	10.40	3.31	2.54	2.01	1.30	2.72
Ab	25.30	26.99	26.40	20.82	24.63	25.47	24.37
An	36.97	18.28	26.23	31.84	38.05	32.28	37.70
Di	9.19	12.35	10.95	15.35	10.17	10.90	8.76
Hy	16.71	16.32	21.10	23.94	17.23	20.00	17.04
Ol	---	---	---	---	---	---	---
Mt	1.69	1.97	2.17	1.69	1.78	2.05	1.86
Il	3.19	4.02	3.63	3.19	2.79	3.71	3.02
Ap	0.69	0.65	0.63	0.55	0.49	0.65	0.51

TABLE IV-1 (cont.)

major oxides (wt%)	GWW 82-29	GWW 82-41	GWW 82-42	GWW 82-43	GWW 82-45	GWW 87-81	GWW 99-83
SiO2	50.90	51.30	50.62	52.99	50.91	59.80	52.21
TiO2	1.36	2.05	1.67	1.55	2.61	0.92	1.10
Al2O3	20.46	15.39	18.96	18.80	14.46	13.82	17.70
FeO*	8.90	12.64	9.77	10.45	12.90	6.01	6.90
MnO	0.25	0.31	0.27	0.26	0.48	0.17	0.20
MgO	3.68	5.15	3.59	3.97	4.00	3.44	5.08
CaO	11.32	9.01	10.47	10.31	8.50	6.65	8.96
Na2O	2.45	2.95	2.95	3.43	3.68	3.94	3.35
K2O	0.37	0.57	0.21	0.20	0.45	1.62	0.71
P2O5	0.21	0.27	0.28	0.22	0.99	0.21	0.28
total	99.90	99.64	98.79	102.18	98.98	96.58	96.49
trace elements(ppm)							
V	211.8	339.5	262.2	270.8	318.0	138.9	162.5
Zr	84.6	116.8	99.2	95.1	130.6	207.3	235.5
Nb	12.0	17.9	14.0	14.2	15.6	14.9	13.3
C.I.P.W. NORMS(WT%)							
Q	3.08	1.63	2.52	1.63	2.00	11.80	2.35
Or	2.17	3.37	1.24	1.18	2.66	9.57	4.20
Ab	20.73	24.96	24.96	29.04	31.14	33.34	28.35
An	43.75	27.07	37.87	35.30	21.61	15.24	31.16
Di	9.23	13.24	10.27	12.09	11.87	13.50	9.40
Hy	16.40	22.76	16.48	17.77	20.33	9.89	17.16
Ol	---	---	---	---	---	---	---
Mt	1.59	2.26	1.75	1.87	2.31	1.07	1.23
Il	2.59	3.89	3.18	2.94	4.95	1.76	2.09
Ap	0.48	0.63	0.64	0.50	2.29	0.50	0.65

TABLE IV-1 (cont.)

major oxides (wt%)	GWW 102-83	GWW 103-83	GWW 104-83	GWW 107-83	GWW 113-83	GWW 114-81	GWW 190-81
SiO2	54.12	53.09	57.55	51.29	53.16	61.96	50.56
TiO2	1.36	1.25	0.84	2.83	1.06	0.96	1.35
Al2O3	16.64	16.50	16.63	13.11	15.50	16.11	18.07
FeO*	8.53	8.69	5.87	13.44	7.38	6.00	11.04
MnO	0.24	0.23	0.18	0.31	0.20	0.17	0.29
MgO	4.20	6.01	3.14	4.53	6.54	3.29	5.72
CaO	7.98	8.65	6.87	7.92	9.33	6.34	10.79
Na2O	3.63	3.32	3.40	3.02	2.96	3.87	2.30
K2O	0.89	0.71	1.69	1.18	1.70	2.32	0.23
P2O5	0.59	0.50	0.21	0.47	0.44	0.19	0.14
total	98.18	98.95	96.38	98.10	98.27	100.61	100.49
trace elements(ppm)							
V	176.4	171.1	131.4	412.4	176.4	142.1	262.2
Zr	265.6	181.0	227.0	154.9	87.5	222.3	62.9
Nb	19.1	15.6	14.9	20.8	19.1	15.6	14.7
C.I.P.W. NORMS(WT%)							
Q	4.77	2.17	10.52	3.09	0.62	11.27	1.21
Or	5.26	4.20	9.99	6.97	10.05	13.71	1.38
Ab	30.72	28.10	28.77	25.56	25.05	32.75	19.46
An	26.48	28.02	25.12	18.73	23.99	19.74	38.30
Di	7.68	9.58	6.28	14.65	15.81	8.67	11.86
Hy	17.92	21.93	12.65	20.41	18.50	11.84	23.57
Ol	---	---	---	---	---	---	---
Mt	1.53	1.55	1.05	2.40	1.32	1.07	1.97
Il	2.57	2.37	1.59	5.37	2.02	1.82	2.57
Ap	1.36	1.15	0.49	1.10	1.03	0.44	0.33

TABLE IV-1 (cont.)

major oxides (wt%)	GWW 191-81	M2-17	M2-19	M2-22	M2-23	M2-24	M2-25
SiO2	50.09	51.47	50.77	56.25	58.07	50.26	51.40
TiO2	1.33	1.44	1.25	1.58	1.13	1.00	1.51
Al2O3	18.15	15.93	18.38	15.19	15.47	17.96	18.13
FeO*	11.40	9.60	9.57	10.18	6.71	9.05	10.35
MnO	0.31	0.26	0.28	0.24	0.21	0.25	0.26
MgO	5.70	4.59	4.69	3.33	3.14	6.52	4.28
CaO	10.73	10.02	10.41	7.85	6.91	11.07	9.51
Na2O	2.23	2.91	2.74	3.29	3.77	2.24	3.10
K2O	0.21	0.52	0.49	0.86	1.49	0.58	0.22
P2O5	0.13	0.23	0.22	0.24	0.32	0.19	0.21
total	100.28	96.97	98.80	99.01	97.22	99.12	98.97
trace elements(ppm)							
V	256.9	232.2	232.2	289.0	192.5	256.9	151.8
Zr	64.3	147.6	100.4	128.2	111.8	108.0	252.7
Nb	15.6	15.6	12.5	14.2	12.0	12.9	16.4
C.I.P.W. NORMS(WT%)							
Q	0.90	3.24	1.29	9.49	10.29	---	2.41
Or	1.24	3.07	2.90	5.05	8.81	3.43	1.30
Ab	18.87	24.63	23.19	27.84	31.90	18.96	26.23
An	38.90	28.86	36.41	24.16	20.89	37.24	34.91
Di	11.19	16.05	11.47	11.09	9.41	13.50	9.13
Hy	24.46	16.26	19.09	16.13	11.94	21.86	19.93
Ol	---	---	---	---	---	0.31	---
Mt	2.04	1.72	1.71	1.82	1.20	1.62	1.85
Il	2.53	2.73	2.37	3.01	2.14	1.90	2.88
Ap	0.31	0.54	0.50	0.56	0.73	0.43	0.48

TABLE IV-1 (cont.)

major oxides (wt%)	M3-25	M3-26	M3-27	M3-29	M3-30	M3-31	M3-32
SiO2	53.68	52.94	54.86	47.95	68.05	60.59	60.63
TiO2	0.90	1.14	1.20	1.26	0.34	0.80	0.93
Al2O3	18.21	16.88	19.15	16.06	12.94	15.85	15.85
FeO*	7.04	8.12	7.05	8.87	4.04	5.42	6.14
MnO	0.19	0.21	0.18	0.23	0.21	0.17	0.17
MgO	4.94	6.06	3.06	8.68	0.24	2.95	3.29
CaO	9.61	8.49	7.84	9.90	1.95	6.74	6.52
Na2O	2.75	3.52	4.02	3.11	4.90	3.36	3.06
K2O	0.80	0.85	1.25	0.92	2.61	1.15	1.81
P2O5	0.19	0.36	0.33	0.45	0.08	0.17	0.18
total	98.31	98.57	98.94	97.43	95.16	97.20	98.58
trace elements(ppm)							
V	146.4	165.7	171.1	189.3	31.7	119.6	144.3
Zr	135.0	159.6	204.4	177.1	388.7	195.0	191.5
Nb	10.9	13.8	13.8	11.2	26.5	13.6	14.9
C.I.P.W. NORMS(WT%)							
Q	5.29	0.61	3.44	---	23.27	16.59	15.32
Or	4.73	5.02	7.39	5.44	15.42	6.80	10.70
Ab	23.27	29.79	34.02	24.68	41.47	28.43	25.89
An	34.99	27.75	30.52	27.15	5.61	24.77	24.17
Di	9.41	9.86	5.18	0.89	3.13	6.25	5.81
Hy	17.32	21.20	14.19	15.48	4.99	11.56	13.51
Ol	---	---	---	18.91	---	---	---
Mt	1.26	1.45	1.26	1.59	0.72	0.97	1.10
Il	1.72	2.17	2.27	2.38	0.64	1.51	1.76
Ap	0.43	0.83	0.77	1.03	0.18	0.40	0.42

TABLE IV-1 (cont.)

major oxides (wt%)	M3-33	M3-34	M3-35	M3-36	M3-37	M3-38	M3-39
SiO2	56.23	51.10	50.79	62.54	51.10	63.91	53.05
TiO2	1.46	1.18	1.34	1.20	1.09	0.91	1.32
Al2O3	15.95	17.09	16.69	12.21	17.87	13.57	17.22
FeO*	8.12	8.37	9.28	5.65	8.50	4.88	9.04
MnO	0.22	0.22	0.25	0.23	0.28	0.20	0.23
MgO	3.53	6.41	5.65	1.49	6.51	1.20	4.31
CaO	7.33	8.43	8.39	4.53	10.97	3.99	9.35
Na2O	4.11	3.52	3.79	4.02	2.22	4.30	2.74
K2O	0.77	0.66	1.05	1.19	0.48	1.57	0.18
P2O5	0.30	0.44	0.55	0.30	0.18	0.19	0.23
total	98.02	97.42	97.78	93.36	99.20	94.72	97.64
trace elements(ppm)							
V	205.4	176.4	184.0	108.9	203.0	87.4	221.5
Zr	171.3	161.6	195.6	266.8	113.9	219.9	131.4
Nb	16.9	14.2	15.6	25.2	12.3	21.2	14.5
C.I.P.W. NORMS(WT%)							
Q	7.01	---	---	22.17	1.73	21.39	7.43
Or	4.55	3.90	6.21	7.03	1.30	9.28	1.06
Ab	34.78	29.79	32.07	34.04	26.23	36.39	23.19
An	22.80	28.88	25.43	11.74	34.91	13.09	34.15
Di	9.67	8.26	10.36	7.43	9.13	4.62	8.90
Hy	14.41	18.58	9.88	7.05	19.93	6.98	18.39
Ol	---	3.38	8.47	---	---	---	---
Mt	1.45	1.50	1.66	1.01	1.85	0.87	1.62
Il	2.77	2.24	2.54	2.28	2.88	1.74	2.51
Ap	0.70	1.02	1.28	0.69	0.48	0.45	0.54

Precision (1σ) - AA: Al2O3(2.3%), MgO(2.3%), Na2O(0.7%), K2O(0.3%)
Colorimetric: SiO2(0.8%)
XRF: P2O5(9.3%), CaO(2.6%), TiO2(2.7%), MnO(2.3%)
FeO(2.7%), V(23.7 ppm), Zr(10.0 ppm),
Nb(1.3 ppm)

FeO* = total iron calculated to Fe^{2+}

Normative Mineral Calculations: The Fe2O3 value was assumed to be 10% of the total FeO*. Q=quartz, Or=orthoclase, Ab=albite, An=anorthite, Di=diopside, Hy=hypersthene, Ol=olivine, Mt=magnetite, Il=ilmenite, Ap=apatite.

Major Elements

The Western Cascade rocks from this study are composed primarily of basalts (57%) and basaltic andesites (27%), with minor amounts of andesite (12%), dacite and rhyodacite (2% each). The nomenclature is based on silica contents in the following manner: basalt, <53% SiO2; basaltic andesite, 53-58% SiO2; andesite, 58-63% SiO2; dacite, 63-68% SiO2; rhyodacite, >68% SiO2.

Harker diagrams for all of the samples analyzed are shown in Figure IV-1. The major oxides versus SiO2 are plotted for the early Western Cascades of 42-18 m.y., open circles, and the late Western Cascades of 18-10 m.y., closed circles. K2O and SiO2 correlate in a positive linear fashion, in general, for all samples. The K2O values are higher and increase less rapidly relative to SiO2 for the younger (18-10 m.y.) than the older (42-18 m.y.) samples. Na2O increases only slightly with SiO2 for the younger samples, but shows a strong positive correlation for the older samples. This suggests that K and Na are more incompatible in the early and middle stages of fractionation in the older lavas.

The CaO and Na2O plots appear as mirror images of one another, the former decreases as the latter increases. This suggests that a Ca-rich plagioclase was crystallizing in the early stages and it became more Na-rich with increasing fractionation. Both early and late Western Cascades CaO values decrease linearly relative to SiO2, but the former decrease more rapidly than the latter. This is probably a function of the Ca-content of the plagioclase and pyroxene which were crystallizing. The early Western Cascades

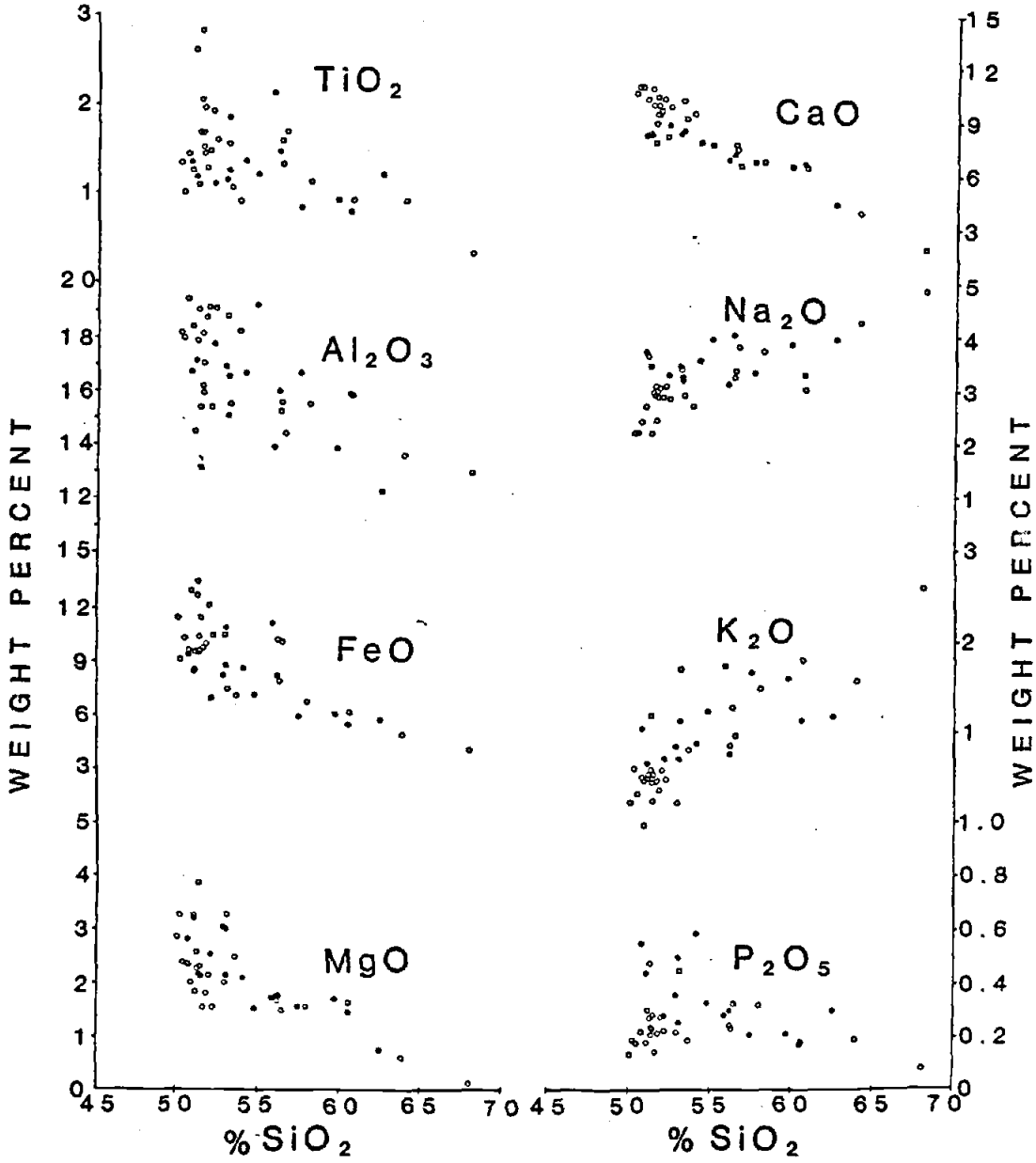

Figure IV-1 - Weight percent major oxides vs. SiO_2.
Open circles: 32 to 18 m.y. age samples,
closed circles: 18 to 10 m.y. age samples.

fractionation sequence was probably dominated by Ca-rich minerals such as anorthite and augite.

A negative correlation between TiO2 and SiO2 is indicative of magnetite fractionation because the distribution coefficient for TiO2 in the magnetite solid solution series is >>1. Magnetite fractionation suppresses Fe-enrichment and is therefore thought to occur throughout the fractionation sequence in calcalkaline suites (Miyashiro, 1974). In the late Western Cascades samples TiO2 contents correlate negatively with SiO2, which suggests a calcalkaline affinity. Crystallization of titaniferous magnetite is delayed until a late stage in the tholeiitic series which results in FeO and TiO2 enrichment in the late stage magmas. TiO2 contents in the early Western Cascades lavas decrease relative to SiO2 when SiO2 >58%. There is a wide range of TiO2 values when SiO2 is F58%. This suggests that magnetite did not begin to crystallize until the SiO2 values exceeded 58% and may be indicative of a tholeiitic affinity in the early Western Cascades samples.

MgO and FeO* contents correlate negatively with SiO2 for both early and late Western Cascade rocks, as expected. When SiO2 <57%, the older basalts contain approximately 2 weight percent higher FeO values than the younger samples, which is compatible with the tholeiitic trend observed in the older lavas.

Phosphorous contents have been observed to show contrasting behavior in calcalkaline and tholeiitic suites (Anderson and Gottfried, 1971). A negative correlation between P2O5 and SiO2 is characteristic of calcalkaline suites. The late Western Cascades exhibit a strong negative correlation. Conversely, in tholeiitic

suites P205 contents increase relative to Si02. If the cluster of data from the early Western Cascades plot is examined, the P205 values gradually increase as the Si02 increases from 50-58%. The three data points above 58% Si02 decrease in a linear fashion. The vast majority of P205 values correlate positively, however, and therefore suggest a tholeiitic affinity.

Al203 contents decrease with increasing Si02 but there is significant scatter in the correlation, which is not uncommon in Al203 vs. Si02 variation diagrams from island arc suites. Gill (1981) suggested that this scatter is a result of plagioclase removal and accumulation.

Figure IV-2 compares Western Cascades basalt samples only, on a K20 vs Si02 variation diagram. The rocks are divided into three age groups: 32-24, 24-17, 17-10 m.y.. The oldest basalts have the lowest K20 content, the youngest basalts have the highest K20 content, and the intermediate age group have a range of K20 values. This indicates an increase in K20 relative to Si02 with time for Western Cascades basaltic lavas. It is consistent with many other volcanic arcs around the world, such as the Aleutians, the Andes and Japan, and implies an increase in the depth of melting (or distance from the trench), an increase in fractional crystallization or a decrease in the percent partial melting with time (Gill, 1981 and McBirney, 1978).

Another factor which may influence the K content is alteration. The older samples may have been subject to more extensive weathering and contain less K due to leaching. In order to test this alternative, the samples which appear to be most altered in thin

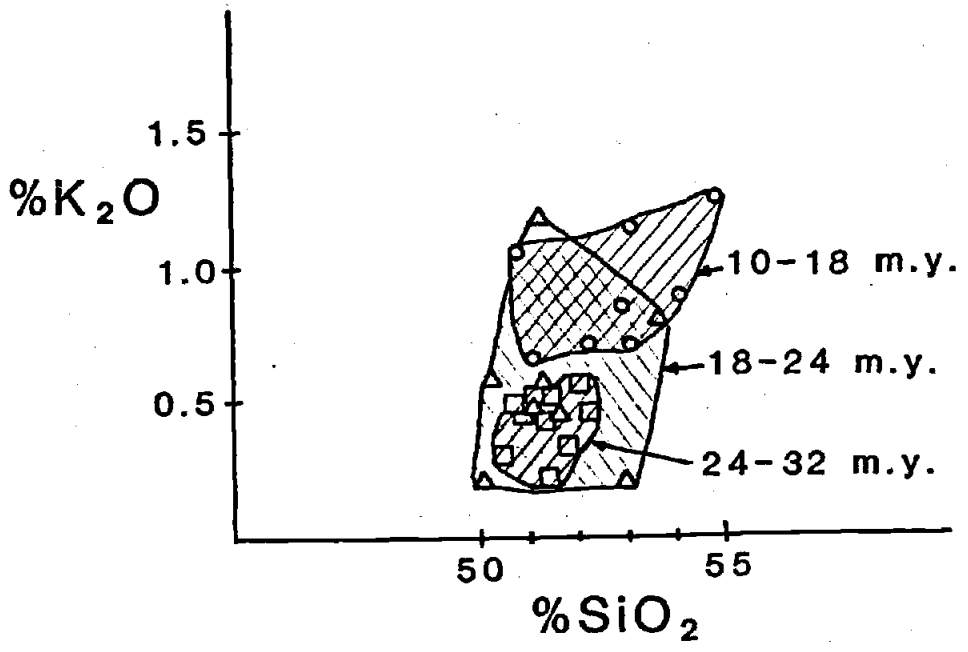

Figure IV-2 - Weight percent K_2O vs. SiO_2. The Western Cascades samples are divided into three age groups: 10-18 m.y., 18-24 m.y. and 24-32 m.y.

section were compared to samples with similar SiO2 contents and no evidence of alteration. The K2O contents of the two groups were indistinguishable, therefore the temporal variations in K2O content probably reflects a change in the processes of magma genesis. Lastly, selective contamination of the basaltic magmas by a crustal component might explain the increase in K2O with time (Watson, 1982).

Recent major element geochemical data from the central Western Cascades in Oregon from Lux(1981) and Priest and Vogt(1983) (open circles) are combined with the present study (closed circles) in Figures IV-3 and IV-4, and sum to a total of 80 analyses. The FeO*/MgO vs. SiO2 diagrams compare the relative proportions of tholeiitic and calcalkaline samples in the early (42-18 m.y.) and late (18-10 m.y.) Western Cascades samples. The tholeiitic/calcalkaline discrimination line is from Miyashiro(1974), and is based on the Fe-enrichment trend characteristic of the tholeiitic series. The results indicate a decrease in tholeiitic relative to calcalkaline volcanism with time. Seventy-eight percent of the early Western Cascades samples fall into the tholeiitic field, and seventy-one percent of the late Western Cascades samples lie in the calcalkaline field.

The same data set is plotted on an AFM (alkalies, iron, magnesium) triangular diagram in Figure IV-4. A similar trend from tholeiitic to calcalkaline volcanism with time is observed. Over one-half of the early Western Cascade samples plot in the tholeiitic field and all but one of the late Western Cascade samples plot in the calcalkaline field.

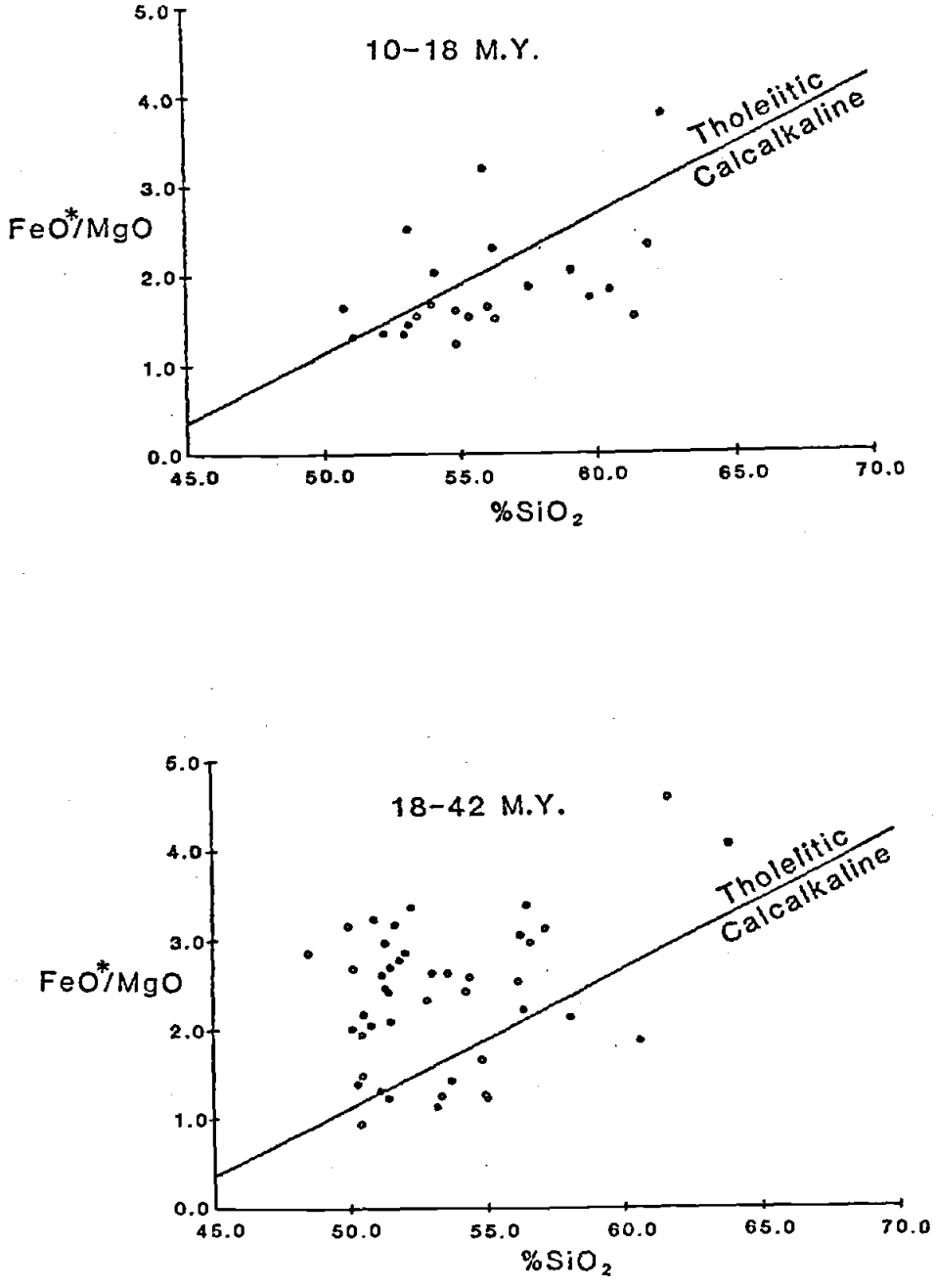

Figure IV-3 - FeO*/MgO ratio vs. $\%SiO_2$. The Western Cascades samples are divided into two age groups: 10-18 m.y. and 18-24 m.y. Tholeiitic and calcalkaline discrimination line is from Miyashiro(1974). Closed circles: this study. Open circles: Lux(1981, 1982) and Priest and Vogt(1983).

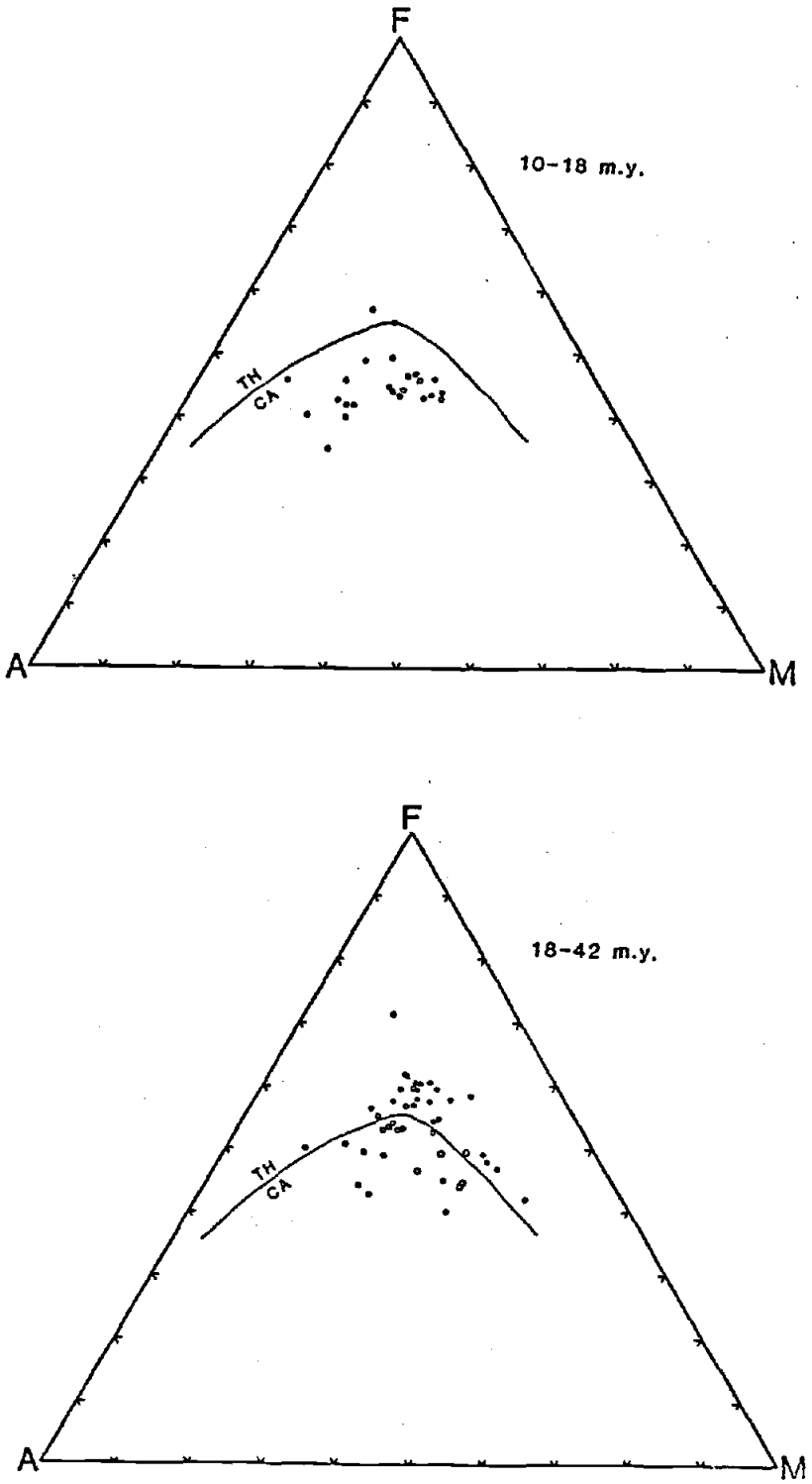

Figure IV-4 - AFM diagrams. The Western Cascades samples are divided into two age groups: 10-18 m.y. and 18-32 m.y. A = Na_2O + K_2O, F = FeO*, M = MgO. Tholeiitic and calcalkaline discrimination line is from Irvine and Baragar(1971). Closed circles: this study. Open circles: Lux(1981, 1982) and Priest and Vogt(1983).

Trace Elements

Vanadium, zirconium and niobium concentrations (ppm) are listed in Table IV-1 for the 49 Western Cascades samples. Vanadium behaves in a similar manner to titanium and therefore readily substitutes into ilmenite and titanomagnetite. Their parallel behavior is illustrated in Figure IV-5, a Ti(%) vs. V(ppm) plot.

The occurence of magnetite fractionation causes the Ti/V ratio to increase (Shervais, 1982), therefore calcalkaline series rocks generally have higher Ti/V ratios than tholeiitic series rocks. Figure IV-6 indicates that there is a slight increase in the Ti/V ratio at about 20 m.y. The samples >20 m.y. have an average Ti/V=38 and those <20 m.y. have an average Ti/V=43. This agrees with the major element data which also indicate a shift from tholeiitic to calcalkaline volcanism with time. The three highest ratios, >60, are also the only three samples with SiO2>62%. These samples are more evolved and therefore are presumably derived from later stage magmas which have been subject to more magnetite fractionation.

Zirconium and niobium are both highly incompatible elements and therefore are expected to increase in the late stage, more evolved magmas (Perfit et al., 1980). Their ratio is indicative of the source region because it is unaffected by the percent melting and also neither Zr or Nb is fractionated into the dominant crystallizing phases, such as olivine, pyroxene and plagioclase. Figure IV-7 is a plot of the Zr/Nb ratio versus age for all the

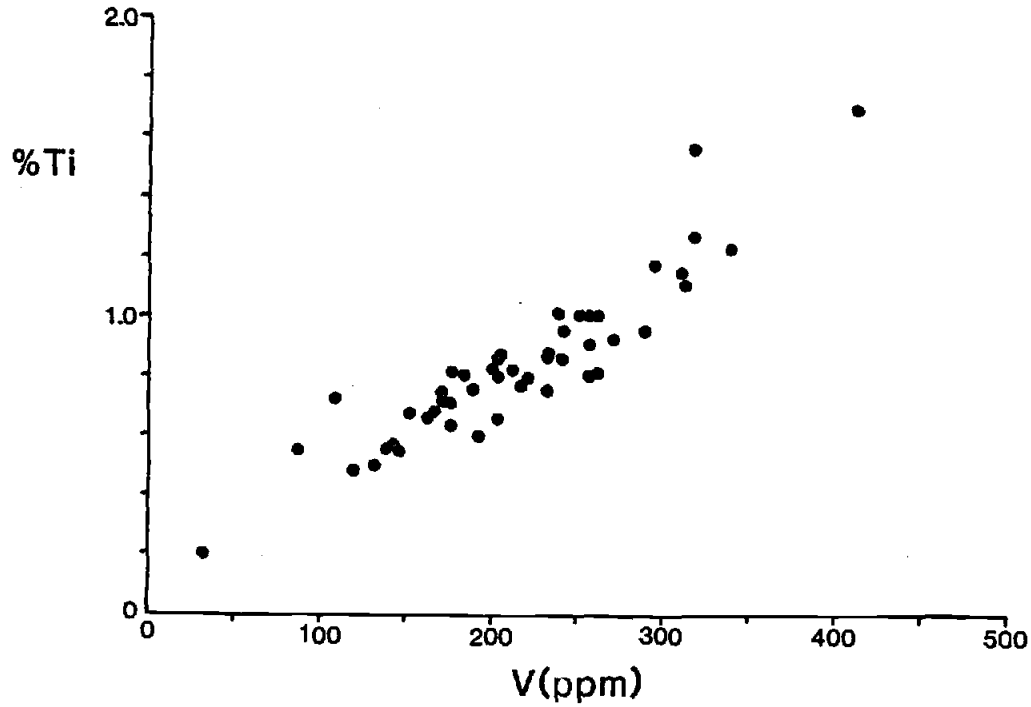

Figure IV-5 - %Ti(ppm/10^4) vs. V(ppm).

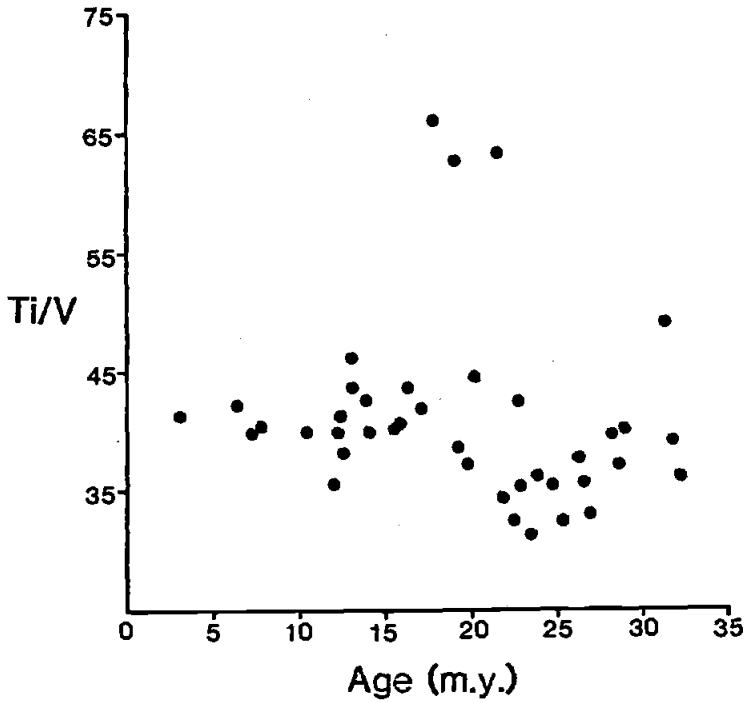

Figure IV-6 - Ti/V ratio vs. age (m.y.).

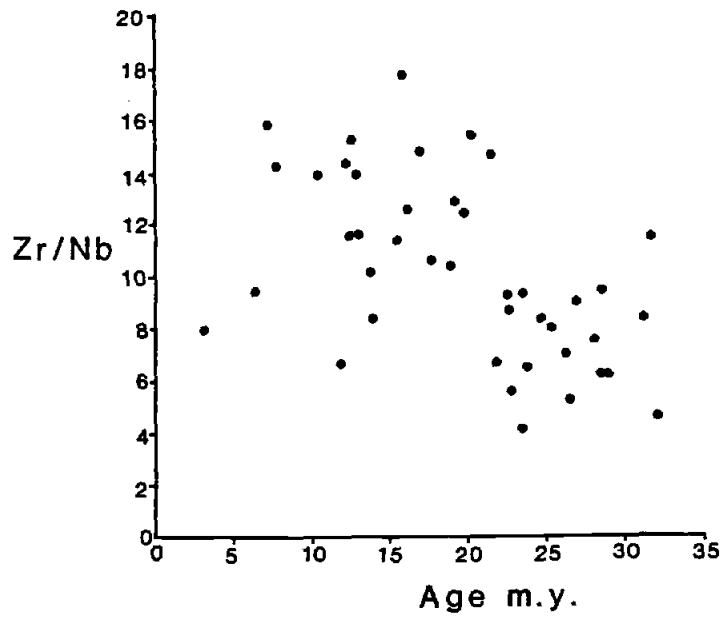

Figure IV-7 - Zr/Nb ratio vs. age (m.y.).

samples. The results fall into two groups: an older group (>20 m.y.) with Zr/Nb<10 and a younger group (<20 m.y.) with Zr/Nb>10. There are a few extraneous data points but the majority of the data suggests two separate source regions of magma genesis. The older samples are depleted in Zr and the younger samples enriched in Zr relative to Nb.

Pearce and Cann(1973) report Zr and Nb data on samples from ocean ridges, oceanic islands, volcanic arcs and continental basalts. The average Zr/Nb ratios of the calcalkaline and low-K tholeiitic volcanic island arc samples are 42 and 35, respectively. These values are significantly greater than the Western Cascades ratios. This may be because island arcs have different Zr/Nb ratios than continental volcanic arcs. The type and amount of sediment that is subducted to the depths of magma genesis may influence the Zr/Nb ratios. Also, there may be contamination from the continental lithosphere. The average Zr/Nb ratios for ocean ridges is 18, for oceanic islands is 7 and for continental basalts is 11, but there is a wide range of values. These three groups are closer to the Western Cascades ratios than the island arcs are. The Zr/Nb ratios from this study range from 4 to 18 and have an average value of 9.7.

Zirconium and vanadium correlate in a linear, negative manner (Figure IV-8). Zr increases with differentiation and is therefore a useful fractionation index (Shervais, 1984; Gill, 1981). V, as mentioned above, behaves similarly to Ti, and therefore decreases as fractionation proceeds if magnetite is a crystallizing phase. The negative correlation between V and Zr is expected, and indicates the importance of magnetite fractionation.

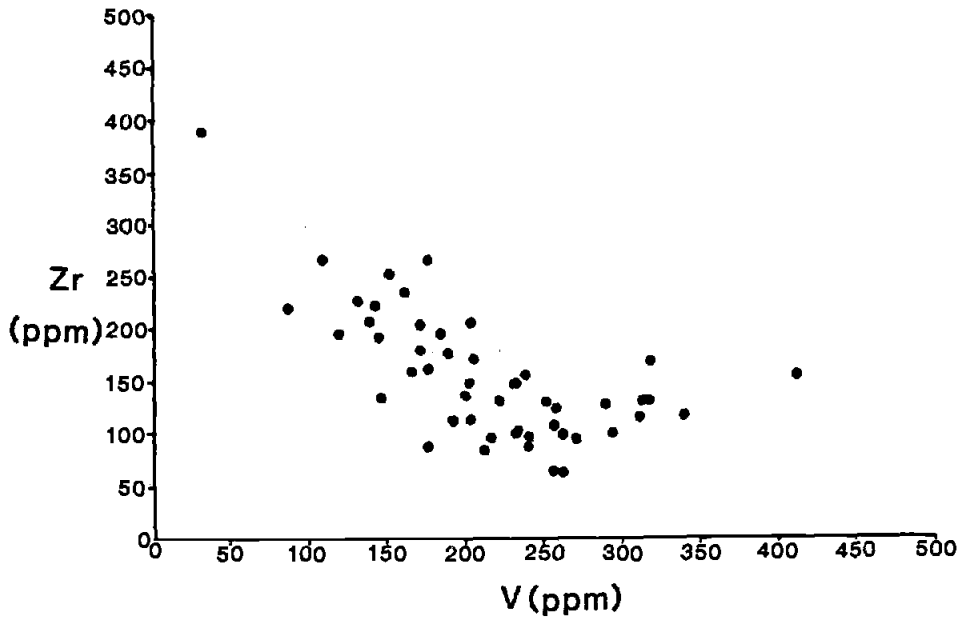

Figure IV-8 - Zr(ppm) vs. V(ppm).

Correlation of Geochemical Variations with Convergence Model

The convergence rate and orthogonal component have decreased during the volcanic evolution of the Cascade volcanic arc. At the same time, volcanism has changed from predominantly tholeiitic to calcalkaline series magmas. The early Western Cascades lavas of 42-18 m.y. age are primarily tholeiitic, and have lower K2O/SiO2 and Zr/Nb ratios. The late Western Cascade lavas of 18-10 m.y. age are dominantly calcalkaline and have higher K2O/SiO2 and Zr/Nb ratios.

Figure IV-9 illustrates two models porposed to explain the petrogenesis of the early Western Cascades when the subduction rate was faster (4-9 cm/y, orthogonal component) and the late Western Cascades when slower subduction took place (2-4 cm/yr, orthogonal component). Tholeiitic series are suggested to be the product of a greater percent partial melting at shallower depths and calcalkaline series are thought to be produced by less percent partial melting at greater depths (Miyashiro, 1974). Presumably, faster convergence results in more volatiles transported to the depth of melting, a greater percent partial melting, and therefore the magmas have lower incompatible element concentrations and tholeiitic affinities. Conversely, slower convergence results in dehydration reactions at a shallower depth because the slab heats up faster. Most of the volatiles escape at depths too shallow for magma genesis. Greater temperature conditions are required to generate partial melts when fewer volatiles are present. Therefore, slower convergence results in an increase in the depth of melting. Also, less percent partial

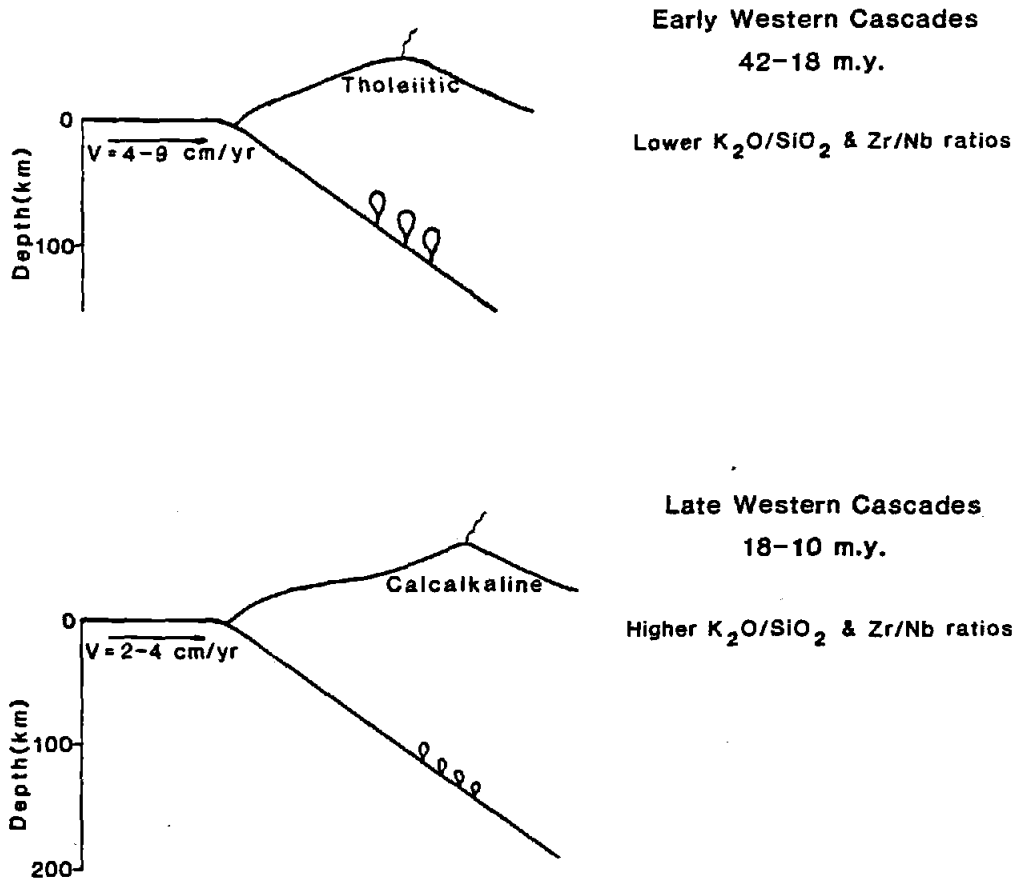

Figure IV-9 - Petrogenetic models for the volcanic evolution of early and late Western Cascades (W.C.). Faster convergence rates (4-9 cm/yr) during the evolution of early W.C. results in predominantly tholeiitic compositions and lower K_2O/SiO_2 and Zr/Nb ratios. Partial melting at 60 to 100 km depth is a likely source region for the early W.C. lavas.

Slower convergence rates (2-4 cm/yr) during the evolution of the late W.C. results in predominantly calcalkaline compositions and higher K_2O/SiO_2 and Zr/Nb ratios. Partial melting at depths $\geq$100 km is a likely source region for the late W.C. lavas.

melting occurs because there are fewer volatiles present. The end result is a higher content of incompatible elements, such as K and Zr, and calcalkaline volcanism.

One possible inconsistency with this model is that it indicates lower volatile contents in the region of calcalkaline magma genesis, but calalkaline magmas contain a greater percent of H2O and CO2 than tholeiitic magmas. One explanation for this is that there is less percent partial melting and therefore the percentage of volatiles in the calcalkaline magmas could still be greater. Alternatively, the inconsistency may be due to the composition of the volatiles. Changes in the relative proportions of H2O and CO2 may control the geochemical characteristics of the resultant magmas.

Future geochemical work on samples from the Western Cascades and other volcanic arcs will lead to a more thorough understanding of subduction-related volcanism. Isotopic ratios (e.g. 87Sr/86Sr and 143Nd/144Nd) can reveal contamination by continental crust or subducted sediment. Rare earth element data can be indicative of the source region, the degree of partial melting and the controlling phases during crystal fractionation.

CHAPTER V SUMMARY

The major objective of this study was to correlate time variations in eruptive history and geochemical character of Western Cascades volcanism with changes in the convergence pattern between the Farallon and North American plates. In order to accomplish this, the first step was to model the history of convergence between the subducting Farallon plate and North America. The model is based on the absolute reference frame, assuming hotspots fixed with respect to the mantle, and calculates that convergence direction has become more oblique and the convergence rate has decreased by a factor of five during the volcanic evolution of the Western Cacades.

The second step was to characterize the eruptive history using the geochronological data from this study and other reported ages. The results indicate that the oldest material is exposed on the western margin and the ages decrease with increasing elevation and distance eastward, which agrees with the expected volcanic outcrop patterns because the Western Cascades flows and tuffs have a gentle ($5-10^{o}$) eastward dip. Volcanism has been continuous throughout the evolution of the Western Cascades, with some periods of more active volcanism: 13-16 m.y., 22-26 m.y. and 29-31 m.y. Most important, the age data were used to estimate eruption rates in the Western Cascades. The results indicate that there was approximatley twice as much volcanic material deposited between 30 and 20 m.y. as between 20 and 10 m.y. The Late Western Cascades eruption rates have decreased by one-half relative to the Early Western Cascades.

The third step was to characterize major and trace element

geochemical variations during the Western Cascades eruptive history. The results indicate an increase in calcalkaline relative to tholeiitic volcanism and an increase in K2O/SiO2 and Zr/Nb ratios with time.

The changes in direction and rate of convergence directly influence the volume and geochemical character of volcanism in the associated volcanic arc. The decrease in convergence rate results in less material being subducted and a corresponding decrease in the amount of magma produced and erupted. Apparently the slower convergence rate results in a shallower loss of volatiles and therefore a decreasing degree of partial melting at depth. Smaller degrees of partial melting result in calcalkaline volcanism and higher proportions of incompatible elements, as seen in the late Western Cascade lavas. More partial melting results in tholeiitic volcanism and lower proportions of incompatible elements, as seen in the early Western Cascades volcanism.

The correlation of subduction rate with eruption rate and geochemical character is an important result because subduction related volcanism occurs in many areas around the globe. This study supports the hypothesis that changes in the subduction rate influence both the volume of erupted material and the geochemical character of the volcanism. It will be useful to compare these results to those of other convergent plate boundaries in future studies, to test whether this hypothesis is valid at other volcanic arcs. Additional trace element and isotopic analyses will lead to a more thorough understanding of the variation in the source region with time.

BIBLIOGRAPHY

Abbott, D., and M. Lyle, 1984, Age of oceanic plates at subduction and volatile recycling, Geophys. Res. Lett., (in press).

Abbott, D.H., and S.E. Hoffman, 1984, Archaean plate tectonics revisited, 1. Heat flow, spreading rate and the age of subducting oceanic lithosphere and their effects on the origin and evolution of continents, Tectonics, 3: 429-448.

Abbott, D.H., M. Lyle and M. Fisk, 1985, Age of the oceanic lithosphere at the start of subduction and the return of volatiles to the mantle: implications for planetary degassing, Geophys. Res. Lett., (in press).

Anderson, A.T. and D. Gottfried, 1971, Contrasting behavior of P, Ti and Nb in a differentiated high-alumina olivine tholeiite and a calcalkaline andesite suite, Geol. Soc. Am. Bull., 82: 1929-1942.

Atwater, T., 1970, Implications of plate tectonics for the Cenozoic tectonic evolution of western North America, Geol. Soc. Am. Bull., 81: 3513-3536.

Atwater, T., and H.W. Menard, 1970, Magnetic lineations in the north-east Pacific, Earth Planet. Sci. Lett., 7: 445-450.

Beck, M.E., Jr., 1980, Paleomagnetism of intrusive rocks in the Coast Range of Oregon: microplate rotations in middle Tertiary time, Geology, 8: 573-577.

Burke, K., W.S.F. Kidd and J.T. Wilson, 1973, Relative and latitudinal motion of Atlantic hotspots, Nature, 245: 133-137.

Callahan, E., 1933, Some features of the volcanic sequence in the Cascade Range in Oregon, Am. Geophys. Union Trans., 14th Ann. Mtg.: 243.

Callahan, E. and A.F. Buddington, 1938, Metalliferous mineral deposits of the Cascade Range in Oregon, U.S. Geol. Surv. Bull. 893, 141 pp.

Carey, S.W., 1958, A tectonic approach to continental drift, in: S.W. Carey (ed.), Continental Drift, A Symposium, Univ. of Tasmania, Hobart, Tasmania: 177-355.

Carlson, R.L., T.W.C. Hilde and S. Uyeda, 1983, The driving mechanism of plate tectonics: relation to age of the lithosphere at trenches, Geophys. Res. Lett., 10:297-300.

Cawthorne, R.G., and M.J. O'Hara, 1976, Amphibole fractionation in calc-alkaline magma genesis, Am. J. Sci., 276: 309-329.

Clague, D.A., G.B. Dalrymple and R. Moberly, 1975, Petrography and K-Ar ages of dredged volcanic rocks from the western Hawaiian Ridge and the southern Emperor seamount chain, Geol. Soc. Am. Bull., 86: 991-998.

Cloos, M., 1984, Quantitative modeling of sediment subduction, melange formation, and accretion at convergent plate margins, Geol. Soc. Am., Abstr. Programs, 16(6): 473.

Couch, R., 1984, Structures in the Cascade Range in Oregon: implications for mineral exploration, Pac. N.W. Metals and Min. Conf. Abs., Portland, Oregon.

Couch, R.W. and R.W. Foote, 1983, Graben structures of the Cascade Range in Oregon (abs.), EOS, 64: 887.

Crosson, R.S., 1976, Crustal structure modeling of earthquake

data, 2. Velocity structure of the Puget Sound region, Washington, J. Geophys. Res., 81: 3047-3054.

Dalrymple, G.B. and M.A. Lanphere, 1969, Potassium-Argon Dating, W.H. Freeman and Co., San Francisco, 258 pp.

Duncan, R.A., 1982, A captured island chain in the Coast Range of Oregon and Washington, J. Geophys. Res., 87: 10827-10837.

Duncan, R.A., 1981, Hotspots in the southern oceans -- an absolute frame of reference for motion of the Gondwana continents, Tectonophysics, 74: 29-42.

Duncan, R.A., 1984, Age progressive volcanism in the New England seamounts and opening of the central Atlantic Ocean, J. Geophys. Res., (in press).

Duncan, R.A., and D.A. Clague, 1984, Pacific plate motion recorded by linear volcanic chains, J. Geophys. Res., (in press).

Duncan, R.A., and K.R. McElwee, 1984, Tertiary plate reconstructions for the western margin of Oregon and Washington, in: L.D. Kulm, et. al., (eds.), Atlas of the Ocean Margin Drilling Program, Western Oregon-Washington, Continental Margin, and Adjacent Ocean Floor, Region 5, Joint Oceanog. Inst., Inc., Marine Sci. Intl., Woods Hole, Mass., (in press).

Engebretson, D., 1982, Relative motions between oceanic and continental plates in the Pacific Basin, Ph.D. Diss., Stanford Univ., 211 pp.

Fiebelkorn, R.B., G.W. Walker, N.S. MacLeod, E.H. McKee and J.G. Smith, 1983, Index to K-Ar age determinations for the state of Oregon, Isochron/West, 37: 3-60.

Forsyth, D., and S. Uyeda, 1975, On the relative importance of the driving forces of plate motion, Geophys. J. R. Astr. Soc., 43: 163-200.

Fukui, S., 1976, Laboratory techniques used for atomic absorption spectrophotometric analysis of geologic samples, School of Oceanography, Oregon State University, Ref. 76-10: 151 pp.

Ganoe, S., and M. Fehler, 1984, Investigation of Pn propogation in Oregon, J. Geophys. Res., (in press).

Gill, J.B., 1981, Orogenic Andesites and Plate Tectonics, Springer-Verlag, New York: 390 pp.

Green, D.H., and A.E. Ringwood, 1967, An experimental investigation of the gabbro to eclogite transformation and its petrological applications, Geochim. Cosmochim. Acta, 31: 767-833.

Green, T.H., and A.E. Ringwood, 1968, Genesis of the calc-alkaline igneous rock suite, Contrib. Mineral. Petrol., 18: 105-167.

Green, T.H., 1972, Crystallization of calcalkaline andesite under controlled high-pressure hydrous conditions, Contrib. Mineral. Petrol., 34: 150-166.

Green, T.H., 1980, Island arc and continent-building magmatism... A review of petrogenetic models based on experimental petrology and geochemistry, Tectonophysics, 63: 367-385.

Grellet, C., and J. Dubois, 1982, The depth of trenches as a function of the subduction rate and age of the lithosphere, Tectonophysics, 82: 45-56.

Hammond, P.E., 1979, A tectonic model for the evolution of the Cascade Range, in: J.M. Armentrout, M.R. Cole and H.

TerBest, Jr. (eds.), Cenozoic Paleogeography of the Western United States, Soc. of Econ. Paleont. Mineral.: 219-237.

Harland, W.B., A.V. Cox, P.G. Llewellyn, C.A.G. Pickton, A.G. Smith and R. Walters, 1982, A Geological Time Scale, Cambridge Univ. Press, Cambridge: 131 pp.

Heller, P.L. and P.T. Ryberg, 1983, Sedimentary record of subduction to forearc transition in the rotated Eocene basin of western Oregon, Geology, 11(7): 380-383.

Helz, R.T., 1976, Phase relation of basalts in their melting ranges at P=5 Kb. Part II, Melt compositions, J. Petrol., 17: 139-193.

Jurdy, D., 1984, The subduction of the Farallon plate beneath North America, as derived from relative plate motions, Tectonics, 3: 107-113.

Karig, D.E., 1982, Temporal relationships between back-arc basin formation and arc volcanism with special reference to the Phillipine Sea, in: D.E. Hayes (ed.), The Tectonic and Geologic Evolution of Southeast Asian Seas and Islands, Part 2, Geophys. Monograph 27, Am. Geophys. Union, Washington, D.C.: 318-325.

Karig, D.E., and R.W. Kay, 1981, Fate of sediments on the descending plate at convergent margins, Phil. Trans. R. Soc. Lond., A301: 233-251.

Kennett, J.P., and R.C. Thunell, 1975, Global increase in Quaternary explosive volcanism, Science, 187: 497-502.

Kennett, J.P., A.R. McBirney and R.C. Thunell, 1977, Episodes of Cenozoic volcanism in the circum-Pacific region, J.

Volcanol. Geotherm. Res., 2: 145-163.

Kennett, J.P., 1982, Marine Geology, Prentice-Hall, Inc., Englewood Cliffs, N.J., 813 pp.

Langston, C.A., 1981, Evidence for the subducting lithosphere under southern Vancouver Island and western Oregon from teleseismic P wave conversions, J. Geophys. Res., 86: 3857-3866.

Leeds, A.R., L. Knopoff and E.G. Kausel, 1974, Variations of upper mantle structure under the Pacific Ocean, Science, 186: 141-143.

Lux, D.R., 1981, Geochronology, geochemistry and petrogenesis of basaltic rocks from the Western Cascades, Oregon, Ph.D. Diss., Ohio State Univ., Columbus, Ohio: 171 pp.

Lux, D.R., 1982, K-Ar and 40Ar-39Ar ages of mid-Tertiary volcanic rocks from the Western Cascade Range, Oregon, Isochron/West, 33: 27-32.

Magill, J., and A. Cox, 1980, Tectonic rotation of the Oregon Western Cascades, Oregon Dept. Geol. Min. Ind., Spec. Pap. 10: 67 pp.

McBirney, A.R., J.F. Sutter, H.R. Nalund, K.G. Sutton and C.M. White, 1974, Episodic volcanism in the central Oregon Cascade Range, Geology, 2: 585-589.

McBirney, A.R., 1978, Volcanic evolution of the Cascade Range, Ann. Rev. Earth Planet. Sci., 6: 437-456.

McKenzie, D.P., 1969, Speculations on the consequences and causes of plate motions, Geophys. J. R. Astr. Soc., 18: 1-32.

Minster, J.B., T.H. Jordan, P. Molnar and E. Haines, 1974,

Numerical modeling of instantaneous plate motions, Geophys. J. R. Astr. Soc., 36: 541-576.

Minster, J.B., and T.H. Jordan, 1978, Present day plate motions, J. Geophys. Res., 83: 5331-5354.

Miyashiro, A., 1974, Volcanic rock series in island arcs and active continental margins, Am. J. Sci., 274: 321-355.

Molnar, P., and T. Atwater, 1973, Relative motions of hotspots in the mantle, Nature, 246: 288-291.

Molnar, P., and J. Francheteau, 1975, The relative motion of hotspots in the Atlantic and Indian Oceans during the Cenozoic, Geophys. J. R. Astr. Soc., 43: 763-774.

Morgan, W.J., 1971, Convection plumes in the lower mantle, Nature, 230: 42-43.

Morgan, W.J., 1972, Deep mantle convections: plumes and plate motions, Am. Assoc. Petrol. Geol. Bull., 56: 203-213.

Morgan, W.J., 1981, Hotspot tracks and the opening of the Atlantic and Indian Oceans, in: C. Emiliani (ed.), The Sea, vol. 7, Interscience-Wiley, New York: 443-475.

Nicholls, I.A., and A.E. Ringwood, 1973, Effect of water on olivine stability in tholeiites and the production of SiO2-saturated magmas in the island-arc environment, J. Geol., 81: 285-300.

Peck, D.L., A.B. Grigg, H.G. Schlicker, F.G. Wells and H.M. Dole, 1964, Geology of the central and northern parts of the Western Cascade Range in Oregon, U.S. Geol. Surv. Prof. Pap. 449: 56 p.

Perfit, M.R., D.A. Gust, A.E. Bence, R.J. Arculus and S.R.

Taylor, 1980, Chemical characteristics of island-arc basalts: implications for mantle sources, Chem. Geol., 30: 227-256.

Priest, G.R., and B.F. Vogt, 1983, Geology and geothermal resources of the central Oregon Cascades, Oregon Dept. Geol. Min. Ind., Sp. Pap. 15: 123 pp.

Rea, D.K. and K.F. Scheidegger, 1979, Eastern Pacific spreading rate fluctuation and its relation to Pacific area volcanic episodes, J. Volcan. Geotherm. Res., 5: 135-148.

Riddihough, R.P., 1977, A model for recent plate interactions off Canada's west coast, Can. J. Earth Sci., 14: 384-396.

Ringwood, A.E., 1975, Composition and Petrology of the Earth's Mantle, McGraw-Hill, San Francisco, Calif.: 618 pp.

Robinson, P.T., G.F. Brem, and E.H. McKee, 1984, John Day Formation of Oregon: A distal record of early Cascade volcanism, Geology, 12: 229-232.

Scheidegger, K.F., and L.D. Kulm, 1975, Late Cenozoic volcanism in the Aleutian arc: Information from ash layers in the northeastern Gulf of Alaska, Geol. Soc. Am. Bull., 86: 1407-1411.

Shervais, J.W., 1982, Ti-V plots and the petrogenesis of modern and ophiolitic lavas, Earth Planet. Sci. Lett., 59: 101-118.

Simpson, R.W., and A.V. Cox, 1977, Paleomagnetic evidence for tectonic rotation of the Oregon Coast Range, Geology, 5: 585-589.

Smith, J.G., N.J. Page, M.G. Johnson, B.C. Moring and Floyd Gray, 1982, Preliminary geologic map of the Medford 1^{o} by 2^{o} quadrangle, Oregon and California, U.S. Geol. Surv. Open-file

Rept., No. 82-0955.

Snavely, P.D., Jr. and N.S. MacLeod, 1977, Evolution of the Eocene continental margin of western Oregon and Washington (abs.), Geol. Soc. Am., Abstr. Programs, 9(7): 1183.

Sutter, J.F., 1978, K/Ar ages of Cenozoic volcanic rocks from the Oregon Cascades west of 121 30', Isochron/West, 21: 15-21.

Taylor, E.M., 1978, Field geology of S.W. Broken Top Quadrangle, Oregon, Oregon Dept. Geol. Min. Ind., Sp. Pap. 2: 50 pp.

Taylor, E.M., 1980, Volcanic and volcaniclastic rocks on the east flank of the central Cascade Range to the Deschutes River, Oregon, in: K.F. Oles, J.G. Johnson, A.R. Niem and W.A. Niem (eds.), Geologic Field Trips in Western Oregon and Southwestern Washington, Oregon Dept. Geol. Min. Ind. Bull., 101: 1-7.

Taylor, E.M., 1981, Central High Cascade roadside geology -Bend, Sisters, McKenzie Pass, Santiam Pass, Oregon, in: D.A. Johnston and J. Donnelly-Nolan (eds.), Guides to Some Volcanic Terranes in Washington, Idaho, Oregon and Northern California, U.S. Geol. Surv. Circ. 838: 55-58.

Thayer, T.P., 1936, Structure of the North Santiam River section of the Cascade Mountains in Oregon, J. Geol., 44: 701-716.

Thorpe, R.S., P.W. Francis, M. Hamill and C.W. Baker, 1982, The Andes, in: R.S. Thorpe (ed.), Andesites: Orogenic Andesites and Related Rocks, John Wiley and Sons, New York: 724 pp.

Tobin, D.G., and L.R. Sykes, 1968, Seismicity and tectonics of the northeast Pacific Ocean, J. Geophys. Res., 73: 3821-3845.

Uyeda, S., and H. Kanamori, 1979, Back-arc opening and the mode of

subduction, J. Geophys. Res., 84: 1049-1061.

Walker, G.W., 1984, Geology of the Salem 2-degree Quadrangle, Oregon, U.S. Geol. Surv. Pub., (in prep).

Watson, E.B., 1982, Basalt contamination by continental crust: some experiments and models, Contrib. Mineral. Petrol., 80: 73-87.

Wells, F.G., 1956, Geology of the Medford Quadrangle, Oregon-California, U.S. Geol. Surv. Geol. Quad. Map, GQ-89, scale 1:96000.

Wells, R.E., D.C. Engebretson, P.D. Snavely, Jr. and R.S. Coe, 1984, Cenozoic plate motions and the volcanotectonic evolution of Western Oregon and Washington, Tectonics, 3: 275-294.

White, C.M., 1980, Geology and geochemistry of volcanic rocks in the Detroit area, Western Cascade Range, Oregon, Ph.D. Diss., Univ. of Oregon, 245 pp.

White, C.M., and A.R. McBirney, 1979, Some quantitative aspects of orogenic volcanism in the Oregon Cascades, Geol. Soc. Am. Mem. 152: 369-388.

White, W.M. and J. Patchett, 1984, Hf-Nd-Sr isotopes and incompatible element abundances in island arcs: implications for magma origins and crust-mantle evolution, Earth Planet. Sci. Lett., 67: 167-185.

Wilson, J.T., 1963, A possible origin of the Hawaiian islands, Can. J. Phys., 41: 863-870.

APPENDIX

APPENDIX A - K-AR AGE EQUATION AND LIST OF CONSTANTS

K-AR Method of Dating

$N = N_0 e^{-\lambda t}$

t = time
N = number of parent atoms
N_0 = number of initial parent atoms
λ = decay constant
D = number of daughter nuclides

Assume $N_0 = N+D$:

General age equation: $t = 1/\lambda \ln(1 + D/N)$

For K-Ar:

$$t = \frac{1}{\lambda_\varepsilon + \lambda_\beta} \ln \left[{}^{40}Ar_{rad} / {}^{40}K \left([\lambda_\varepsilon + \lambda_\beta] / \lambda_\varepsilon + 1 \right) \right]$$

List of Constants

1.	Fractonation factor	1.0181
2.	Depletion constant	3.2900 E -5
3.	CC of ^{38}Ar initially	7.0200 E -6
4.	Decay constant λ_ε	5.8100 E -11
5.	Decay constant λ_β	4.9630 E -10
6.	Ratio of 40/38 in spike	1.8800 E -3
7.	Ratio of 36/38 in spike	2.8800 E -5
8.	Ratio of 40/38 in air	1.5810 E +3
9.	Ratio of 36/38 in air	5.3492
10.	Fraction of K that is ^{40}K	1.167 E -4

APPENDIX B - PETROGRAPHIC DESCRIPTIONS

GWW-56-81 Basalt
45% Phenocrysts: Plagioclase, up to 5 mm
55% Groundmass: 30% plagioclase
18% clinopyroxene
3% opaque minerals

GWW-76-81 Basalt
40% Phenocrysts: 30% plagioclase, 1-2 mm
5% olivine, replaced mainly by opaque minerals (magnetite), subhedral, 1mm
5% clinopyroxene, up to 5 mm, slight alteration on rims
60% Groundmass: very fine-grained, plagioclase, clinopyroxene, opaque minerals +olivine

GWW-87-81 Andesite
55% Phenocrysts: bimodal size distribution, .25 mm and 1 mm
35% plagioclase
20% clinopyroxene
5% orthopyroxene
5% opaque minerals
45% Groundmass: extremely fine-grained, plagioclase, clinopyroxene

GWW-81-141 Basalt
40% Phenocrysts: 35% plagioclase, up to 3 mm
5% olivine, subhedral relict crystals, replaced by clay (iddingsite)
60% Groundmass: medium-grained, plagioclase, clinopyroxene, opaque minerals

GWW-114-81 Andesite
40% Phenocrysts: 20% plagioclase, up to 3 mm, An48 composition
10% clinopyroxene, 1-2 mm, glomeroporphyritic
10% orthopyroxene
60% Groundmass: fine-grained, some reddish-brown clay alteration plagioclase, clinopyroxene, opaque minerals

GWW-190-81 Basalt
30% Phenocrysts: plagioclase, up to 4 mm, slight sericite alteration
70% Groundmass: 35% plagioclase, 20% clinopyroxene, opaques, glass

GWW-191-81 Basalt
15% Phenocrysts: 13% plagioclase, up to 5 mm
2% clinopyroxene, replaced by clay
85% Groundmass: 60% plagioclase, 20% clinopyroxene, 5% opaque minerals

GWW-82-18 Basalt
60% Phenocrysts: plagioclase, up to 3 mm
40% Groundmass: medium-grained, 20% plagioclase, 18% clinopyroxene, 2% opaque minerals

GWW-82-29 Basalt
45% Phenocrysts: plagioclase, up to 5mm, An38 composition
55% Groundmass: fine-grained, 30% plagioclase, 20% clinopyroxene, 5% opaque minerals

GWW-82-41 Basalt
2% Phenocrysts: plagioclase, up to 2 mm
98% Groundmass: uniform, fine-grained, 40% plagioclase, 45% clinopyroxene, 13% opapue minerals

GWW-82-42 Basalt
45% Phenocrysts: 40% plagioclase, up to 5 mm
5% oxyhornblende, rims replaced by extremely fine-grained mineral
55% Groundmass: very fine-grained, 30% plagioclase, 20% clinopyroxene, 5% opaque minerals

GWW-82-43 Basalt
50% Phenocrysts: 45% plagioclase, up to 3 mm
5% olivine or clinopyroxene, relict crystals altered to clay
50% Groundmass: 25% plagioclase, 22% clinopyroxene, 3% opaque minerals (magnetite), 5% glass (devitrified)

GWW-82-45 Basalt
2% Phenocrysts: plagioclase, 1mm
glass
98% Groundmass: medium-fine grained, 60% plagioclase, 25% clinopyroxene, 8% opaque minerals, minor glass

M2-17 Basalt
25% Phenocrysts: 22% plagioclase, up to 3 mm, slight sericite alteration
3% olivine or clinopyroxene, relict crystals replaced by clay
75% Groundmass: trachytic texture, 40% plagioclase, 15% clinopyroxene, 10% opaque minerals (magnetite), 5% glass (devitrified)

M2-19 Basalt
40% Phenocrysts: 30% plagioclase, up to 3 mm, slight sericite alteration
8% olivine, replaced by iddingsite
2% clinopyroxene
60% Groundmass: trachytic texture, 30% plagioclase, 20% clinopyroxene, 10% opaque minerals

M2-22 Basaltic andesite
25% Phenocrysts: 22% plagioclase, moderate sericite alteration
3% clinopyroxene, glomeroporphyritic
75% Groundmass: very fine-grained, 40% plagioclase, 15% clinopyroxene, 15% glass, 5% opaque minerals

M2-23 Andesite
50% Phenocrysts: 30% plagioclase
20% clinopyroxene
50% Groundmass: very fine-grained, plagioclase, clinopyroxene, opaque minerals, minor calcite fracture fillings

M2-24 Basalt
60% Phenocrysts: 45% plagioclase, 1-2 mm
15% clinopyroxene, 5 mm, sub-euhedral, fresh
40% Groundmass: plagioclase, clinopyroxene, opaque minerals

M2-25 Basalt
40% Phenocrysts: 35% plagioclase, up to 2 mm, fresh
5% relict olivine or clinopyroxene, replaced by clay

M3-25 Basaltic andesite
40% Phenocrysts: 30% plagioclase, up to 3 mm, slight alteration
8% clinopyroxene, up to 2 mm, slight alt.
2% relict olivine, clay infilled
60% Groundmass: fine-grained, 0.1-0.5 mm, felty texture, 45% plagioclase, 10% clinopyroxene, 5% opaque minerals

M3-26 Basalt
5% Phenocrysts: clinopyroxene, up to 2 mm, yellowish alteration rims minor plagioclase
95% Groundmass: very fine-grained, trachytic texture, 60% plagioclase, 30% clinopyroxene, 5% opaque minerals

M3-27 Basaltic andesite
50% Phenocrysts: 45% plagioclase, fresh
5% relict olivine or clinopyroxene, clay infilled
50% Groundmass: felty texture, 30% plagioclase, 12% clinopyroxene, 10% opaque minerals

M3-29 Basalt
20% Phenocrysts: olivine, 1mm, iddingsdite alteration rims clinopyroxene?
80% Groundmass: 45% plagioclase, 15% olivine, 15% clinopyroxene, 5% opaque minerals

M3-31 Andesite
40% Phenocrysts: 35% plagioclase, up to 5 mm, slight alteration, contain glass inclusions
3% clinopyroxene
2% quartz
60% Groundmass: fine-grained, 30% plagioclase, 20% glass, 5% clinopyroxene, 5% opaque minerals

M3-32 Andesite
60% Phenocrysts: 45% plagioclase, up to 5 mm, slight alteration
15% clinopyroxene
40% Groundmass: very fine-grained, 20% plagioclase, 10% variolitic glass, 5% clinopyroxene, 5% opaque minerals

M3-33 Basaltic andesite
3% Phenocrysts: plagioclase, up to 2 mm, fresh
97% Groundmass: very fine-grained, trachytic texture, 60% plagioclase, 30% variolitic glass, 10% clinopyroxene, 7% opaque minerals

M3-34 Basalt
50% Phenocrysts: 25% olivine, iddingsite alteration on rims mainly
25% plagioclase
50% Groundmass: fine-medium grained, felty texture, 35% plagioclase, 10% clinpyroxene, 5% opaque minerals, olivine?

M3-35 Basalt
5% Phenocrysts: olivine, 1 mm, fresh
95% Groundmass: fine-grained, trachytic texture, 60% plagioclase, 20% clinopyroxene, 15% opaque minerals

M3-37 Basalt
60% Phenocrysts: 42% plagioclase, 2-4 mm
15% clinopyroxene, 1 mm crystals
3% olivine, clay infilled, rims replaced by cpx
40% Groundmass: 20% plagioclase, 12% clinopyroxene, 5% opaque minerals, minor glass, vesicles infilled with clay

M3-38 Dacitic vitrophyre
10% Phenocrysts: 6% plagioclase, 1 mm, fresh
2% orthopyroxene
2% opaque minerals
90% Groundmass: flow-banded glass, concoidal fractures

M3-39 Basaltic andesite
35% Phenocrysts: 32% plagioclase, agglomerates up to 2 mm
3% clinopyroxene, 0.1-0.4 mm
65% Groundmass: fine-grained, felty texture, 40% plagioclase, 20% clinopyroxene, 5% opaque minerals

GWW-10-83 Basaltic andesite
4-5% Phenocrysts: plagioclase
95% Groundmass: medium-grained, 55% plagioclase, 25% clinopyroxene, 10% opaque minerals, 5% glass

GWW-15-83 Basaltic andesite
50% Phenocrysts: 30% plagioclase, up to 4 mm, fresh, An55 composition
15% clinopyroxene
5% olivine, replaced by opaque mineral
50% Groundmass: fine-grained, plagioclase, clinopyroxene, opaque minerals, glass

GWW-21-83 Basalt
25% Phenocrysts: Plagioclase, up to 5 mm , An62 composition
75% Groundmass: medium-grained, 50% plagioclase, 20% clinopyroxene, minor opaque minerals and glass

GWW-28-83 Basaltic andesite
5% Phenocrysts: plagioclase, up to 1 mm
95% Groundmass: medium-fine grained, trachytic texture, 60% plagioclase, 25% clinopyroxene (slight alteration), 10% opaque minerals

GWW-32-83 Basalt
15% Phenocrysts: 10% clinopyroxene, up to 2 mm
5% plagioclase
olivine?
85% Groundmass: medium-fine grained, 50% plagioclase, 40% clinopyroxene, 15% opaque minerals

GWW-42-83 Basalt
50% Phenocrysts: 45% plagioclase, up to 6 mm, altered slightly to sericite, An46 composition
5% clinopyroxene
50% Groundmass: medium-grained, 35% plagioclase, 13% clinopyroxene, 2% opaque minerals

GWW-67-83 Basaltic andesite
1% Phenocrysts: plagioclase, 1-2 mm, slight alteration on rims
99% Groundmass: fine-grained, 50% plagioclase, 40% clinopyroxene, 9% opaque minerals(magnetite)

GWW-73-83 Basalt
10% Phenocrysts: plagioclase, up to 3-4 mm, fresh
90% Groundmass: fine-grained, trachytic texture, 45% plagioclase, 30% clinopyroxene, 10% opaque minerals, 5% glass

GWW-99-83 Basalt
40% Phenocrysts: 30% plagioclase, up to 1-2 mm, slight sericite alteration
10% clinopyroxene
60% Groundmass: very fine-grained, 45% plagioclase, 10% clinopyroxene, 5% opaque minerals and clay-filled vesicles

GWW-102-83 Basaltic andesite
50% Phenocrysts: 45% plagioclase, up to 2 mm
5% clinopyroxene, up to 2 mm
50% Groundmass: very fine-grained, 30% plagioclase, 15% clinopyroxene, 5% opaque minerals and glass

GWW-103-83 Basaltic andesite
5% Phenocrysts: plagioclase
relict clinopyroxene or olivine, replaced by clay
95% Groundmass: fine-grained, 60% plagioclase, 30% clinopyroxene, 5% opaque minerals

GWW-104-83 Basaltic andesite
30% Phenocrysts: plagioclase, up to 5 mm, reddish alteration common along fractures in crystals
70% Groundmass: very fine-grained, numerous fractures throughout, 40% plagioclase, 12% clinopyroxene, 12% glass, 6% opaque minerals

GWW-107-83 Basalt
2% Phenocrysts: plagioclase, up to 1 mm
98% Groundmass: fine-grained, 50% plagioclase, 30% clinopyroxene, 14% opaque minerals (distinctive long ilmenite needles), 4% glass

GWW-113-83 Basaltic andesite
20% Phenocrysts: plagioclase, up to 5 mm
clinopyroxene
relict olivine, replaced by iddingsite
80% Groundmass: 50% plagioclase, 23% clinopyroxene, 7% opaque minerals

P84-1 Basalt
32% Phenocrysts: 28% plagioclase
2% clinopyroxene
2% oxyhornblende, rims replaced by fine-grained groundmass minerals
68% Groundmass: very fine-grained, 33% plagioclase, 25% clinopyroxene, 10% opaque minerals

P84-2 Basalt
25% Phenocrysts: 20% plagioclase
3% olivine, replaced by clay
2% clinopyroxene, fresh
75% Groundmass: fine-grained, trachytic texture, 55% plagioclase, 12% clinopyroxene, 8% opaque minerals

P84-3 Basalt
2% Phenocrysts: plagioclase, up to 1 mm
98% Groundmass: medium-grained, slight greenish alteration, 85% plagioclase, 12% clinopyroxene, 5% opaque minerals

P84-6 Basalt
15% Phenocrysts: 13% plagioclase, 1 mm
2% clinopyroxene
85% Groundmass: fine-grained, 65% plagioclase, 12% clinopyroxene, 8% opaque minerals

P84-65 Basalt
40% Phenocrysts: 35% plagioclase, up to 5 mm
5% relict clinopyroxene, replaced by extremely fine-grained mineral
60% Groundmass: fine-grained, 35% plagioclase, 20% clinopyroxene, 5% opaque minerals